AQUEOUS CORROSION OF URANIUM AND SOME URANIUM-RICH ALLOYS

Submitted for
the degree of Ph.D.
in
The University of London

by

Ajay Yashvant Nehru

1962

ABSTRACT

The aqueous corrosion of uranium and some uranium-zirconium alloys has been studied as a function of several variables including hydrogen activity, pH, temperature and the oxygen content of the test solution. Two main experimental techniques were employed: an optical method designed to measure the rate and kinetics during the corrosion process, and an electronic technique to measure changes in the electrode properties under similar conditions. Both techniques were selected to permit careful control of the test conditions and measurement without removal of the specimen from the environment.

The results of the investigation emphasise the importance of the protective oxide film formed during corrosion, and suggest that the rate-controlling steps in the process occur within this film. The effects, both of cathodic polarisation in a variety of conditions and alloying with zirconium, on the diffusivity in and the thickness of the oxide have led to a discussion of the protective film in terms of an ionic diffusion-barrier, a solid electrolyte and a non-stoichiometric semi-conductor, and, further, to a consideration of the methods by which this oxide may be deformed.

TABLE OF CONTENTS

SECTION I

INTRODUCTION

I(a) Basis of the Investigation

The contemporary development of nuclear reactor technology has aroused an interest in the corrosion behaviour of several metals including uranium, aluminium, zirconium and niobium. These metals which are of particular importance in the fabrication of fuel elements are thermodynamically unstable in the presence of water or steam. This property would normally preclude their use under operating conditions where an aqueous coolant is employed, if it were not for the protective nature of the initially-formed oxide films which decreases the rate of the subsequent corrosion.

Detailed studies[1,2,3] of the corrosion behaviour of these metals at high temperatures have shown in many cases that the growth of the protective oxide, resulting in a corrosion rate which decreases with time, precedes a period of corrosion where the rate is constant with respect to time. For the particular case of uranium, the rate of the time-independent corrosion has been shown to be temperature-dependent, and there exists experimental evidence[1] that the duration of this process is shortened and its rate increased by a rise in temperature. Furthermore, after a length of time dependent on the test

temperature, and without apparent change in the conditions, this first period of linear corrosion can be succeeded by a second of greater rate. This linear-linear transition is termed "breakaway" and, in some instances, the ratio of the first linear rate to the second has been found to be of the order 1 : 20 (see Fig. 1).[1]

The general aqueous corrosion reaction for these metals is of the type :

$$xM + yH_2O = M_xO_y + yH_2$$

and a survey of the literature indicated that many of the effects described above were attributed to the corrosion-product hydrogen, but that of the various mechanisms proposed to explain the phenomena, few, if any, had been substantiated by experiment.

Early research into the corrosion behaviour of uranium, initiated in the U.S.A. during the War, was confined mainly to the practical aspects of the problem. Most succeeding investigations, too, maintained a non-theoretical bias. This led to the suggestion[3], as recently as 1957, that a fundamental approach would be of considerable value. In the present study, therefore, an attempt has been made to assess qualitatively the relative importance of the various environmental factors involved in the corrosion process.

I(b) Scope of the Investigation

The dominant role of hydrogen in the corrosion processes of uranium was established chiefly by means of high-temperature testing in autoclaves. Following this work, Draley and Ruther[3] suggested three alternative mechanisms by which hydrogen might alter the protective properties of the oxide film. These were by (1) diffusion into the metal and consequent blistering of the surface, (2) formation of gas bubbles at the metal-oxide interface causing rupture of the oxide, and (3) formation of a metal hydride leading to reduction of film adhesion and possible recrystallisation of the oxide.

The models based on these proposals emphasised the mechanical failure of the oxide film due to the action of the corrosion-product hydrogen.

Later work by Leach[4] attempted to relate the electrical properties of the oxide formed to the corrosion rate of the metal. He pointed out that the effect of the Draley-Ruther mechanisms would be primarily to alter the thickness or porosity of the oxide. However, while proposing a fourth mechanism, Leach suggested that the incorporation into the oxide lattice of ionic hydrogen might influence the diffusion of other ionic species without causing a change in the structure. Measurements of the conductivity and capacity of U/UO_2 electrodes

were made at cathodic potentials and the results were interpreted as showing that an increase in hydrogen activity caused an increase in the conductivity of the oxide layer without appreciable change in its thickness - suggesting the probable existence of the fourth mechanism and a relationship between oxide conductivity and corrosion rate.

The present investigation has been carried out in order to examine in detail the effect on the oxide film, and, hence, on the corrosion rate of the metal, of alloying additions, particularly of hydrogen. Both electrical and mechanical models of damage are considered.

The basic experimental techniques employed in the research are electrochemical and have been chosen to allow control over some of the influencing variables (e.g. the hydrogen activity at the electrode surface), and to enable measurement without removal of the specimen from the corrosion environment.

The results obtained fall naturally into two categories; the first concerned with the electrode properties of the U/UO_2 cathode, and the second pertaining directly to the corrosion rate and corrosion kinetics of the metal. A scheme for dual presentation has been adopted, therefore, and will be maintained on this basis throughout, except in the Discussion where a division

has been made for different reasons. The main emphasis of the thesis is on the corrosion behaviour and the majority of the Discussion will be devoted to this aspect of the work.

SECTION II

PREVIOUS WORK

SECTION II

PREVIOUS WORK

The literature survey is divided into two parts, in accordance with the general scheme outlined in the preceding section, and is confined almost entirely to the properties of uranium and the theories relevant to the corrosion behaviour of this metal.

The first part considers the electrode properties of uranium and uranium oxides and includes discussion of the following topics: general electrode properties, anodic and cathodic processes, hydrogen overpotential, conductivity and diffusion mechanisms, and capacity.

The second section is concerned primarily with mechanical aspects of the corrosion of uranium. Space is also given to a general consideration of the kinetics of oxide growth. The subjects reviewed in detail are: film-growth laws, methods of corrosion rate testing, evidence for hydrogen-induced damage to uranium, structural properties of uranium metal and the effect of alloy additions, explanatory models for hydrogen-induced damage, and the corrosion of uranium-zirconium alloys at low temperatures.

PART ONE - ELECTRODE PROPERTIES

II(a) Introduction

Any enumeration of the electrochemical variables which influence corrosion must include the following four factors associated mainly with the properties of the metal:-

(a) The effective electrode potential in a solution.

(b) The ability to form an insoluble protective film.

(c) The hydrogen overpotential.

(d) The chemical and physical homogeneity of the surface.

The electrode potential of a metal, in a particular solution of its own salt, determines its position in the Electrochemical Series. The electrode potential of hydrogen is taken arbitrarily as zero, and metals of negative electrode potential are capable of liberating the gas from water. The rate of the hydrogen evolution process for uranium would be extremely rapid but for two distinct phenomena - the formation of a protective oxide and the overpotential of the reaction. A protective oxide generally fulfils two functions: it prevents access of the environment to the metal surface, and raises* the electrode potential. Measurement of the direction of

*N.B. The convention adopted in this thesis defines 'rising' or increasing potentials as changes occurring in the anodic (noble or positive) direction; decreasing potentials are associated with changes in the opposite sense.

change of potential is commonly employed as a method for determining whether corrosion or passivation is occurring. The effect of oxygen in solution and the rise in potential associated with the healing of oxide films are relevant in this context; the model derived by Hoar and Evans[5] to explain these phenomena is, perhaps, the most widely known.

In any corrosion process where the rate is influenced to a great extent by the presence of hydrogen, a knowledge of the overpotential of the reaction becomes important. In the case of an oxide-covered metal, the rate of the electrochemical processes is controlled by the diffusion of various species through the film. The interdependence of overpotential and oxide conductivity will be shown later.

A common method for the prevention of hydrogen-induced damage to uranium and other reactive metals is the introduction of alloying elements of lower overpotential into the base. One theory of the mechanism by which alloying elements function is that they alter the chemical homogeneity of the surface by providing cathodes for rapid discharge of molecular hydrogen[2].

II(b) Anodic and Cathodic Processes

Electrochemical reactions occurring at "clean" metal surfaces have been the subject of numerous invest-

igations. Theories derived from these studies, however, must be modified for the case of uranium and similar reactive metals to allow for the presence of semi-conducting oxide films on the surface.

The corrosion reactions proceeding at an oxide-free electrode are restricted to a single interface; the corrosion of uranium, however, involves the diffusion of both ionic and electronic charge-carriers through a conducting oxide, and the reactions which are possible can take place at two interfaces. Thus, an uranium cathode in an electrolytic cell may be considered to function as a bi-polar electrode, i.e. in addition to its behaviour as a cathode in the accepted sense, the uranium metal-oxide interface can be regarded as the negative electrode in a cell in which the outer interface is the anode and the conducting oxide is the electrolyte. It is necessary, therefore, that the existence of both concentration and potential gradients within the growing oxide be taken into consideration in any study of the electrode properties. A generalised diagram of the relevant interfaces and gradients is given in Fig. 2.

A metal placed in an aqueous solution tends to ionise and an equivalent amount of hydrogen is produced. The following types of reaction may be said to take place :

Anodic		Cathodic
$M = M^{x+} + xe^-$	potential dependent	$xH^+ + xe^- = xH$
	or	
$M^{x+} + x/2\ OH^- = MO_{x/2} + \frac{xH^+}{2}$	pH dependent	$x/2\ H_2O = x/2\ OH^- + x/2\ H^+$

When it occurs, the growth of an oxide film involves the anodic reaction, and takes place by either the outward diffusion of metal ions or the inward diffusion of oxygen ions. It is clear from Fig. 2 that both ionic transfers must be accomplished <u>against</u> a potential gradient. An increase in electronic conductivity of such a film will reduce this gradient and consequently stimulate oxide growth.

The cathodic reaction, directly responsible for hydrogen depolarisation, can proceed by at least three mechanisms. Two of these which occur at the oxide-electrolyte interface are discussed later in this section.

Several models have been derived describing the anodic and cathodic processes at an oxide-covered cathode; two are given below. These differ mainly in the assumptions concerning the electronic charge-carriers within the oxide.

A simple theory suggested by Draley and Ruther[3] is shown diagrammatically in Figs. 3a and 3b. Here, the anodic transfer is accomplished under the influence of

a concentration gradient. The cathodic current, on the other hand, is considered to be inversely proportional to the energy requirements of the following four processes:- (1) the cathodic reduction at the oxide-electrolyte interface, (2) incorporation of the diffusing species into the oxide, (3) diffusion, and (4) liberation and disposal of the products. It can be seen from Fig. 3b that the diffusion of electrons and protons is aided by both a concentration and a potential gradient (a concentration gradient of electrons is itself equivalent to a potential gradient). The protons are believed to migrate either via interstitial positions or by combining with oxygen ions in the lattice. It should be pointed out, however, that the entry of protons into the oxide and the formation of molecular hydrogen at the outer interface are competing reactions, and that an increase in the electronic conductivity of the oxide is likely to favour the latter.

Waber[6] has proposed an alternative model for the corrosion of uranium in which the cathodic formation and discharge of H^+ ions are not emphasised. He suggests that hydrogen migrates to the metal in the form of hydroxyl ions which are produced at the oxide-electrolyte interface by either the reduction of adsorbed oxygen or the decomposition of water, and diffuse through the oxide

as part of the anodic current. In support of this argument, there is evidence for the presence of the hydroxide $U(OH)_4$ in the corrosion-product.

The main cathodic reactions which Waber considers as taking place are given below :-

(1) When the electrolyte contains a high concentration of oxygen :

$$\tfrac{1}{2}\, O_2 \longrightarrow O^-_{ads} + \oplus$$

$$O^-_{ads} \longrightarrow O^{=} + \oplus$$

$$\tfrac{1}{2}\, O_2 + H_2O \longrightarrow 2OH^- + 2\oplus$$

(2) When insufficient oxygen is present :

$$H_2O_{ads} \longrightarrow H_{ads} + OH_{ads}$$

$$OH_{ads} \longrightarrow OH^- + \oplus$$

The symbol $\oplus$ represents a positive hole - an electronic species carrying a single positive charge. The transfer of electrons across the oxide-electrolyte interface, facilitating the cathodic reactions, results in a space-charge of positive holes on the film side of the interface. If the oxide is conducting, the space-charge is annihilated by the inward diffusion of the species. The formation of positive holes will be considered in sub-section II(d). It is sufficient, here, to say that the inward diffusion of a positive hole towards the metal-oxide interface

accomplishes the same net charge transfer as the outward movement of an electron.

Draley and Ruther[3] have acknowledged the possibility of anodic hydroxide diffusion, but consider it unlikely. They base this conclusion on the observation that accumulation of corrosion-product hydrogen in the metal is decreased by anodic polarisation and increased by cathodic polarisation.

It is established[7] that the aqueous corrosion of uranium is under anodic control, i.e. the overall rate is dominated by the anodic reaction. To enable the corrosion represented by the anodic reactions to proceed, it is necessary that the hydrogen liberated simultaneously be removed, since, otherwise, it would produce a polarising film and arrest further action. Two methods of hydrogen removal which are considered relevant are given here. The first requires the presence of sufficient oxygen or other oxidising agent in the electrolyte, when the following reactions may occur :

$$2H + \tfrac{1}{2}O_2 = H_2O$$

$$2H_2O + O_2 + 4e^- = 4\,OH^-$$

$$H^+ + OH^- = H_2O$$

This is known as corrosion by oxygen depolarisation.

The second mechanism is of greater interest to

this research and functions when oxygen activity in the solution is low. If electrons are available from the metal to convert protons to hydrogen, then

$$H^+ + e^- = H$$

$$H + H = H_2$$

and this is known as corrosion by hydrogen evolution.

II(c) Hydrogen Overpotential

The hydrogen overpotential is a measure of the ease with which the evolution reaction can take place, and may be expressed by :

$$\eta = e_i - e_r$$

where η is the overpotential at current density i ; e_r is the reversible hydrogen potential, i.e. the potential of an unpolarised hydrogen electrode in the same solution; e_i is the electrode potential when i amps./cm^2 is passing across the electrode-electrolyte interface.

There are three generally accepted causes for the departure of the electrode potential from its reversible value during passage of a current. The most significant of these, known as the activation overpotential, is related to the energy requirements of the various steps which occur during the discharge of molecular hydrogen at a cathode. Fig. 4 shows a proton produced by

electrolysis and solvated by the base which, here, is assumed to be water. For discharge to occur, it is necessary that the solvation bonds holding the proton at the centre of the complex be broken and the proton itself be drawn to the metal surface. The next stage might entail the temporary formation of a complex M(H) or a metastable hydride MH before the hydrogen now in the atomic stage (having received an electron from the metal) is catalysed to the gas.

The relationship of overpotential to activation energy is shown by the expression :

$$\left(\frac{\partial \ln i}{\partial T}\right)_v = \frac{E}{RT^2}$$

where T is the absolute temperature; v is the potential of the electrode; i is the current density; E is the activation energy, and R is the gas constant.

The continuation of the discharge reaction is dependent upon the constant replacement of the ions removed from the electrolyte in the immediate vicinity of the electrode. At high current densities, when the rate of electrolysis exceeds the rate at which ions arrive at the cathode by convection or migration, the ionic concentration in the electrolyte adjacent the metal may become lower than in the bulk solution. This leads to <u>concentration overpotential</u> and a numerical

increase in the electrode potential. The effect of concentration overpotential can be reduced by stirring, agitation, etc.

The presence of a resistant oxide film or other substance on the surface of the metal can create an ohmic overpotential by impeding the discharge of hydrogen. The magnitude of this effect is the product IR (where, I is the impressed current and R is the resistance of the surface film). A related phenomenon is the ohmic pseudo-overpotential caused by the IR drop in the electrolyte between the electrode and the potential-measuring device.

The relationship between the activation over-potential and the impressed current is given by the Tafel equation :-

$$\eta = a + b \log i$$

where, a and b are constants; i is the current density; η is the activation overpotential.

It must be stressed that the validity of this equation is restricted to the limited current range where the effects of concentration and ohmic overpotentials can be neglected. Fig. 5 illustrates an idealised Tafel line (derived from the equation) for an oxide-free cathode. A change in the constants (as shown at B) may take place if the rate-determining step of the

discharge reaction is altered at higher current densities.

Several authors[4,6,8,9] have reported measurements of the hydrogen overpotential on uranium and uranium-base alloys. Of these, the first three have observed marked inflections in the Tafel line at intermediate current densities, and also the occurrence of a hysteresis loop. The inflections indicate a change in mechanism and are not comparable to the change in slope shown in Fig. 5 where only the rate of the existing process is affected by high current densities. Fig. 6 shows the general type of curve obtained by these workers. The hysteresis shown here is of significant magnitude and in all cases takes the same form. Over the relevant portion of the curve, the current at a given potential is less in value when measured at decreasing potentials than when approached from below.

Losco[8] has calculated numerical values for the constants in the Tafel equation, and proposes a relationship between the transition in kinetics and the absorption of atomic hydrogen by the electrode surface. He explains the hysteresis of the curve as resulting from the surface hydriding of the metal at high current densities. The validity of the latter explanation, however, is questionable in view of its inconsistency both with his own results and those of other workers.

Measurements, under identical conditions, have been made by Losco for two specimens, one normal, and the other heavily hydrided. The hydrided specimen appears to display the greater overpotential, contra-indicating the explanation offered. Further, the existence of a hysteresis similar to that of uranium has been shown in the Tafel line of the non-hydride forming metal, aluminium. This will be illustrated in a later section.

Leach[4] has provided evidence indicating a relationship between the overpotential and the conductivity of the oxide formed. He has measured a significant increase in oxide conductivity at potentials which correspond to those of the inflection in the overpotential curves, and has shown that both conductivity and overpotential curves display similar hysteresis.

These observations are supported separately by both Isaacs[9] and Fawkes[10]. Isaacs has derived a mathematical relationship between overpotential and current which can be applied equally well to both 'clean' and oxide-covered metals. He explains the inflection in the overpotential curve for U- 12 wt % Mo on the basis of a change from oxygen depolarisation to the hydrogen evolution reaction. Further, an investigation of the properties of hydrided specimens was conducted and showed that the formation of UH_3 on the metal surface did not significantly

influence the kinetics of the process.

Hitherto unpublished data obtained by Fawkes indicate an increase in electronic conductivity deriving from an increase in the activity of ionic hydrogen within the oxide. This provides a justifiable interpretation for the hysteresis effect, in that it follows that any increase in oxide conductivity would tend to diminish the overpotential of the hydrogen evolution reaction at the surface. It has been assumed in this work that high current densities are likely to increase the concentration of protons within the oxide.

II(d) Conductivity and Diffusion

Wagner[11] has discussed the conductivity mechanism in ionic crystals in terms of lattice defects, and has demonstrated the existence of a relationship between the electronic conductivity and the mobility and diffusion of ions for the system Ag-Ag_2S-S. A similar relationship may be possible for the system U-UO_2-O in which the oxide formed during aqueous corrosion is likely to possess a defect structure.

Fig. 7 shows the pH-potential diagram derived by Pourbaix and co-workers[12] from thermodynamic data for the uranium-water system. This figure has been redrawn on the basis of hydrogen activities to conform to the method adopted for the plotting of results. The method

of presentation allows the effect, on a given variable, of the amount of hydrogen produced to be seen easily. The hydrogen activity potential E_{HA} is a function of the logarithm of hydrogen activity or pressure $\propto$: its relationship to the hydrogen potential E_H is given by the expression :-

$$E_{HA} = E_H + 0.0591\ pH$$

Two points should be stressed: (1) that the Pourbaix diagram is truly representative only of a system in equilibrium, and (2) that it is derived from thermodynamic data which could possibly be in error. At this point, however, these factors may be ignored, and it will be assumed that the data presented in the diagram are qualitatively applicable to the system under consideration.

It is implicit in the construction of the diagram that the oxides shown are stoichiometric and not liable to a change in phase. However, there is convincing evidence[13,14,15] in the literature which establishes both the non-stoichiometry of uranium oxides over wide ranges of composition and the occurrence of other phases between UO_2 and U_3O_8.

The oxidation of UO_2 to higher oxides is accompanied by changes in the type of semi-conductivity. Willardson, Moody and Goering[15] have identified the following at

high temperatures :-

UO_2	stoichiometric phase,	intrinsic conductor
UO_{2+x}		p-type "
U_4O_{9-x}		n-type "
U_4O_9	stoichiometric phase,	intrinsic "
U_4O_{9+x}		p-type "
U_3O_{7-x}		n-type "
U_3O_7	stoichiometric phase,	intrinsic "

Extrapolating further, it is reasonable to expect from the available evidence that higher oxides than U_3O_7 would be the following :-

U_3O_{7+x}		p-type conductor
U_3O_{8-x}		n-type "
U_3O_8	stoichiometric phase,	intrinsic "
U_3O_{8+x}		p-type "
UO_{3-x}		n-type "
UO_3	stoichiometric phase,	intrinsic "

The total electrical conductivity of a compound is the sum of both the ionic and electronic contributions, and is closely related to the diffusion mechanism and the lattice structure. The conductivity of uranium oxides is believed to be predominantly electronic; the lattice which is of the fluorite type can tolerate both excess anions and anion vacancies, and the current, therefore,

can, in theory, be carried by either positive holes or excess electrons.

Fig. 8 shows the lattice structure common to fluorite type compounds. In the case of p-type uranium oxides, the electrical imbalance resulting from the random distribution of excess oxygen ions in interstitial positions would be neutralised by the formation of positive holes in the immediate vicinity. Holes are charge-carriers which are positive in comparison to an ideal lattice region, and are produced by the exchange of electrons between ions with normal shells and ions with incomplete shells. It must be pointed out that the holes themselves are incapable of independent movement; only the electrons of the system may move. Conduction by migration occurs as the location of the hole passes through the lattice by the successive movement of electrons between neighbouring ions.

n-type semi-conduction in uranium oxides, on the other hand, is favoured when the number of anions in the lattice is insufficient to balance the total positive charge of the metal ions. The imbalance is neutralised by the formation of excess electrons in a manner similar to the formation of positive holes.

The ionic current in uranium oxides, several orders of magnitude less than the electronic contribution, is

responsible for the growth of the oxide and is maintained primarily by the inward diffusion of oxygen ions via interstitial positions[6,15,16]. Belle and Lustman[16] have calculated the activation energy for self-diffusion of oxygen ions in the UO_2 lattice as 29.7 Cals./gm. mole which contrasts with a value of 90-125 Cals./gm.mole for the self-diffusion of the metal. The ease with which the UO_2 lattice accommodates excess oxygen, without significant change in parameter, suggests that the inward diffusion of anions is only slightly impeded by other oxygen ions in the lattice.

The effect of alloying components on the diffusion processes and conductivity of ionic crystals has been investigated in detail. Wagner[17] has shown that both ionic and electronic conductivity can be greatly altered by additions of small amounts of ions of higher or lower valency. The entry of ionic hydrogen into an uranium oxide film has been considered on this basis by some workers.

Leach[4] and Isaacs[9] have measured the conductivity of U/UO_2 electrodes at cathodic potentials and have obtained similar results. Leach has discussed the results in terms of a relationship between the hydrogen content of the oxide, conductivity, and corrosion rate. He suggests that the quantity of hydrogen which enters the

oxide will depend upon the activity of hydrogen at both the outer and inner interfaces of the metal-oxide-solution system; an increase in activity at either or both of these interfaces will result in a corresponding increase in the hydrogen concentration within the oxide.

Isaacs acknowledges the existence of contributing reactions within the oxide, but does not consider them in his interpretation. He makes use of the theory of Faradaic admittance developed by Grahame[18] to explain some of the conductivity phenomena purely on the basis of electrochemical reactions occurring at the oxide-electrolyte interface. This model provides an explanation for the observed increase in electrode conductivity at cathodic potentials but can explain neither the changes observed at more positive potentials nor the hysteresis in the conductivity curve.

It is unfortunate that the experimental technique employed by both workers is unable to provide any indication of the type of conductivity prevailing in the oxide. No satisfactory interpretation of the conductivity mechanism at U/UO_2 electrodes will be possible without the use of a measuring technique which can differentiate between n- and p-type semi-conductivity and detect the effect of variables, such as H^+ ion concentration and alloy additions, upon them.

II(e) Capacity

Capacity measurements have been employed for several years as a standard technique for determining both the thickness and the protective character of oxide films.

The majority of thickness measurements have been made on compact anodic films. Young[19] has studied the dependence of film capacity and resistance on frequency, and treats the oxide as the dielectric of a leaky condenser of which the metal-oxide interface is one plate and the oxide-electrolyte interface is the other. The thickness of the oxide is given as proportional to the reciprocal of the measured capacity. Other workers who have applied similar methods are Petrocelli[20], Charlesby[21], and Wanklyn and Silvester[22]. In all cases where the capacity of the oxide film was measured, the value was found to be less than about 5μF/cm.^{2}.

A loss in the protective properties of an oxide film has been found by numerous authors[20,22,23] to be accompanied by an increase in the capacity. This is attributed to a reduction in the effective thickness of the dielectric following the formation of defects which arise from factors such as local stresses or dissolution and allow the corrosion environment easier access to the substrate metal. Wanklyn[24] has used capacity measurements

to study the influence of hydrogen on the oxidation rates of zirconium in several media. He finds that the capacity decreases during the initial stages of oxidation, but when cracking commences, however, there is an increase and the capacity finally reaches a constant value independent of the total film thickness. It is believed that in the latter period of oxidation, the greater part of the oxide is fissured, especially on the surface, and the growth rate is controlled by the diffusion of ions across a region where the film is thin and contains no macro-defects.

The measurements reviewed above were made on oxide films not likely to be altered by the application of a few volts of a.c. from a conventional impedance-measuring bridge. In the case of films formed on reactive metals during aqueous corrosion at room-temperature, the formation potential is of the order of -1.0V and the conventional technique would most probably affect the corrosion process. A method developed by Denholm[25] appeared to overcome this difficulty and was employed by Leach[4] to study the capacities of cathodically-formed films on pure uranium and U-12 wt % Molybdenum.

The results showed that the capacity was not significantly influenced by the presence of hydrogen, but that there was an increase with time. Since the

values of capacity, which were of the order of hundreds of microfarads/cm.^{2} and the increase with time both contra-indicated the usual relationship between capacity and thickness, a different interpretation appeared to be necessary. It was proposed that the high measured capacities could be associated with a change in the valence state of the metal ions in the oxide; this would allow the metal-oxide-electrolyte condenser to absorb charge without a change in potential. It was also suggested that, at potentials where high capacities were observed, the capacity was probably directly related to the film thickness. These, and other similar results, are discussed in detail by Isaacs[9].

PART TWO - CORROSION BEHAVIOUR

II(f) Kinetics of Film-growth Processes

A consideration of the relevant thermodynamic data shows that practically no metal is totally unaffected by exposure to aqueous or gaseous environment. The purpose of this section is to review the various theories related to the growth of reaction films with time - with particular reference to oxidation processes. It should be noted that although the fundamental relationships described here were originally conceived to account for atmospheric oxidation, they are equally applicable to aqueous reactions.

The growth of an oxide film is typified, at any given stage during the process, by obedience to a particular time-law. The following laws are the most frequently encountered*: the logarithmic law, the parabolic law, and the linear law. The first two laws are responsible for the formation of protective films while the third is indicative of non-protective kinetics.

The term 'logarithmic law' is a generic classification comprising three algebraically distinct low-temperature processes which lead to exceedingly slow rates in the later stages of film growth. Logarithmic oxidation is controlled by either the inverse logarithmic law, the direct logarithmic law, or the asymptotic law. The inverse and direct laws are considered here. Both are believed to be operative only during the formation of very thin films.

The inverse logarithmic law is representative of a process in which the transport of normally immobile ions results from the existence of a strong electric field. The theoretical derivation of this law is attributed to Cabrera and Mott[26] although modifications

*N.B. The existence of other more complex laws has been observed during the present research. The application of these to the corrosion of uranium will be considered in the Discussion section. No interpretations are provided at this stage.

have been proposed by both Evans[27] and Dewald[28]. The law is expressed mathematically by :-

$$1/y = 1/y_o - K \log \{a(t - t_o) + 1\}$$

where, y is the film thickness at time t; y_o is the film thickness at time t_o (when the steady state has been established); K is a constant and a is a constant of dimensions $(\text{time})^{-1}$.

The direct logarithmic law is operative when the rate-controlling factor in oxidation is the transfer of electrons and not the movement of ions. The explanation of the process is based on an assumption of the electron-tunnel effect[29]. The equation for the direct logarithmic law is :-

$$y = K \log (at + 1)$$

where, y is the film thickness at time t; K is a constant and a is a constant of dimensions $(\text{time})^{-1}$.

The parabolic law governs reactions under conditions where thermal mobility of the ions is assured. Film growth proceeds by uniform ionic diffusion - the driving force arising from metal-oxygen affinity. It is important to note that the effect of the 'field' is directive and not causative (as during inverse logarithmic growth). In its simple form, the parabolic law is expressed as :-

$$y^2 = kt$$

where, y is the film thickness at time t and k is a constant.

The parabolic law is of particular relevance to the growth of semi-conducting films. Wagner[30] has discussed the effect of both the lattice structure and the electrical properties of the oxide on the diffusion rate. He proposes a relationship between these factors which is expressed mathematically in terms of an equation for the parabolic rate constant k. It is assumed that both a potential gradient and a concentration gradient actively influence the diffusion.

A simplified version of the theory has been derived by Hoar and Price[31] who base their model on the concept of a purely electrical gradient.

Linear oxidation differs from logarithmic and parabolic growth in that the thickness of the existing film does not influence the reaction rate. The process may be written as :-

$$y = kt$$

where, y is the film thickness at time t and k is a constant. Obedience to this law, clearly, results in a constant rate of oxidation.

Linear kinetics can result from one of several causes. These may be either environmental effects or

inherent in the film itself. The following causes will be considered: non-coherency of the oxide, extreme mobility of the reactants, breakdown of the oxide, and deficiency of the oxidising phase.

The growth of non-protective films was considered in a classical work by Pilling and Bedworth[32]. It was predicted that the linear law would apply to cases of oxidation which resulted in the formation of a surface-layer of lesser specific volume than that of the parent metal. Under such conditions, coherency of the oxide is not possible and fresh metal surface is continuously exposed to the environment.

The oxidation of barium and calcium has been found to obey the Pilling-Bedworth principle although it is doubtful, in the light of more recent work[33], whether the facts are equally simple for all other metals of similar characteristics. Further, linear kinetics have been observed even in the presence of an intact, coherent surface oxide (when parabolic growth would normally be expected). In such instances, it has been concluded that the diffusion of reactants through the film is extremely rapid as compared to the interfacial reaction rate, and the rate of the process is, therefore, constant and independent of the oxide thickness.

Physical breakdown of a coherent film is often

responsible for a transition from protective to non-protective kinetics[33]. The growth of a parabolic film generally proceeds by the inward diffusion of anions or the outward diffusion of cations. The former process has been found to result in straining of the oxide while the latter encourages the formation of cavities near the metal-oxide interface. Both phenomena can eventually lead to failure of the film and, thereby, to a change in the rate-controlling mechanism.

The effect of temperature on the transition in kinetics requires some comment. An increase in temperature generally hastens the initiation of linear oxidation although certain unexpected observations[34] have indicated that, in some cases, temperature may be responsible for improved plasticity of the oxide film and temporary postponement of failure. This observation is of considerable importance to the present research.

The linear law has been found[33] to govern reactions in which the rate of replenishment of the oxidising-agent is inadequate to the requirements of the film-thickening process. Thus, for example, in atmospheres where the oxygen content is low, the replenishment rate may assume complete control of the process and result in constant oxidation.

For the sake of convenience, oxidation reactions

may be defined as either low-temperature or high-temperature processes. The mutual interdependence of the three main laws governing film growth is summarised below on the basis of this classification.

Low temperature (only slight ionic mobility)	High temperature (ions mobile)
1. Logarithmic growth (general case)	1. Partial logarithmic control (during formation of initial very thin film) ↓ Parabolic growth ↓ Linear growth (if failure of parabolic film occurs).
2. Linear growth (special case – when formation of a coherent oxide is impossible).	2. Linear law (at very high temperatures the other two processes may occur too rapidly to be measured).

II(g) Estimation of Film Thickness

Numerous methods are available for the assessment of film thickness; these can be separated into gravimetric, electrometric, capacity, and optical techniques.

Several indirect procedures are also known although these will not be considered here.

Gravimetric techniques record either weight-increment or weight-loss during the oxidation of a metal. In both cases, sensitive balances are employed to measure the change in weight. If oxidation after the appropriate time produces a weight increase of W grams on a specimen with a surface area of A cms.^{2}, then the thickness of the film in centimetres is given by the expression :

$$\frac{W}{AD} \cdot \frac{M}{M - m}$$

where, D and M are respectively the density and molecular weight of the oxide, and m is the weight of metal in M of oxide.

Specialised methods which enable continuous measurement of weight-gain during the actual process of film growth have been developed, but are suitable only for testing during atmospheric corrosion. When tests are conducted in aqueous environments, removal of the specimen from the cell or autoclave is necessary before drying and weighing.

Weight-loss measurements require either mechanical or chemical removal of the corrosion-product film before weighing of the metal. The loss in weight of the specimen

plotted against time is indicative of the corrosion rate. The majority of the published data for the corrosion of uranium has been accumulated by use of this technique.

Electrometric determinations of film thickness are made by the cathodic reduction of the oxide at a constant current I. The appearance of a potential change signals the completion of reduction. If the time required for the process is t, then the thickness is given by :

$$\frac{JIt}{FAD}$$

where, F is the Faraday number; A is the area of the specimen; J is the equivalent weight of the film-substance, and D is the density of the oxide.

Two obvious disadvantages of this method are that (1) it does not permit continuous measurement of corrosion rate, and (2) it is successful only when applied to easily reducible oxides.

Capacity measurements have already been discussed in sub-section II(e).

Two types of optical technique are commonly employed for the measurement of film thickness. The first depends upon the detection of interference colours and the subsequent assessment of film thickness either

spectrometrically or by comparison with a standard; the second method considers the optical phase-change, induced by the presence of the oxide film, when polarised light is reflected from the face of the specimen.

Both techniques require removal of the specimen from the environment prior to examination. Again, while the polarised light method is perhaps the most accurate for even very thin films, the theoretical basis is complicated and a lengthy mathematical procedure is necessary for the translation of measured values into units of film thickness.

II(h) Evidence for Hydrogen-Induced Corrosion Damage to Uranium.

Certain aspects of the corrosion behaviour of uranium in high-temperature water have been attributed by investigators to the effect of the hydrogen formed as the corrosion product. The purpose of this section is to summarise the evidence, both direct and indirect, which has led to this belief, preparatory to a discussion of the specific models proposed to account for the damage.

Hydrogen analyses of specimens withdrawn periodically from autoclave tests are reported by Burkart[1] to have revealed that the hydrogen concentration was a function of the exposure time. An increase in test

temperature, accelerating the formation of hydrogen, decreased the time to 'breakaway'. Further analyses showed that the hydrogen concentration of the metal was directly related to the amount of corrosion (measured by a weight-loss method) which had taken place.

The same author[1] has observed that the introduction of hydrogen into the metal, prior to testing, either in an aqueous electrolytic cell or by ionic bombardment in a discharge tube also increased the corrosion rate.

The majority of methods which have found application in minimising the corrosion damage to uranium can be interpreted as owing their success to the prevention of hydrogen-induced effects. It is found that alterations to the metal or environment which tend to decrease the activity of hydrogen in the oxide are likely to result in lower rates of corrosion. For instance, it was predicted that the rate of hydrogen pick-up would be reduced by using low-overvoltage metals such as platinum or nickel to provide points for easy evolution of the gas. It has been found[1] that such elements, whether alloyed to the metal or dissolved in the solution as salts, do, in fact, reduce hydrogen accumulation in the metal by decreasing the concentration of protons at the oxide-electrolyte interface. In the

same context, however, it is significant that although the presence of cathodic depolarisers, such as oxygen, in the solution encourages the formation of protective films, it does not always directly influence hydrogen pick-up. When conditions are such that electrons are not available at the oxide-electrolyte interface, protons rather than hydrogen atoms are abundant and the oxygen depolarisation reaction is not effective.

The service life of uranium can be prolonged by heat treatments which induce a phase transformation to a lattice with a greater solubility for hydrogen[1,35,36]. The dissolution of the gas in the metal decreases the activity of hydrogen within the oxide and at the metal-oxide interface. Additions of alloying constituents are necessary in order to retain the high solubility structure of uranium at low temperatures. Both the heat treatments and the alloying requirements will be discussed in greater detail in the next sub-section.

It should be noted that the evidence collected by early workers and presented here was based mainly on quantitative measurements of corrosion rate. The qualitative approach was neglected in comparison, and, for example, no attempt was made to consider the effect of hydrogen on the kinetics of the corrosion mechanism.

II(i) Structural Properties of Uranium and the Effect of Alloying.

The allotropic crystal structures normally encountered in uranium and uranium alloys are (1) the alpha phase (orthorhombic) which usually exists at temperatures below about 660°C, (2) the beta phase (complex tetragonal) limited to the temperature range 660°-770°C, and (3) the gamma phase (BCC) which persists above 770°C to the melting point at 1130°C. Some properties of the two phases, alpha and gamma, of chief interest to this research, are reviewed below.

The gamma-structure has good resistance to hydrogen-induced corrosion. An important reason for this resistance is the relatively high hydrogen-solubility of the gamma lattice. This property results in the dissolution within the metal of much hydrogen which would otherwise have been available to take part in the corrosion-attack. The solubility in γ -uranium at 650°F is given as 19.7 ppm compared to a figure of 0.34 ppm which is the calculated hydrogen-solubility in alpha-uranium[1]. (Other sources[37] differ in the values which are assigned but there is general agreement that solubility in the gamma phase

is much greater). The retention at room-temperature of the resistant γ-phase is dependent upon two requirements: rapid quenching from the gamma region and the use of stabilising alloy elements.

The alpha-structure is characteristic of pure uranium at room-temperature. However, it may be encountered in alloys when the concentration of the additions is not sufficient to retain the gamma-structure, and, in special cases, as the relatively corrosion-resistant alpha prime phase (of similar structure) produced by the martensitic transformation of gamma uranium.

The choice of alloying elements that are used with uranium is, in view of the specialised nature of its employment, restricted to a small number which possess a low cross-section for neutron capture. Three metals commonly employed as alloy constituents are molybdenum, niobium and zirconium.

The chief use of molybdenum is in its capacity as a gamma stabiliser. The usual minimum addition for this purpose is approximately six weight percent, although alloys containing less molybdenum can retain the gamma-phase if quenched extremely rapidly. Optimum corrosion-resistance is obtained with U-12 wt % molybdenum[1]. It is interesting that, in all cases, annealing at temperatures between 300°-400°C, and the

consequent transformation to the alpha prime phase, is beneficial and prolongs the service life[1].

The incorporation of molybdenum oxide into the urania lattice might also exert a beneficial influence on the corrosion properties, but the author is not aware of any published evidence concerning this.

Uranium containing more than six weight percent of niobium and water-quenched from above 800°C is found to retain the gamma-phase at room-temperature and show good corrosion properties[1]. Smaller alloying additions lead to the formation of the martensitic alpha prime structure which, in this case, is only moderately resistant. It is believed that, in small quantities, niobium is beneficial only as a hydrogen getter and a grain-refiner[38]. In the latter role, it is responsible for the optimum distribution of the alpha prime phase.

Ternary alloys containing both molybdenum and niobium also display good corrosion properties. Prolonged service life is obtained with alloys containing from 10-12 wt % molybdenum and 1.5-2.5 wt % niobium[1]. Gamma-quenching is a pre-requisite for resistance; annealing at lower temperatures is detrimental.

Zirconium is a less effective gamma-stabiliser than either niobium or molybdenum. γ-quenched alloys containing as much as 40 wt % zirconium still retain

sufficient alpha uranium, as a continuous network in the gamma matrix, to cause rapid failure in water at high temperatures (315°C.)[6,39]. Alloys in the range 40-70 wt % zirconium are more resistant. The corrosion behaviour of these alloys is determined by the amount and distribution of the relatively corrosion-resistant delta-phase (UZr s.s.). However, the service life of alloys in the upper portion of this composition range is reduced by the partial transformation of the gamma phase, at relatively low temperatures, to a mixture of alpha zirconium plus the UZr solid solution. Optimum resistance is obtained with gamma-quenched U- 50 wt % zirconium[40].

The uranium-rich side of the U-Zr phase diagram is shown in Fig. 9.[41] Low zirconium alloys (0-10 wt % zirconium) are not found to retain any gamma-phase at room-temperature[6]. Rapid quenching from the gamma region leads to the formation of either alpha uranium plus small amounts of UZr (in the lower half of the composition range) or alpha prime phase plus UZr (in the upper half). The latter mixture is fairly resistant to aqueous corrosion at low temperatures (~100°C). A detailed review of the corrosion behaviour of low Zr alloys follows in a later section.

II(j) Models for Hydrogen-induced Damage to Uranium and its Alloys

Extensive research into the corrosion properties of uranium has evolved no entirely convincing theory to account for all aspects of the process. However, several plausible mechanisms have been proposed which allow an interpretation of the general behaviour in terms of hydride formation, local stresses in the metal, lattice mismatch, etc. Some of these are reviewed below.

The first important development in the field of uranium corrosion must be credited to Draley and Ruther[3]. They proposed that the formation of a hydride at the metal-oxide interface could be one possible explanation for the corrosion damage to uranium (see sub-section I(b)), and attributed the following harmful effects to the compound: (1) disruption of the metal to oxide bonding mechanism, and (2) recrystallisation of the oxide with the subsequent formation of a granular, non-adherent material. Further, Draley and Ruther suggested that the hydride could be held indirectly responsible for an increase in the corrosion rate by virtue of its reaction with water to form UO_2 and liberate hydrogen, thereby providing an ample supply of the gas for the continuation of the corrosion process.

Draley's argument is based on observations of the presence of UH_3 in the corrosion-product oxide formed

during prolonged testing at high temperatures. Under such conditions, the protective film is subject to local breakdown which becomes generalised with time. It is considered that the points of breakdown lie immediately above areas where corrosion-product hydrogen has combined with the metal to form hydride.

The validity of the hydride theory is debatable. Although the phase is thermodynamically stable at fairly high temperatures, several workers have been unable to verify its presence after corrosion tests. Burkart[1] reports evidence both for and against hydride formation and concludes, for the particular case of alpha uranium, that -

> "the corrosion rate is primarily determined by the formation and subsequent oxidation of a non-adherent hydride layer".

However, a detailed study of the corrosion behaviour of gamma-phase alloys has led him to propose a modification to the above theory. Burkart considers that, in the case of these alloys, the hydrogen released by the corrosion reaction at high temperatures, rather than forming a stable UH_3 phase, dissolves (at least in part) in the base metal, where, when the concentration exceeds ~20 ppm, a metastable hydride, of formula approximating UH, is precipitated some distance below the surface.

Two properties of the phase are considered

responsible for accelerating the attack. First, UH is a hard, acicular material which can cause local stresses in the metal, and second, it has a higher corrosion rate than the alloy, and this can lead to preferential attack. Both effects are able to cause failure of the metal.

A totally different explanatory model has been proposed by Chirigos[42]. The lack of compelling evidence that hydrogen accumulation in the metal reduced the service life of certain gamma-phase alloys led him to a consideration of the role of the corrosion-product oxide on the rate of attack. Chirigos suggests that two properties of the reaction film are likely to influence the corrosion process: (1) high compressive stresses resulting from conversion of the metal to an oxide having a lower density, and (2) coherency stresses resulting from the discrepancy between the lattice parameters of the two materials.

The strains which arise during the oxidation of a metal are determined by the percentage increase in the volume ratio of oxide to metal, and the compressibility of the oxide. As long as the oxide remains adherent, the compressive stresses must be balanced by equally large tensile stresses in the metal. Cubiciotti[43] has estimated the approximate strains produced during oxide growth on

several metals; the value calculated for uranium is exceptionally high. Waber[6] has shown that a thin foil of uranium can be deformed significantly by the oxide film formed even at temperatures as low as 75°C.

The influence of lattice parameter mismatch has been demonstrated to a limited extent for some U-Nb-Zr ternary alloys. Chirigos[42] has made use of a theory of oriented overgrowths in his interpretation. It is pointed out that, if the lattice parameters of the base and oxide differ by 9 to 15 percent, the mating plane will include a large number of dislocations. Epitaxy is not expected if the difference exceeds 15 percent. Chirigos has calculated a lattice mismatch of 11 percent between a U-10 wt % niobium alloy and the reaction film.

The above theory assumes that the stresses arising from either of the two effects described can result in failure of the metal. However, in view of the relative thicknesses of the coherent oxide layer and the underlying metal, the first effect is unlikely to be sufficient cause for serious damage. Again, the second explanation appears doubtful since it has not always been found possible to correlate the measured corrosion rate of various members of an alloy series to the degree of parameter mismatch.

II(k) Resumé of Data for the Corrosion of Uranium Alloys containing up to 10 wt % Zirconium

The data relating to the aqueous corrosion of uranium alloys at low temperatures are poorly represented in the literature. A survey[35] of the corrosion resistance of uranium alloys in the composition range 0-100 wt % zirconium produced the generalisation that at least 20 wt % zirconium was required for resistance when the alloy was alpha-annealed (furnace cooled from 600°C.) while only 5 or 6 wt % zirconium was necessary when the alloy was gamma-quenched.

It is reported[35] that alloys containing two or three weight percent zirconium developed porous oxide films in boiling distilled water and corroded rapidly. In boiling water containing oxygen some parts of the alloy surface formed protective films, but these broke down upon continuous exposure.

Gamma-quenched five weight percent alloys showed good corrosion resistance at 100°C and formed adherent tarnish films, but only when oxygen was present in the water. Tests in boiling water saturated with several ratios of hydrogen to oxygen showed that the maximum ratio to which the alloy was resistant appeared to lie between 25 : 1 and 35 : 1. In the total absence of oxygen these alloys failed within 24 hours in boiling water and in

three weeks in water at 80°C.

The saturation of the test water by gases such as hydrogen or nitrogen was used solely as a method for the elimination of oxygen. Neither gas was found to have a significant effect of its own on the corrosion behaviour. The addition of 7.5 wt % zirconium appeared to be the minimum requirement for an alloy resistant to rapid failure in either hydrogen - or nitrogen - saturated water at 100°C. The films formed on U - 10 wt % zirconium (gamma-quenched) were found to resist breakdown for at least three months under such conditions.

It is clear that the addition to uranium of more than the minimum amount of zirconium reduces the apparent sensitivity to hydrogen-induced corrosion. Draley and co-workers[38] postulate three mechanisms to account for the protection given to the base metal by alloy additions of zirconium of up to 10 wt %.

(1) That the incorporation of zirconia into the urania lattice aids the formation of an inherently more protective film, and also hinders the diffusion of hydrogen through it. (The presence of ZrO_2 in the oxides formed on these alloys has been observed to reduce UO_2 lattice parameters).

(2) That metallic zirconium in the surface layers of the uranium behaves as a getter and, thus, increases the solubility for hydrogen.

(3) That alloying with zirconium aids the formation of the alpha prime phase on quenching from the gamma-region, and the increase in lattice parameters (compared with those of normal α-U) which accompanies this transition reduces the effective resistance of the metal to hydrogen entry.

However, there is little reference in the literature to the effect of zirconium on the protective properties of the surface oxide film. The rate of oxide growth depends on the ionic flux through the film, and this may be influenced independently by changes in the diffusion constants of the film or changes in the diffusion distance, both of which can be caused by the addition of an alloying constituent.

II(1) Conclusions

It is clear from the literature that much of the understanding of the corrosion mechanisms of uranium was influenced by considerations of the mechanical aspects of the attack. The early American work[1,3,38,42] accentuated the importance of phenomena such as physical breakdown of the oxide and the discontinuous failure of the metal due to internal stresses.

More recent work[4,9] concerned with the electrode characteristics of uranium, suggested that the rate-

controlling steps in the corrosion process may occur within the oxide which is formed and that damage probably results from changes in the electrical properties of the protective film rather than from mechanical failure. The possibility of a relationship between the conductivity of the oxide and the corrosion rate was proposed. However, although the theoretical basis has been laid by these studies, there appeared to be no factual evidence available in the literature which could establish such changes in the properties of the protective film as would result from additions of hydrogen and/or other alloying constituents and, thus, lead to a higher or lower rate of corrosion.

Bearing in mind the lack of qualitative data, it was decided to investigate the effect of alloying content and several other variables both on the electrochemical characteristics of the oxide and the kinetics of film growth. Two main experimental techniques were selected; the one, designed to measure changes in the properties of an oxide-covered electrode during corrosion, and, the other, to measure the rate of the corrosion. The selection of both techniques was determined by the fulfilment of the following requirements: (1) The ability to control the test conditions - in particular the hydrogen activity at the specimen surface. The

reason for this is made clear later. (2) The ability to make the necessary measurements without removal of the specimen from the environment. It is believed that an interruption of the corrosion process would be likely to influence the subsequent rate.

The materials examined in the present research were: U-12 wt % molybdenum and the alloy series, uranium, U-5 wt % zirconium and U-10 wt % zirconium. The molybdenum alloy was used only in preliminary studies. The zirconium series, which was examined in detail, was chosen since it was known from the data that identifiable changes in corrosion behaviour would occur within reasonably short periods of time at test temperatures below the boiling-point of water. The documentation of previous work and the difficulties associated with making electrochemical measurements at temperatures above 100°C both contributed towards the final selection of these materials. The inclusion of the ten weight-percent alloy provided an opportunity for comparing the properties of a resistant alloy with those of less resistant materials under identical conditions.

SECTION III

EXPERIMENTAL TECHNIQUES AND PROCEDURE

SECTION III

EXPERIMENTAL TECHNIQUES AND PROCEDURE

The experimental methods employed in this research will be considered separately under the broad headings : Electrode Properties and Corrosion Behaviour. The first section will be devoted to an examination of the various equipment and procedures necessary to the measurement of the hydrogen overpotential and the capacity and conductivity of U/UO_2 cathodes. The second section will consider the optical device and techniques developed for the estimation of corrosion rates. A simple arrangement which enabled simultaneous measurement of both the corrosion rate and the capacity and conductivity of the electrode will also be described in this section.

PART ONE - ELECTRODE PROPERTIES

III(a) Hydrogen Overpotential Measurements

The hydrogen overpotential characteristics were investigated by two separate methods. In the initial stages of the research, a conventional variable-resistor technique was employed. This was discarded later in favour of a potentiostatic method which was used in conjunction with an impedance bridge and permitted simultaneous measurement of both the overpotential and the capacity and conductivity of the electrode. This technique enabled accurate correlation of the results and the observation of certain relationships which might otherwise have been obscured.

Some variables which were included in the preliminary studies were not repeated later. Hence, neither the experimental details involved nor the results obtained will be considered in full within this thesis.

(i) Variable-Resistor Method

Overpotential tests involve a measurement of the potential difference between the polarised cathode and a standard electrode when a given current is flowing between the cathode and the anode. Fig. 10 shows in scheme the circuit employed in the variable-resistor technique of measurement. The potential difference between the test electrode and the reference electrode

(standard calomel ½-cell) was recorded by a valve-voltmeter with an input impedance of 10^{13} ohms (E.I.L. pH meter Model 23A). The current passing between the test electrode and the auxiliary anode of platinum foil was measured by a sensitive galvanometer ('Scalamp' Pye 7893/S) with a built-in shunt. The high impedance of the valve-voltmeter restricted the current drain from the cell, and accurate measurements were, therefore, possible even at voltages where the resultant current density was very low.

During measurements at high current values, the potential of the test electrode was adjusted by means of the two variable resistors A and B; fine adjustments were made with the 6 ohm resistor B. Measurements of potential at equivalent current values below $\sim 100\mu A$, however, required a different method of control. Depression of switch C altered the circuit to a potentiometric system which was able to fulfil the necessary requirement.

The technique described above was used to examine the effect on the overpotential of the following environmental variables :-

(1) Gas content of the electrolyte: oxygen-free, air-saturated and oxygen-saturated.

(2) Temperature of the electrolyte: 2°C, 18°C and 80°C.

(3) pH of the electrolyte: 1, 2.4, 9.7 and 13.

Fig. 11 shows the cell employed for the measurement of overpotential in oxygen-free solutions at room-temperature. The anode and cathode compartments are connected by a bridge containing the electrolyte. Isolation of the auxiliary electrode was necessary in order to prevent depolarisation of the reaction by the anodically-formed oxygen. The probe P is connected to the reference cell by a salt-bridge and is allowed to rest very near the surface of the cathode. This device minimises the ohmic pseudo-overpotential caused by the IR drop in the electrolyte. Provision is made for the bubbling of gas into the solution. In this case, oxygen-free nitrogen was used to reduce the concentration of oxygen in the electrolyte to a minimum.

Separation of the two electrodes was unnecessary during measurements in either air-saturated or oxygen-saturated solutions, and these tests were conducted in a single compartment. A water suction-pump was used to induce a flow of air through the electrolyte; cylinder oxygen was introduced via the gas inlet.

Tests at temperatures other than room-temperature were again conducted in single compartments. The low-temperature and high-temperature conditions were achieved

by the use of an ice bath and a heating mantle respectively. Frequent thermometer readings were taken, and overpotential measurements were commenced only after a constant value of temperature had been attained.

The compositions of the various electrolytes used is given in the list below :

pH 1	IN HCl
pH 2.4	Na_2HPO_4 + citric acid (Buffer)
pH 9.7	0.2N Na_2CO_3 + 0.2N $NaHCO_3$ (")
pH 13	0.1N NaOH

All solutions were prepared from distilled water and Analar grade reagents.

The test specimen was a U-12 wt % molybdenum alloy which had been arc-cast and certified as 99.95 pure (A.E.R.E. Harwell). Before examination, it was given the following heat-treatment: The specimen was enclosed in a tantalum foil envelope and placed in a silica tube which was then evacuated and sealed. Strips of zirconium foil contained in a side-extension of the tube provided a getter for any remaining air. The specimen was heated in a furnace at 1000°C for seven days and then water-quenched from this temperature.

After the heat-treatment, the specimen was cut and mounted in a cold-setting synthetic resin (Ciba Araldite) to fit the socket at the base of the test cell.

A brass screw provided the electrical contact to the back of the specimen.

The experimental procedure employed is given below:-

(1) The specimen is wet-polished on emery papers (down to grade 600), and is fitted to the cell.

(2) The cell is filled with electrolyte and flushed with the appropriate gas for approximately one hour.

(3) Measurements are commenced as near E_H= OV as possible; the potential is decreased in steps of about 100 mV. Readings of potential and current are taken after one minute at a given potential.

(4) At very negative potentials bubble formation makes accurate readings difficult. The procedure is reversed and measurements are made at intervals of increasing potential.

(5) The specimen is removed from the cell and its surface area is measured with a travelling microscope.

(6) E_H is plotted against the logarithm of current density per cm.^{2} (see Fig.6). $\therefore E_H = -E + E_{SCE}$ where, E_H is the potential with respect to the hydrogen scale, E is the measured potential, and E_{SCE} is the potential of the reference electrode on the hydrogen scale (+0.250V).

(ii) Potentiostatic Method

The procedure followed during potentiostatic measurements was essentially the same as that given above. Modifications were necessary only to the electrical circuit and the construction of the test cell.

The modified circuit is complex and cannot be separated from that of the impedance bridge; it will be described in the next sub-section. The potentiostat[44,45] (A.E.R.E. type 1465A) is shown schematically in Fig.12. It can be seen from the figure that electrical connection was made to the anode and to a silver-silver chloride reference electrode. This electrode was prepared by immersing a silver strip in concentrated hydrochloric acid.

The potentiostat was used to control the voltage by impressing a current on the specimen. The resulting voltage was measured, with reference to a standard calomel half-cell, by a valve-voltmeter. The current was measured by a galvanometer connected to the terminals A and B of the potentiostat.

Measurements were conducted in a single compartment (see sub-section III(b). The cell was adapted to provide for the presence in the solution of two reference electrodes (Ag/AgCl and S.C.E.) and a tubular specimen holder.

The materials examined were natural uranium, uranium- 5 wt.% zirconium and uranium- 10 wt.% zirconium. The natural uranium was supplied by A.E.R.E. and certified as 99.95% pure (impurity analysis - O = 40 ppm, N = 10 ppm, C = 30 ppm, Si = 8 ppm, Fe = variable 10-90 ppm, Al = 3 ppm). It was not subjected to a preliminary heat-treatment since there is only one lattice structure (α) which is possible for the pure metal. The alloys, prepared from 99.95% pure uranium and low hafnium 99.9% pure zirconium (Van Arkel), were supplied in the arc-cast condition and, after receiving the same heat-treatment as the uranium-12 wt.% molybdenum alloy, were water-quenched from the γ-temperature region.

After heat-treatment, the specimens were cut and spot-welded to a tantalum strip which was in turn spot-welded to a thin brass rod; the whole was then mounted with Araldite in a glass tube. Electrical contact was made to the rod.

Measurements were made at room-temperature in either oxygen-free or oxygen-saturated solutions of pH 9.7 and the results plotted as current density vs. E_{HA}.

III(b) Impedance Measurements

The details of the technique for measuring capacity and conductivity have been reported previously[4, 9, 25], and some results have been published. It is

intended, therefore, to describe only the principles of the method in this sub-section.

The schematic diagram of the equipment is shown in Fig. 13. A large square wave a.c. signal (about 100V RMS) is applied across two networks of which the first consists of a large resistance in series with the cell containing the test electrode, and the second of a large resistance in series with an analogue circuit composed of a capacity and resistance in parallel. The purpose of the series resistance is, effectively, to convert the voltage source to a current source.

The response of the test electrode to the square wave current is measured by the Ag/AgCl reference electrode, and balanced, in both magnitude and phase, against the voltage developed across the analogue. Both responses are amplified and compared on a cathode ray oscilloscope. Balance which is achieved by varying the capacity and resistance of the analogue is indicated on the CRO by a straight line inclined at an angle of 45^{o}.

The equipment was built to fulfil the following requirements :-

(1) The ability to achieve a rapid balance. Prolonged periods, especially at negative potentials, are likely to influence the properties of the electrode.

(2) The ability to polarise the electrode to a given d.c. potential.

(3) The ability to measure values of resistance between 10^3 and 10^6 ohms, and values of capacity ranging from a few microfarads to several hundreds.

The experimental procedure followed during the impedance measurements was essentially the same as that for the potentiostated overpotential tests. The materials and solutions used were common to both types of experiment. During measurement, the capacity and conductivity of the electrode were balanced at each value of the polarising potential. Results were plotted in microfarads/cm.^{2} and ohms^{-1}/cm.^{2} vs. E_{HA}.

PART TWO - CORROSION BEHAVIOUR

III(c) Corrosion Rate Measurements

The equipment developed for the estimation of corrosion rates has been adapted from a previous design[46,47] with some minor alterations. The operating principle of the technique involves a continuous measurement of the intensity of light reflected from a metal corroding in an aqueous environment, and calculation of film thickness by comparison with the intensity reflected from a clean surface. The growth of an optically-

absorbent film results in a continuous reduction of reflected intensity; the relationship between light intensity and thickness of film is given by one of the following two expressions :-

(1) When monochromatic light is used :

$$(y + x) = (\frac{2r - 1}{2})(\frac{\lambda}{2n_1 \text{Cos } \emptyset_1})$$

where, y is the thickness of the oxide at which minima occurs in the reflectivity; x is a constant which allows for the reflection phase changes; r = 1,2,3 etc.; λ is the wavelength of the light; $\emptyset_1$ is the angle of refraction, and n_1 is the refractive index of the oxide at wavelength λ.

(2) When 'white' light is used :

$$I = I_o \, e^{-2 \theta y}$$

where, I_o is the intensity of light reflected from the clean metal surface; I is the reflected intensity when the thickness of the oxide is y, and θ is the optical absorption coefficient of the oxide.

The equipment is shown diagrammatically in Fig. 14. Light from a high pressure mercury lamp S (Phillips HPK/125) is focussed by a condensing lens on the mirror M which is mounted inside the main tube A at an angle of about 45°. It is then reflected as a divergent beam through the lens L mounted in the front of the test cell. The main tube is adjustable in length and the

distance from M to L has previously been made equal to the focal length of the lens; the transmitted beam is, therefore, rendered parallel before reflection from the specimen which is positioned immediately behind the lens. After passage through the tube, the intensity of the reflected light is measured by the photoelectric cell P_1.

When required, monochromatic light was obtained by the interposition of a filter (Ilford type 808) between the light source and the condensing lens. The filter was chosen to transmit the high intensity yellow doublet lines (5771-5791 Å) from the spectrum of the mercury lamp.

Photocurrents caused by extraneous light or light reflected from surfaces other than that of the specimen were 'backed-off' by a monitor ~~as a standard~~ photocell P_2 which was connected in opposition to P_1 and also acted as a standard for light intensity. The counter-current was generated by light from the source transmitted through a variable iris-diaphragm to the photocell P_2. The diaphragm, mounted within the secondary tube B, served as course control for the back-off current. Fine control was provided by the potentiometer R_2 included in the measuring circuit.

The measuring circuit is shown in Fig. 15. The function of the potentiometer R_2 has already been mentioned. Optimum adjustment for extraneous currents

was indicated by zero deflection of the galvanometer G. The potentiometer R_1 served to adjust the photocurrent, developed by the initial reflection from the polished specimen, to give full-scale deflection on the 0 - 1 mV scale of the recorder (Cambridge Electronic Recorder Model D.E.). During the test, the decrease in intensity due to film growth was converted to voltage and automatically recorded. The ripple imposed on the light source and, hence, on the photocurrent by the 50 cycle mains current was found to decrease the stability of the recorder. The capacitors, shown connected in parallel with the galvanometer, provided a damping circuit which reduced this effect.

Especial care was taken in the construction of the equipment to prevent leakage of light from external sources. All interior surfaces were finished in matt-black in order to decrease the possibility of interference from stray reflections.

The two photocells (Megatron type B) were specified to have a linear response over the range of intensities used. The light source was stabilised by the incorporation of a constant voltage transformer (Advance Components Ltd. type M.T. 267A) in the mains circuit. Experiment showed that a 5% fluctuation in mains voltage resulted in a change of less than 1% in the light intensity.

The test cell (Fig. 16) was fabricated from a black, sheet plastic (¼" thick). The sheets were cut to the required dimensions and the joints were first cemented, and then bolted together to provide a rigid, leak-proof structure. The lens was cemented in position with Araldite. The cell was mounted on a table with adjustable three-point suspension which enabled optimum alignment of the cell with the aperture of tube A.

The equipment described above was employed to examine the effect on the corrosion behaviour of the following variables: polarisation, alloy composition, gas-content of the electrolyte, pH of the electrolyte, and temperature of the electrolyte.

The majority of corrosion rate tests was made potentiostatically at cathodic potentials. The potential was measured, with respect to a calomel reference electrode, by a valve-voltmeter. A potentiostatic technique was employed since it permitted a qualitative estimation of the effect on the corrosion rate of corrosion-product hydrogen (hydrogen activity can be calculated if the impressed potential is known (see sub-section II(d)). Free-corrosion measurements do not allow a similar estimation. Fig. 17 illustrates some time vs. potential curves for freely-corroding uranium; it is clear that the potential is unstable in all cases

and varies considerably with time.

The materials examined (pure uranium, uranium- 5 wt % zirconium, uranium- 10 wt % zirconium) by the optical technique were, except for size, identical in all respects to the specimens tested with the impedance bridge. Each specimen was approximately 1 cm. in diameter, and was mounted at one end of a glass tube of previously determined length (see Fig. 16). Care was taken to ensure that the tube, when inserted in the cell, would position the specimen directly behind and parallel to the lens. Electrical contact to the metal was provided by the same method as used in the preparation of the impedance test electrodes.

Measurements were conducted in either oxygen-free or oxygen-saturated solutions. A fine dispersion of the appropriate gas (oxygen-free nitrogen or pure oxygen) was obtained by using a capillary inlet in the solution (Fig. 16).

The compositions of the various electrolytes used in corrosion rate measurements are given in the list below:-

pH 5.4	0.1 N K_2SO_4
pH 9.7	0.2 N Na_2CO_3 + 0.2N $NaHCO_3$
pH 11.6	0.1 N Na_2CO_3
pH 13	0.1 N NaOH

The choice of these solutions was influenced by the pH-potential diagram (Fig. 7), which shows that uranium oxides are stable at these values of pH over a wide range of potentials.

All solutions were prepared from distilled water and Analar grade reagents.

The influence of solution temperature on the corrosion rate was investigated. Measurements were made at various impressed potentials in the temperature range 30° - 60°C. A special test cell was constructed from a plastic (polypropylene) capable of withstanding temperatures as high as 125°C. without loss of rigidity. In addition to the features incorporated in the room-temperature cell, provision was made for the use of an immersion heater, a temperature-controlling thermometer and a reflux condenser.

The heater was especially prepared to fit the bottom of the cell by bending a silica tube which contained a heating-coil and powdered alumina. Power was supplied through a variac and the output, during operation, was maintained at approximately 100 watts. The thermometer (Electromethods) was positioned at one inch from the specimen, and could be set to control at any temperature between 0° and 100°C. within certified limits of accuracy $\pm$ 0.1°C. A relay, activated by the thermometer, switched the heater circuit.

The experimental procedure followed during both room-temperature and high-temperature tests is given below:

(1) The cell is filled with electrolyte and flushed with the appropriate gas for one hour. Electrolytes are allowed to stabilise at the required temperature for half an hour.

(2) Extraneous light is backed off with potentiometer R_2.

(3) The specimen is wet-polished to a mirror-finish on emery papers down to grade 600 and then washed and dried.*

(4) The specimen is inserted in the cell within a half minute of drying and adjusted to give maximum reflection of the incident light beam on to the photocell P_1 (this is indicated by maximum deflection of the galvanometer).

*N.B. Wet polishing on abrasive papers is reported[36] to be a satisfactory method of surface preparation for corrosion rate tests on uranium and uranium alloys. Good reproducibility is obtained when specimens are tested shortly after polishing. An examination was made, during the present work, to determine whether air-exposure of the specimen, prior to testing, affected the subsequent corrosion rate. The results indicated that exposure times as long as 20 minutes produced no significant change in the initial rate of corrosion.

(5) Adjustment is made with potentiometer R_1 to give full-scale deflection of the recorder.

(6) The potential of the specimen is adjusted to the required value with the potentiostat (free-corrosion measurements naturally, do not require this step).

(7) The test is continued until a ten-fold decrease in the reflected light intensity is indicated by a recorder reading of 0.1 mV on the 0 -1 mV scale.

III(d) Simultaneous Measurement of Impedance and Corrosion Rate

An attempt was made to establish whether a change in the corrosion kinetics of uranium involved a corresponding change in the electrode properties. A number of tests was conducted in which the impedance of the specimen was measured during corrosion at fixed cathodic potentials.

Connection was made between the impedance bridge (described previously) and the corrosion cell by replacing, in the cell, the Luggin capillary from the calomel electrode by the silver-silver chloride reference electrode from the bridge. The reference electrode was used to measure the response of the specimen to the applied signal. Polarisation of the specimen was induced by the potentiostat incorporated in the bridge.

Measurements of capacity and conductivity were made at intervals of approximately fifteen minutes during the period of recorded corrosion.

All tests were conducted on pure uranium in oxygen-free solutions of pH 5.4.

SECTION IV

R E S U L T S

SECTION IV - RESULTS

PART ONE ... ELECTRODE PROPERTIES

IV(a) Overpotential Measurements

Measurements of the overpotential on uranium-12 wt % molybdenum electrodes have established the existence of two transitions in the hydrogen evolution kinetics. The first transition results in a rapid increase in current density indicating easier kinetics while the second, occurring at more negative potentials, has the opposite effect and involves a return to a higher overpotential. All curves obtained exhibited a marked hysteresis similar to that described by Losco[8].

Fig. 18 shows the effect of solution pH on the overpotential. It is clear that, although the general shape of the curve remains unaltered by changes in pH, increasing acidity causes the transitions to occur at more positive potentials.

The influence of solution temperature on the overpotential of the alloy can be seen from Fig. 19. It is interesting that an increase in temperature and a decrease in pH both appear to have a similar effect on the transitions. Again, the shape of the curves seems to be virtually independent of the test conditions.

Fig. 20 illustrates overpotential curves obtained

for measurements in solutions of varying oxygen-content. An increase in oxygen concentration has two apparent effects: (1) it allows higher current densities to be achieved at potentials down to about -1.4 V E_H (indicating an easier discharge mechanism), and (2) tends to eliminate the two transitions to give an almost straight Tafel line.

Although a quantitative estimation was beyond the limits of accuracy of the measuring technique, it can be seen from Figs. 18 to 20 that the hysteresis in the curves was unaffected by changes in the environment. Fig. 21 shows that a similar hysteresis is common to the overpotential curves obtained for some other oxide-covered metals (including aluminium, see sub-section II(c)).

IV(b) Simultaneous Electrode Measurements

Simultaneous measurements of both the hydrogen overpotential and the impedance of pure uranium, uranium -5 wt % zirconium and uranium-10 wt % zirconium electrodes were made potentiostatically in solutions of pH 9.7.

Figs. 22 to 24 record the results obtained in oxygen-free solutions. The following observations are of interest:-

(1) The rapid increase in current density at negative potentials can be compared to the similar increase in the conductivity. Addition of the alloying constituent appears to lower the potential at which the transition

in kinetics occurs.

(2) Hysteresis is common to measurements of both overpotential and impedance. There is a tendency at intermediate potentials for the effect to be of the opposite type to that normally encountered.

(3) The unusually large values of capacity measured at potentials above about E_{HA} = 0 V can be compared to the high conductivity of the oxide at corresponding potentials.

(4) The effect of increasing the zirconium content of the specimens is to decrease the capacities and conductivities of the oxides formed, to lower the potentials at which the capacity and conductivity peaks occur, and to increase the overpotential.

Fig. 25 illustrates for one specimen (pure uranium) the general effect on the electrode properties of oxygen additions to the electrolyte. Several significant differences between these results and results obtained in oxygen-free solutions have been identified; some are listed below:-

(1) Higher values of capacity and conductivity are obtained.

(2) Higher values of current density are obtained at intermediate potentials.

(3) A significant change in the kinetics of the hydrogen discharge reaction is found to occur near the hydrogen evolution potential (E_{HA} = 0 V). This is shown

by the sharp "break" in the slope of the Tafel line.

(4) The interrelated "breaks" in the conductivity and overpotential curves occur at more negative potentials, and appear to be less clearly defined.

A number of tests was conducted in which the impedance and overpotential were measured independently in solutions of pH other than 9.7. The results were similar in character to those obtained during simultaneous measurements, but precise correlation between overpotential and impedance was difficult due to slight differences in the experimental conditions. Since the main intention here is to show the existence of such relationships, these independent measurements are not reported.

PART TWO ... CORROSION BEHAVIOUR

IV(c) Technique

The type of result obtained with the optical equipment was determined by the nature of the incident light beam, following the two intensity-thickness relationships stated earlier. If the incident light were rendered monochromatic with the optical filter, interference maxima and minima were obtained superimposed on an absorption curve while 'white' light measurements gave a simple absorption curve. Records made by both techniques are shown in Figs. 26a and 26b.

The monochromatic-light technique involved no assumption about the absorption coefficient of the oxide, and could be employed to give accurate measurements of relative film thickness. Calculation of absolute thicknesses required knowledge of the refractive index of the oxide. However, the relatively low intensity of the monochromatic lines from the mercury light source and the high optical absorption coefficient of uranium oxides precluded the measurement of all but thin films. Furthermore, it was difficult to obtain sufficient points with this technique for an accurate representation of the different growth-processes since only the maxima and minima could be plotted.

The second technique, due to the greater light intensities available, could be used to measure much thicker films, but assumed an absorption coefficient which is independent of thickness. Over the range of oxide thicknesses where both the first and second methods of measurement were applicable, the results were, within the experimental error, the same.

The results reported in this thesis are derived from 'white' light measurements. If, in the expression $I = I_o e^{-2 \theta y}$, y is considered to be some function of time t, then

$$I = I_o e^{-2 \theta f(t)}$$

and,

$$\log_e I - \log_e I_o = 2\theta f(t)$$

A plot of ($\log I_o - \log I$) vs. t gives relative film thickness as a function of time.

The 'white' light technique was recommended by its ability to (1) measure the rate of the initial stages of corrosion with accuracy, and (2) procure a continuous record of the corrosion process and, hence, allow identification of the various transitions in kinetics.

IV(d) Calculation of Data

The aqueous corrosion of uranium is known to be governed by more than one growth law, and, in many cases, proceeds in the following sequence: parabolic - linear_1 - linear_2. The corrosion behaviour cannot, therefore, be truly represented in terms of the total thickness of oxide formed in a given period of time, but must take into consideration the separate kinetic processes which are involved and the effect of environmental variables and alloy additions upon them. The following parameters are of major interest:- (1) k_p, the parabolic rate constant, (2) k_1', the constant of the first linear period, (3) k_1'', the constant of the second linear period, (4) T, the apparent film thickness at which the parabolic-linear transition occurs, and (5) T_{theo}, the theoretical film thickness at which the transition occurs.

The values of these parameters are calculated from the relative thickness vs. time curves by the methods described below.

Fig. 27a which illustrates the corrosion of a cathodically-polarised uranium alloy in pH 5.4 solution is taken as typical of the majority of corrosion rate results obtained. The initial curved portion of the graph represents adherence to the parabolic law; linear growth is shown by the two straight lines. The apparent parabolic-linear transition occurs at T. The linear time-ordinate which has been used does not allow the calculation of k_p from this figure, but k_1' and k_1'' are given by the slopes (change in thickness/100 mins.) of the two straight lines. T_{theo} is the limiting thickness of the diffusion layer, and is calculated by drawing, tangentially to the parabolic curve, a line of gradient k_1'. The point of tangential contact, then, defines the film thickness at which linear growth commences, and to which the oxide 'cracks-back' from the non-equilibrium value T.

The parabolic rate constant, k_p, is calculated from Fig. 27b. Here, the film thickness values of Fig. 27a are plotted against a $t^{\frac{1}{2}}$ ordinate, and the straight line obtained denotes the parabolic region. The numerical value of k_p is obtained by squaring the

gradient (change in thickness/100 root-mins.) of the line. The additional constant, incurred by the deviation of the straight line from the origin, is probably due to a surface effect resulting from either the air-formed oxide present on the specimen or from adsorbed oxygen, and has been ignored for the sake of simplicity.

In special cases, where oxide growth is neither linear nor parabolic, the order of the growth law is calculated from the slopes of log (log I_o - log I) vs. log t graphs.

IV(e) Effect of Cathodic Polarisation on Corrosion Rate

Fig. 28 shows the corrosion, in pH 5.4 solution, of pure uranium at several cathodic potentials. The following observations are of interest :-

(1) The total corrosion increases with decreasing potential, i.e. with increasing hydrogen activity.

(2) k_p increases with decreasing potential (this can be seen even from the linear plot).

(3) T and T_{theo} are not significantly affected by cathodic polarisation.

(4) At very negative potentials, there is a tendency for parabolic growth to occur too rapidly to be detected, and the corrosion appears to be linear.

The transition from one linear rate to a faster linear rate which has hitherto been observed[1] only at

high temperatures and termed "breakaway" is also evident in Fig. 28. It has been previously reported[1] that an increase in the test temperature leads to a decrease in the duration of the first linear period and to a greater rate constant for both the first and the second. The figure shows that increasing cathodic polarisation has a similar effect upon the growth kinetics.

Some curves of the cathodic corrosion of uranium -5 wt % zirconium in pH 5.4 solution are shown in Fig.29. The results illustrate clearly the marked resemblance in behaviour between the alloy and the pure metal. The time to "breakaway", however, is increased by alloying.

The corrosion behaviour of the uranium-10 wt % zirconium alloy is somewhat different. Parabolic oxide growth on this metal proceeds in successive steps - each step having a greater rate constant than the preceding one (Fig. 30). It is clear, however, that the corrosion rate increases with decreasing potential.

The effect of cathodic polarisation on the corrosion parameters of pure uranium and uranium-5 wt % zirconium in pH 5.4 solution is summarised by the following tabulations of data.

TABLE ONE (Pure uranium)

E_{HA}	k_p	$k_{1'}$	$k_{1''}$	T	T_{theo}
0	0.75	0.35	-	1.1	1.1
-0.2	2.1	0.65	0.85	1.75	1.55
-0.3	5.1	1.45	2.1	1.9	1.5
-0.4	6.4	2.4	5.8	2.0	1.4

TABLE TWO (U-5 wt % Zr)

E_{HA}	k_p	$k_{1'}$	$k_{1''}$	T	T_{theo}
-0.1	2.35	0.45	-	3.6	2.8
-0.2	3.8	0.65	-	3.6	2.8
-0.3	5.5	0.90	1.35	2.8	2.8
-0.4	11.3	1.85	2.4	3.25	2.8

A simple relationship between hydrogen activity and corrosion rate was deduced from the results obtained from measurements at cathodic potentials. Several possibilities were investigated but the best straight-line fit was found when k_p and $k_{1'}$ were plotted against α^2 (Figs. 31 and 32), thus indicating that the corrosion rate of uranium and uranium-5 wt % zirconium appears to be directly proportional to the square of the hydrogen

activity (or pressure).

The influence of alloying constituents on the corrosion behaviour of uranium can also be derived from the results described above. Reference to Tables I and II shows clearly two effects caused by addition of the alloying element : (1) an increase in the parabolic rate constant k_p , and (2) an increase in the value of the film thickness, T_{theo}, at which the parabolic-linear transition occurs. Despite the complexity of the results, measurements on uranium-10 wt % zirconium confirm these trends; it can be seen from Fig. 30 that parabolic oxide growth on this alloy continues to thicknesses of film which are substantially greater than those on the other two materials.

The effect of alloying on the corrosion rate is shown diagrammatically in Fig. 33. Here, the corrosion of uranium-10 wt % zirconium has been illustrated, for the sake of simplicity, by a single smooth curve.

IV(f) Effect of Solution pH on Corrosion Rate

The corrosion processes of both pure uranium and uranium-zirconium alloys were found to be considerably altered in solutions of greater alkalinity than pH 5.4. The results when plotted against a linear time-ordinate were difficult to interpret but, nevertheless, indicate (1) that, in many cases, growth of the oxide film is

governed by complex laws (accelerating film-growth), and (2) the disappearance of the direct relationship between corrosion rate and hydrogen activity. When $\log(\log I_o - \log I)$ vs. log t graphs were plotted, however, certain patterns of behaviour were emergent and these are described below.

Figs. 34a and 34b show the corrosion behaviour of pure uranium in pH 9.7 solution. The following observations are of interest :-

(1) At and above E_{HA} = 0 V (Fig. 34a), corrosion is either parabolic or parabolic changing to approximately linear. The rate increases with decreasing potential.

(2) Between -0.2 E_{HA} and -0.5 E_{HA} (Fig. 34b), corrosion is initially linear (approximately) and changes in time to a complex law. The rate decreases with decreasing potential.

(3) Below -0.5 E_{HA} (Fig. 34b), there is a tendency for the initial corrosion to approximate more closely to the linear law. The rate increases with decreasing potential.

The corrosion of uranium-10 wt % zirconium in pH 9.7 solution is illustrated in Figs. 35a and 35b. It can be seen that the results indicate a continuation of the trends established for the pure metal, with, however, two significant differences which are listed below :-

(1) The overall corrosion rate of the alloy is lower.

(2) The changes in the corrosion process occur at more

negative potentials, i.e. first, between E_{HA} = -0.2 V and E_{HA} = -0.3 V (instead of between E_{HA} = 0 V and E_{HA} = -0.2 V) and, second (apparently), somewhere below -0.7 E_{HA} (instead of between E_{HA} = -0.5 V and E_{HA} = -0.6 V).

The corrosion behaviour of pure uranium in pH 11.6 solution bears a marked resemblance to the behaviour in pH 9.7 solution. Figs. 36a and 36b show that the changes in corrosion process occur at approximately the same hydrogen activity potentials, although the kinetics of the initial growth periods are somewhat different in the more alkaline solutions.

The corrosion in pH 13 solution has not been investigated in detail. However, those measurements which were made (Fig. 37) confirmed the pattern of complex behaviour observed in other alkaline solutions. Again, it can be seen that alloying diminishes the overall corrosion rate at any given potential.

The dependence of the overall corrosion rate of pure uranium (at a given potential) on the pH of alkaline test solutions is illustrated in Fig. 38. It is clear that, for the conditions chosen, the rate increases with increasing alkalinity. Note again the similarity between the corrosion kinetics of uranium in various alkaline solutions.

IV(g) Effect of Solution Temperature on Corrosion Rate

Corrosion rate measurements were conducted on both pure uranium and uranium-5 wt % zirconium cathodically-polarised in pH 5.4 solution. The following potentials were chosen: (pure uranium E_{HA} = + 0.1 V, 0 V, -0.1 V, -0.2 V and -0.3 V; (uranium-5 wt % zirconium) E_{HA} = +0.1 V, 0 V and -0.1 V.

The results show that at temperatures between 30° and 60°C and potentials of -0.2 V and above the corrosion is governed by the usual parabolic-linear kinetics. However, at temperatures above 30°C and potentials negative to -0.2 V E_{HA}, the initial kinetics are linear and are followed in time by complex growth laws (indicating accelerating film growth). Fig. 39 illustrates some results obtained for corrosion under the latter conditions.

The effect of solution temperature on the rate constants of parabolic growth at various potentials is summarised for both pure uranium and the alloy in the following tables :

TABLE THREE (Pure Uranium)

T°C	+0.1 V	0 V	-0.1 V	-0.2 V
	k_p	k_p	k_p	k_p
30		37.8	102	228
35	21.2	45.6	130	275
40			174.2	
45	41	80.1		390
50	50.4		275	
55		139.2		484
60	85.6			

TABLE FOUR (U-5 wt % Zr)

T°C	+0.1 V	0 V	-0.1 V
	k_p	k_p	k_p
30	31.4	69.7	111
35		78.3	
40	45.6	92.2	158.7
45		114.5	
50	64	132	213.2
60	83.9		282

It can be seen from the data (1) that, at a given potential, the corrosion rate increases with increasing temperature, but (2) that at the higher end of the temperature range the growth rate of oxide on the

pure metal becomes more rapid than on the alloy. Observation (2) conflicts with results obtained at room temperature where it was found that for a given potential the parabolic constant, k_p, for uranium-5 wt % zirconium was approximately two times greater than for the pure metal.

Figs. 40 and 41 show the temperature dependence of k_p for cathodically-polarised pure uranium and uranium-5 wt % zirconium respectively. Activation energies for parabolic growth were calculated by the standard method and were found to lie between 6.3 and 11.2 Kcals./gm.-mole for pure uranium and 6.1 and 6.9 Kcals./gm.-mole for the alloy. It is important to note from the figures (1) that alloying with zirconium reduces the activation energy for diffusion, and (2) that cathodic polarisation appears to have a similar effect.

With regard to observation (2), it is believed that, although the error of $\pm$ 10% which is often associated with plots of the type shown in Figs. 40 and 41 may appear to exclude the possibility of this being a significant effect, the fact that both the pure metal and the alloy demonstrate a similar trend (i.e. decreasing activation energy with decreasing potential) provides evidence in favour.

IV(h) Effect of Solution Oxygen-content on Corrosion Rate

The effect of oxygen in solution upon the corrosion rate was investigated and appeared to be difficult to interpret. The kinetics of film growth are affected by the addition of oxygen, and the results (Fig. 42) show that initial corrosion approximating to a parabolic mechanism is succeeded by complex growth. It can also be seen from the figure that the effect of cathodic polarisation on the corrosion rate of pure uranium in oxygen-saturated pH 5.4 solution is contrary to the behaviour in oxygen-free solution in that the corrosion rate is reduced by decreasing potential.

Free-corrosion measurements in oxygen-saturated solutions also obtained unexpected results. It is observed that under these conditions the overall corrosion rate of the pure metal is less rapid than that of the alloys. However, it must be stressed that these tests were for comparatively short periods of time, and that the data obtained are relevant only to the early stages of corrosion.

IV(i) Free Corrosion at Room-Temperature

The free-corrosion behaviour of pure uranium and the two alloys in oxygen-free pH 5.4 solution is illustrated in Fig. 43. It can be seen that the alloys corrode less rapidly than the pure metal although the

sharp increase in the corrosion rate of the ten percent alloy is unexpected. This "break" was found to be reproducible, but could not be related to any change in the electrode potential of the metal.

IV(j) Simultaneous Measurement of Impedance and Corrosion Rate

Measurements were made at several cathodic potentials but the results obtained were not very consistent. In many cases, neither the capacity nor the conductivity of the oxide was significantly altered during the entire period of corrosion. However, in a small percentage of the results, a certain trend was detectable; the best example is shown diagrammatically in Fig. 44. Here, it can be seen that a rapid increase in capacity and conductivity at the initiation of the test is followed by a period when both remain constant. The impedance of the electrode increases again near the linear-linear transition ("breakaway").

SECTION V

DISCUSSION OF RESULTS

SECTION V

DISCUSSION OF RESULTS

V(a) Introduction

An examination of the results obtained during the present work and those obtained by previous investigators has shown that several complications are apparent in the corrosion behaviour of uranium, While it is difficult to provide a comprehensive explanation for the corrosion from the results of the present research, it is possible, without reference to theory, to make two general deductions concerning the experimental approach most likely to contribute to an understanding of the mechanisms involved. In addition, it appears that under certain restricted conditions, simple relationships between the corrosion rate, potential and alloying concentration can be shown.

It seems necessary that, in order to investigate successfully the effect of hydrogen and alloy content on the kinetics of corrosion, the rate-measurements be conducted (1) under potentiostatic control, and (2) over a period of time which comprises both protective and non-protective growth.

In one case (in pH 5.4 solution), the existence of a simple relationship between the corrosion rate and both potential and alloying concentration has been shown.

Here, an explanatory model is derived from considerations of the defect-structure and the mechanical properties of the corrosion-product oxide. In alkaline solutions, the corrosion is more complex and cannot be easily explained. It is possible that the difference in behaviour is related to an unexpected change in the nature and stoichiometry of the oxide. The results are discussed in these terms.

For the sake of clarity, the Discussion is divided into two broad sections: the first deals with corrosion in pH 5.4 solution and the second with the behaviour in alkaline solutions.

V(b) Experimental Techniques

The majority of American data for the aqueous corrosion of uranium was obtained from high-temperature tests in autoclaves. Electrochemical measurements under these conditions present obvious experimental difficulties, and the tests were therefore, confined to freely-corroding specimens. The present research suggests that such measurements are likely to provide information which is less useful in interpreting the effect of hydrogen on the corrosion, and supports the proposal by Draley and Ruther[3] for a fundamental approach.

It can be seen from Fig. 17 that the electrode potential of uranium is subject to a considerable

variation with time during free-corrosion. Since other results (Figs. 28, 29 and 30) have established the marked potential-dependence of the corrosion rate of uranium, it may be concluded that the rate during free-corrosion is influenced by a fluctuating and unknown potential. Furthermore, while it is true that the corrosion rate of uranium increases with temperature, it is difficult, because of the interdependence of the variables, to relate this effect directly to a higher formation rate of corrosion-product hydrogen. Potentiostatic measurements, however, permit the hydrogen activity variable to be controlled, and relationships of the type shown in Figs. 31 and 32 may be derived.

The American corrosion rate tests considered above are subject to a further shortcoming. Most results which are reported are similar in type to Fig. 1 and, due, no doubt, to the difficulties involved in the measurement of very small weight-losses or increments, fail to show the formation of the initial protective oxide. The present investigation emphasises the role of the parabolic film in the corrosion of uranium for two important reasons. First, because the diffusion of ions through the initially-formed barrier film is believed to be the rate-controlling factor during all stages of the corrosion process, and one of the main

effects of hydrogen is to increase the rate of diffusion. Second, because it has been shown that the protection given by alloying can derive from an increase in the limiting thickness to which the parabolic film can grow. The effects of alloying on the corrosion rate are summarised in Tables I and II; it is clear that although the growth rate, k_p, of the protective film is increased, the rate constants of the linear periods are lower, at a given potential, for U-5 wt % Zr than for the unalloyed uranium. It will be shown later that the decrease in the linear corrosion rate is directly related to the increase in the thickness of the protective film.

PART ONE ...CORROSION IN pH 5.4 SOLUTION

V(c) Effect of Cathodic Polarisation on Corrosion Rate

The following observations are of chief interest to the Discussion :

(1) The occurrence of the parabolic-linear$_1$-linear$_2$ sequence of growth-laws.

(2) The almost constant thickness T_{theo} at which the transition from parabolic to linear kinetics occurs at all magnitudes of polarisation.

(3) The increase in k_p with increasing polarisation.

The present author is not aware of any earlier observations of the complete growth-sequence parabolic-linear$_1$-linear$_2$ during the corrosion of uranium. However, evidence in support of such a sequence may be derived by collating the results obtained by other workers under various conditions. High-temperature aqueous measurements have shown[1] the occurrence of the second (linear$_1$-linear$_2$) transition (Fig. 1) although they were not sufficiently sensitive to detect the first (parabolic-linear$_1$). The formation of a protective oxide and the first transition have been shown during the dry oxidation of uranium. Waber[48] has observed parabolic growth extending to a thickness of 750 Å during oxidation at 100°C. Cubiciotti[49] reports initial parabolic oxidation changing to a linear mechanism, at temperatures between 90 and 165°C. A similar transition has also been found[50], in some cases, during the oxidation of certain uranium alloys in both air and carbon dioxide at temperatures of 500°C and above.

In all cases, the transition from protective to non-protective kinetics during the dry oxidation of uranium has been explained in terms of the Pilling-Bedworth ratio. Waber[6] reports that on a mole-for-mole basis UO_2 occupies 1.97 times as much volume as the metal. Oxidation, under these conditions, is likely to

result in high compressive stresses acting at the surface of the coherent protective film and, eventually, in cracking of the film when the stresses have reached a critical value. The average thickness of the uncracked part of the protective oxide should determine the subsequent rate of attack since ionic diffusion through this film will remain the slowest step in the oxidation process.

From the evidence available, there is no reason to believe that the transitions from parabolic to linear growth shown in Figs. 28 and 29 are caused by a mechanism which is in any way different to that operative during dry oxidation. The disparity between the critical thickness T_{theo} and the non-equilibrium value T would appear to suggest that a certain 'supersaturation' of stress may occur before cracking of the film under compression. This behaviour is in accord with the crack-theory of Griffiths[51] which has shown that the energy-requirements for the nucleation of a crack are greater than for the propagation.

Draley and Ruther[3] have discussed the effect of hydrogen on the corrosion of uranium and offer three alternative suggestions to explain the increase in corrosion rate (see sub-section Ib). It is believed likely that the effect of these mechanisms would be to

alter the thickness of the protective film through which the corrosion processes must occur. The present results (Tables I and II), however, show that, although the corrosion-rate is increased, the thickness of the initial protective film, T_{theo}, remains virtually unaffected by increasing hydrogen activity.

It may be concluded, therefore, both from the results and from the similarity between wet and dry kinetics, that the sole effect of hydrogen is to increase the rate of ionic diffusion within the oxide, without causing a change in mechanism. This behaviour has been previously predicted by Leach[4] from conductivity measurements on U/UO_2 cathodes. Wanklyn and Hopkinson[52] give, inter alia, a similar explanation for the increase in the corrosion rate of zirconium caused by cathodic-polarisation during tests in high-temperature water ($325^{o}C$). They reject, on two counts, the cathodic reduction of the oxide as a possible explanation: (1) as thermodynamically unlikely, and (2) as controverted by the enhanced film growth. It should be pointed out that these reasons are equally applicable to uranium oxides.

Since the present hypothesis suggested for the role of hydrogen is supported by the observations of some other workers, it remains to be shown by which method the hydrogen can increase the corrosion rate of

uranium. Two factors are relevant: (1) the state of the hydrogen within the oxide, and (2) its position in the lattice.

A relationship between the electronic conductivity and the ionic diffusion coefficients of semiconducting compounds has been demonstrated. An increase in the conductivity will generally result in enhanced diffusion-rates. Wagner[11] has shown that the diffusion coefficient of Ag in the system Ag-Ag_2S-S is increased by a factor of 3×10^3 due to the increase in conductivity associated with a non-stoichiometric silver excess of 2×10^{-3} gm.-atom of Ag per mole of Ag_2S. An excess of silver in Ag_2S corresponds to a prevalence of excess electrons (i.e. n-type conduction), and the increase in diffusion rate is attributed to a space-charge, created by these electrons, which tends to accelerate the silver ions.

It has already been concluded that hydrogen increases the rate of ionic diffusion within the oxide. Hence, because of the relationship between the diffusion coefficients and the electronic conductivity, it is evident that hydrogen will also influence the latter parameter. It can be argued, therefore, that as the conductivity is likely only to be affected by the presence of charge-carrying species, it is a reasonable assumption that the increase in the corrosion rate of

uranium is caused by the incorporation into the oxide lattice of hydrogen in the ionic state. The direct relationship between the corrosion rate of the metal and the square of the hydrogen activity at the oxide-electrolyte interface (Figs. 31 and 32) is probably relevant to this argument, although it is not possible at the present stage to enlarge on this observation.

Arguing from the stand-point that hydrogen is ionised within an oxide film, there are several possible lattice-sites in which it can be incorporated. Leach[4] has proposed the following :

(1) Sites which are normally occupied by metal ions.

(2) Interstitial sites other than those normally occupied by metal ions.

(3) Sites associated with oxygen ions.

For the particular case of uranium oxides where lattice vacancies do not normally exist, it is reasonable to expect that protons would occupy interstitial sites. Here, the energetics would require the association of H^+ ions with oxygen ions to form hydroxyl ions. Draley and Ruther[3] have acknowledged, inter alia, a similar mechanism.

It is interesting that, from this theory, the increase in the conductivity and consequent increase in the corrosion rate, shown in the results, can only be

caused by the incorporation of protons in the lattice if the oxide itself is an n-type semi-conductor. Consider the arbitrarily chosen n-type oxide U_3O_{7-x} ; this may be written as :

$$U_3O_{7-x} = 2U^{4+} + U^{6+} + 6\ O^{2-} + (1-x)O_i^{2-} + 2x\theta^-$$

where $(1-x)O_i^{2-}$ is the number of excess oxygen ions (in interstitial positions), and θ are excess electrons . It is clear that, in order to maintain the charge balance, the addition of an H^+ ion to the right-hand side of the equation will require the formation of an extra excess electron. The resulting increase in electronic conductivity will tend to reduce the potential gradient opposing the diffusion of negative ions towards the metal (see Fig. 2) and, hence, will encourage further oxide growth. Another example of enhanced oxidation rates caused by externally-induced electronic conductivity is apparent in the work of Jacobs[53]. He has shown that anodic films (Ta_2O_5) on tantalum will continue to grow beyond the thickness defined by a given formation-voltage when the electronic conductivity of the oxides is increased by ultra-violet irradiation.

It follows from the above argument that, in pH 5.4 solution, all corrosion-product oxides (or at least those formed in the potential range 0 to $-0.6\ E_{HA}$) behave as n-type semi-conductors. The

importance of this observation will become evident later in the discussion when it will be used as a basis for differentiating between the corrosion behaviour in pH 5.4 solution and in more alkaline solutions.

The occurrence of the $linear_1$-$linear_2$ transition ("breakaway") during the corrosion of uranium requires some comment - especially since it is believed that the accelerating corrosion observed at higher temperatures and in alkaline solutions is governed by a similar mechanism.

A consideration of the possible explanations suggests that a sharp increase in rate could be incurred either by (1) an increase in the ionic diffusion rates within the oxide, or (2) a decrease in the diffusion distance through which the process must occur.

The first explanation attributes the effect to an increase in hydrogen activity resulting in an increased rate which, in turn, leads to further build-up of hydrogen concentration. However, there exists evidence[10] which may be interpreted to show that the hydrogen activity within the oxide reaches a maximum equilibrium value in a relatively short time and then remains constant. Furthermore, although a "snowball" mechanism of this type might account for a transition to a complex growth law (where the rate increases with time), it is

difficult to ascribe the linear-linear transition to the same model.

A tentative explanation for "breakaway" is, therefore, based on a reduction in diffusion distance, and is modified later to account for the observations of complex growth.

The growth of a coherent protective oxide is accompanied not only by the formation of internal stresses but also by a complementary annealing-action which tends to relieve the stresses. Any increase in the rate of growth, k_p, will reduce the time during which the anneal is operative and, in effect, will increase the magnitude of the stress concentration (provided that any simultaneous increase in the rate of annealing does not compensate). The first crack will appear when the oxide is no longer able to accommodate the stresses, and the subsequent corrosion will be controlled, for a time, by the diffusion of ions through the uncracked film of thickness T_{theo}. It is believed, however, that localised stress-raisers can increase the stress concentration in the coherent barrier layer and propagate further cracks, and that the effectiveness of these stress-raisers will be inversely related to the duration of the anneal. Hence, it may be possible to attribute the transition in rate ("breakaway") to the formation of a new set of cracks which reduce the

thickness of the rate-controlling film T_{theo}. Furthermore, it is clear from this reasoning that increasing the rate of film growth (i.e. reducing the annealing time) in the initial stages will eventually result in deeper cracks and a faster second period of corrosion ($linear_2$). This observation may be compared with both the present results and the results of other workers which show, respectively, that the rate constant of the second linear period is increased by increasing cathodic polarisation and by higher temperatures.

It is possible that some confusion may arise due to the apparent similarity between the mechanism described above and the already disapproved theories of Draley and Ruther[3]. These authors have ascribed increases in the corrosion rate of uranium to three hydrogen-induced effects which are likely to have a direct influence on the thickness of the protective film. Note, however, that the reduction of the protective thickness, in the present hypothesis, is not directly attributed to hydrogen, but only to the stresses arising from high rates of film growth.

Clearly, there are several assumptions implicit in the explanation offered which may detract from its cogency. For example, it has been necessary to reason that some local stresses act in a direction normal to the plane of the metal-oxide interface although the oxide

itself is in compression and, also, that the thickness, T_{theo}, of the protective film is not influenced by the growth rate during the initial parabolic period. However, granted these assumptions, it is believed that a model for "breakaway" based on film-cracking is superior to the alternative hydrogen-based mechanism, especially as the former model may be used to explain both linear to linear and linear to complex-growth transitions without serious modification. Further work will, of course, be necessary to confirm the hypothesis.

It was originally intended that the simultaneous measurements of impedance and corrosion rate would determine the validity of the film-cracking hypothesis for it was hoped that transitions in the growth kinetics would correspond to equally well-defined changes in the capacity and conductivity of the oxide.

Ideally, the capacity of an oxide is expected to decrease parabolically during growth of the protective film, reaching a minimum value at the transition thickness. The capacity should then remain stable at this value throughout the first period of constant corrosion since it is reasonable to assume that the non-protective oxide, by allowing the electrolyte access to the surface of the protective film, would not significantly affect the measured capacity of the electrode. The minimum

value of capacity will be inversely proportional to the thickness of the uncracked film. If, as has been proposed, the second ($linear_1$-$linear_2$) transition is accomplished by cracking of the initial barrier film, a corresponding ihcrease in the capacity should be detectable.

The conductivity of the oxide is also expected to follow a definite pattern under similar conditions. In the initial stages of growth, the build-up of the proton concentration within the oxide should cause an increase in the measured conductivity. The conductivity should then stabilise at a maximum value when the maximum activity of hydrogen has been reached. No change should be detectable at the parabolic-$linear_1$ transition since the measured values always correspond to the conductivity of an uncracked barrier layer, but "breakaway" should be accompanied by an increment.

However, it became obvious from the high values of capacity recorded that the normal inverse relationship between capacity and conductivity could not exist. Instead, it would appear from the results that a direct relationship of the type suggested by some early workers[4,9] is more likely.

The results have proved difficult to interpret and the following discussion must be considered as only tentative. The changes in impedance do not correspond

with any exactitude to the transitions in kinetics. It is interesting, however, that other workers[54] using different experimental methods have encountered similar difficulties. It can be seen from Fig. 44 that the capacity increases at the initiation of the test during growth of the parabolic film, and then, near the parabolic-linear transition, decreases slightly before stabilising for the duration of the first linear period. From the direct relationship between capacity and film thickness, it may be inferred that the decrease in capacity corresponds to a 'cracking-back' of the protective film from the non-equilibrium value (T) to a statistically constant thickness T_{theo} (see sub-section IV(d)). Since the film grown during linear kinetics is cracked, the thickness of the constant protective film will remain the controlling factor; this is seen from the stable value of capacity measured during the major portion of the linear period of corrosion. The decrease in capacity associated with the linear-linear transition ("breakaway") might suggest that this transition is associated with a further cracking-back of the protective film, but this is difficult to reconcile with the observations on the changes in conductivity at this point.

The sharp increase in conductivity during the first few minutes of corrosion may be caused by the

charging of the air-formed oxide film with hydrogen, while the stable value of conductivity during the first linear period may be explained if, as is probable, the hydrogen activity reaches a constant saturation value in the compact protective film within a short time. However, no interpretation is apparent at present for the increase in resistance occurring near the linear-linear transition.

It should be pointed out that one of the difficulties in the interpretation of these results arose from the observation that changes in the hydrogen content of the oxide could significantly alter the measured capacity of the oxide, both when the capacity and oxide thickness are inversely related and when the relationship is direct. It is also clear from these observations that this capacity change is not associated with a change in oxide thickness but arises from the shortcomings of the analogue, consisting of only a simple capacitor and resistor, in the measuring device. This phenomenon has been described in greater detail for the case of a zirconium electrode[55].

Notwithstanding the various difficulties encountered, it is believed that the pattern of behaviour exhibited in Fig. 44 does not confirm any other reasonable explanation for the "breakaway" transition and, hence,

it is not considered as evidence against the film-cracking hypothesis which has been proposed.

V(d) Effect of Alloying on Corrosion Rate

The observations of importance to the Discussion are given below:

(1) The increase in the parabolic rate-constant, k_p, with increasing alloy content.

(2) The increase in the protective film thickness, T_{theo}, with increasing alloy content.

The oxidation behaviour of alloys has been investigated extensively by Wagner, Hauffe[33,56] and their respective schools; results have been obtained for several systems which are similar to the uranium-zirconium system and where the alloying constituent distributes itself through the main oxide phase and forms a mixed oxide in which it replaces some of the cations of the main metal. These data are summarised by the 'Hauffe Valency Rule' which states that the oxidation rate is generally reduced by alloying additions of (1) lower valence than the base metal, when the main oxide is a p-type semi-conductor, and (2) higher valence when the main oxide is n-type. Although the theory is not considered here, it may be deduced that any explanatory model based on these observations will attribute the improvement in oxidation resistance to a decrease in the

ionic diffusion rates of the growing oxide.

The present results are not consistent with the deduction from the Wagner-Hauffe explanations, nor can they be interpreted on the basis of the mechanisms proposed by Draley and co-workers[38] (see sub-section II(k)) to account for the protection given by the addition of small amounts of zirconium to uranium. There is no evidence to suggest that the effect of cathodic polarisation on alloys is in any way different from the effect on the pure metal; this would be expected if the latter theories were applicable.

Fig. 33 shows that increasing amounts of alloying constituent reduce the linear corrosion rate, but, at the same time, increase the diffusion constants of the protective film. The reduction in rate must, therefore, be attributed to the compensatory increase in the protective film thickness, T_{theo}, which accompanies alloying.

Consider the equation for parabolic growth:
$y^2 = k_p t$ which on differentiation becomes $2y\frac{dy}{dt} = k_p$.
At the limiting thickness of the protective film (when $y = T_{theo}$) $\frac{dy}{dt} = k_l$ (where k_l is the linear rate constant).
Therefore, it is clear that $k_p = 2\, k_l \cdot T_{theo}$
It can be seen from the above expression that if the increase in T_{theo}, due to alloying, is proportionately

greater than the increase in k_p, then the rate of the subsequent linear corrosion will be decreased. Reference to Tables I and II shows that this is, in fact, the case.

The effect of zirconium additions on the ionic diffusion rates in the oxide may be discussed with reference to the list of stoichiometric and non-stoichiometric phases given in sub-section II(d). It is established that uranium dioxide (UO_2) possesses a fluorite-type crystal structure (Fig.8). This may be represented by a face-centred cubic array of cations, the tetrahedral interstices of which are occupied by anions in a simple cubic sub-lattice. The oxidation of UO_2 to form higher oxides involves the random occupation of the remaining interstitial positions (the octahedral interstices), of which there are four per unit cell, by additional oxygen ions. The charge imbalance resulting from the excess oxygen ions is neutralised by conversion of the necessary number of U^{4+} ions to U^{6+} ions.

The stoichiometric oxide phases which have been found for uranium can be interpreted as the result of ordering phenomena[57]. Thus, it can be shown, for example, that the two end oxides, UO_2 and UO_3, are ordered in both the cation and anion sub-lattices; in the case of UO_2, all uranium ions are 4-valent and no interstitial positions are occupied by oxygen ions, while in the case

of UO_3, all uranium ions are 6-valent and all interstices are occupied. On the other hand, stoichiometry in oxides of composition intermediate to UO_2 and UO_3 results from ordering of either anions or cations. The compounds U_4O_9 and U_2O_5* can be characterised, respectively, by a UO_2 lattice with one and two interstitial positions per unit cell occupied by oxygen ions. U_3O_7 and U_3O_8 are formed, respectively, when, in a UO_2 lattice, one and two uranium ions in every three display 6-valency. Similar order-disorder transformations have been shown[58] to take place in other oxides where the cation has more than one valency (e.g. Fe_3O_4).

The increase in ionic diffusion rates may now be explained in terms of the random replacement, within the mixed oxide, of a proportion of both 4-valent and 6-valent uranium by the 4-valent zirconium ion. Although U^{4+} and Zr^{4+} should be mutually interchangeable without influencing either the charge balance or the conductivity of the oxide, the replacement of U^{6+} by an ion of lower valency would lead to disorder in the cation sub-lattice, and the resulting defect structure would allow more rapid oxide growth.

*N.B. It should be noted that of the three anion-ordered oxides theoretically possible, U_4O_9, U_2O_5 and U_4O_{11}, there is concrete evidence for the existence of U_4O_9 and U_2O_5.

The observation that alloying of the base metal increases the thickness to which the protective oxide may grow without cracking may involve one or more of several explanations. It is possible either that the corrosion of an alloy is (1) accompanied by a lower concentration of built-in stresses in the oxide, or (2) if the stresses are not significantly affected by alloying, that the mixed oxide is able to accommodate them to greater concentrations.

A reduction of the compressive stresses at the surface of a growing oxide can result from those changes caused by alloying which tend to diminish the difference between the specific volumes of the metal and the oxide. Similarly, a decrease in the lattice-parameter mismatch between the two species may reduce the stress concentration. The author, however, is not aware of any conclusive evidence in support of such mechanisms, (see sub-section II(j)). In any case, it is unlikely that zirconium additions as small as 5 weight percent would result in large enough changes in the specific volume or lattice parameters of either the metal or the oxide to account for the necessary reduction in stress.

The ability to accommodate greater volume changes without breakdown can be related either to an increase in the plasticity (and the consequent relief of stresses)

or in the strength of the oxide. The present results, however, provide no clear method for differentiation between the two alternatives and both must, therefore, be discussed with equal emphasis.

An increase in the plasticity of the mixed oxide may be caused by the accompanying increase in defect (vacancy) concentration associated with alloying. In the same context, it is interesting that alumina, which is not a good electronic conductor and probably has a low defect concentration, forms a very thin protective film, while at the other extreme, magnetite, formed as a protective oxide on boiler steel, is a good conductor and grows to a considerable thickness. In between, it would appear that certain other oxides which grow, without cracking, to intermediate protective thicknesses have intermediate conductivities.

Antill and Peakall[50] have obtained results, for the oxidation of some uranium alloys in both high-temperature air and carbon dioxide, which are best explained by the "plasticity mechanism". In further agreement with this mechanism, they find that the oxidation-products on the least resistant alloys tend to be extremely brittle and fly off violently from the specimens at experimental temperature and on cooling. Other workers who have commented on the plasticity of

uranium oxides are Christie and Williams[59] and Scott and co-workers[60].

On the other hand, the strength of ionic crystals can also be greatly influenced by the presence of foreign ions. Impurities in the lattice tend to restrict the movement of dislocations and result in greater yield strengths (the ultimate strength is difficult to measure experimentally). Numerous examples[58,61,62] of this phenomenon are known, especially for materials such as MgO, TiO_2, and NaCl. It must be pointed out, however, that increases in strength usually accompany impurity concentrations of the order of parts per million, and there is little evidence to suggest that alloying additions as large as 10 weight percent would have a similar effect.

The deformation of crystals generally proceeds either (1) crystallographically, i.e. by the movement of relatively large aggregates along certain preferred slip or glide planes, or (2) by the diffusion of individual ions. In considering the applicability of these mechanisms to the protective film present on uranium, it would appear, at first sight, that both methods of deformation are unlikely under the prevailing conditions - the first, because the protective oxides are almost certainly amorphous, and the second, because it is normally a high

temperature phenomenon and, also, requires the diffusion of both metal and oxygen ions during the growth of the oxide. Results obtained in the present investigation, however, provide a reasonable argument in favour of deformation by diffusion. First, because the ability of uranium to corrode rapidly, even at temperatures as low as 20 to 60°C, is implicit evidence of the existence of a strong diffusion-flux in the oxide formed. Second, because it is clear from Fig. 40 that the activation energies calculated for the corrosion of uranium are significantly lower than would be expected if the process depended solely on the diffusion of oxygen ions through the oxide lattice. And third, because it has recently been shown[63] that the addition of zirconia to UO_2 increases the diffusion rate of uranium ions by an order of magnitude. While, after this increase, the diffusion of metal ions is still much less rapid than that of the anion, the change may be sufficient to permit an increase in deformation. This observation is supported by some results obtained in the present work; these are discussed in the next sub-section.

The limitations of the two theories of protection by alloying (plasticity, strength) may now be considered in terms of the mechanism of deformation by diffusion. Figs. 45a,b,c show the various stages during the growth

and fracture of a coherent oxide under lateral compression. It is clear that failure will occur only after the stored strain-energy in the film has attained a level sufficient to form the two new surfaces (marked A and B). When diffusion in the oxide is possible, stress-relief can result from ionic motion in a direction perpendicular to the force vectors, F and F', and, hence, an increase in plasticity will permit oxide growth to greater thicknesses. It may be deduced from the same model, that an increase in yield strength will probably have the opposite effect. If deformation becomes more difficult due to the greater strength of the film, then the internal stresses will accumulate rapidly and failure might occur at a lesser thickness.

It is apparent that the available evidence tends to favour an explanation based on an increase in plasticity to account for the formation of thicker protective films on alloys. It is necessary, however, to state here that the evidence is by no means conclusive, and that the 'plasticity mechanism' could be invalidated if (1) deformation of the oxide occurs crystallographically, and if (2) the ultimate strength of the oxide is also increased by alloying.

V(e) Effect of Solution Temperature on Corrosion Rate

The following points are considered relevant to

the Discussion :

(1) The low activation energies calculated for the aqueous corrosion of uranium as compared with values obtained by other workers for atmospheric oxidation.

(2) The decrease in activation energy with cathodic polarisation.

(3) The decrease in activation energy with alloying.

(4) The appearance of accelerating corrosion at temperatures above 30°C and potentials below -0.2 V E_{HA}.

Figs. 40 and 41 show that the calculated activation energies for the aqueous corrosion of uranium and uranium-5 wt % zirconium in the temperature range 30° - 60°C lie between 6.1 and 11.2 Kcals./gm.-mole. These values are in reasonable agreement with the activation energies of 7 to 16 Kcals./gm.-mole reported by Waber[6] for the oxidation of uranium in water vapour in the temperature range 50°-226°C, but differ significantly from the values obtained during atmospheric oxidation[49] (22 to 24 Kcals./gm.-mole at temperatures between 90° - 165°C).

It must be pointed out that, while linearity in log rate vs. $^{1}/_{T}$ plots is generally considered to reflect the operation of a single rate-controlling process, it would be unsound to draw this conclusion in the present

case in view of the narrow range of temperature involved. It is equally significant, however, that using a much wider range of temperature, Thomas[64] and Potter and Mann[65] have discovered that the aqueous corrosion of zirconium and mild steel, respectively, involves a much lower activation energy than the corresponding atmospheric oxidation.

Belle and Lustman[16] have measured the activation energy for the self-diffusion of oxygen ions in UO_2 and obtain a value of 29.7 Kcals./gm.-mole in fair agreement with the activation energies for the atmospheric oxidation of uranium. It would appear, hence, that in the absence of water, the oxidation of uranium occurs almost entirely by the inward diffusion of oxygen. This observation makes the lower energy-requirements of aqueous corrosion processes difficult to explain although a different mechanism may be postulated involving a large reduction in the activation energy for metal diffusion.

It may be argued from the results that such a change in mechanism could arise from the presence of hydrogen ions in an oxide formed in aqueous conditions. Thus, Figs. 40 and 41 show that the activation energy for parabolic corrosion is reduced by increasing hydrogen activity. That the addition of small amounts of a foreign cation can lead to an increase in the self-diffusion of

uranium is borne out by the work of McNamara[63]. His observations may be related to the present work which has shown that alloying additions lower the activation energy for parabolic corrosion. It is an interesting speculation that the increase in lattice disorder to which have been attributed the higher parabolic constants, k_p, measured for the alloy (see sub-section V(d)) may be the cause of this decrease in activation energy.

Corrosion measurements on uranium (E_{HA}= -0.3V) in solutions at temperatures above 30°C (Fig.39) fail to observe parabolic growth and instead show that an initial linear period is succeeded by complex growth laws. It is believed, however, that the absence of a parabolic law from the growth-sequence does not indicate the existence of a different corrosion mechanism at high temperatures, but can be explained in terms of the sensitivity of the rate-measuring instrument. It can be estimated from Fig. 39 that the constants of linear corrosion, k_l, for the three curves are of the order of 100 thickness units/100 mins. If, for the sake of argument, it is assumed that the thickness, T_{theo}, of the hypothetical protective film is 3 thickness units,*

*N.B. It is found that the protective oxide film grows to greater thicknesses at higher temperatures. This effect has not been investigated in detail but is believed to be due to some form of annealing-action.

then it can be shown from the expression

$$k_p = 2 k_1 \cdot T_{theo}$$

that the parabolic rate constant will be 600 units/ 100 mins. Taking this value for k_p, and substituting in the parabolic growth equation,

$$y^2 = k_p \cdot t \quad \text{(where } y=T_{theo}=3\text{)}$$

it is evident that the protective film will grow to the critical thickness T_{theo} in the order of 1.5 minutes. Thus, since the instrument is not sufficiently sensitive to measure accurately a complete process occurring within 1 to 2 minutes, the results do not show the existence of the parabolic period.

The occurrence of complex-growth is similar to "breakaway" and can be interpreted on the basis of the film-cracking hypothesis. It is clear that the combined effect of cathodic polarisation and high temperatures leads to enormous increases in the corrosion rate, and it is suggested that the stress concentrations which result from such high rates of corrosion will be sufficient to cause a progressive cracking-back of the protective film, thereby incurring a growth rate which increases with time.

V(f) Effect of Solution Oxygen-Content on Corrosion Rate

Reports[35,36] from America had stressed that

uranium and its alloys were protected by dissolved oxygen in solution. This was interpreted to mean that oxygen caused the formation of more compact protective films. This is not, however, the general case. The presence of large amounts of oxygen is found to increase the initial rate of corrosion, and the films formed consist mainly of a non-adherent green oxide (perhaps U_3O_8). Moreover, the results illustrated in Fig. 42 show that the cathodic depolarisation of oxygen in solution leads to a lower rate of corrosion.

It must be pointed out, however, that the conditions under which the present experiments were conducted differ markedly from the American work, and results from the two sources are not, therefore, directly comparable. The present results were obtained by short-time tests at very high oxygen concentrations. Further, no corrosion tests in oxygenated solutions reported from the U.S.A. were carried out under potentiostatic control. Indeed, it is possible that the presence of small amounts of oxygen under such conditions could depolarise the corrosion-product hydrogen and/or raise the natural corrosion potential and thus cause a decrease in the corrosion rate. In any case, it has been shown even in the present work (sub-section IV(h)) that, when the potential of the specimen is not stabilised, tests in oxygenated-solutions appear to give irrational results.

It has not been established whether the apparently non-protective films observed in the present research can eventually stifle further corrosion, but it is clear from the descriptions that the oxides obtained during tests in America are very different in character. This suggests that the corrosion products of uranium are very sensitive to the concentration of oxygen in the solution.

PART TWO - CORROSION IN ALKALINE SOLUTIONS

V(g) Modification of pH-Potential Diagram for the System U-H_2O.

Visual observations of specimens corroding in alkaline solutions have shown that the corrosion products are generally darker in colour and less compact than their counterparts in pH 5.4. Furthermore, the results show that corrosion in these solutions (pH 9.7, 11.6, 13) is exemplified by (1) complex-growth (under certain conditions), even during room-temperature tests, and (2) the absence of a direct relationship between hydrogen activity and rate. The difference between the behaviour in alkaline solutions and in pH 5.4 is considered to be of sufficient significance to merit separate discussion.

The existence of complex-growth mechanisms (shown in Figs. 34b, 35b, 36a, 36b, and 37) may again be related

to a progressive 'cracking-back' of the protective film due to high rates of corrosion. The normal parabolic-linear combination of growth laws is seen to hold in instances when the corrosion rates are lower (Figs. 34a, 35a). It should be noted that measurements in both alkaline solutions and in pH 5.4 solution were conducted at identical values of E_{HA}. Higher corrosion rates, in the present case, cannot, therefore, be attributed directly to the effect of cathodic polarisation, but appear to indicate a change in the character of the corrosion film formed. In this context, it is perhaps significant that increasing alkalinity has been found to result in higher rates not only for uranium (Fig. 38), but for other materials as well[65].

It can be seen, both from Figs. 34a, 34b, 36a and 36b, and the description of the results, that the corrosion rate of uranium is subject to a complex variation with potential. That this behaviour is primarily a characteristic of the environment is confirmed by the observation of similar variations during the corrosion of the ten weight-percent alloy (Figs. 35a and 35b). Again, it is difficult to interpret these data in terms of the simple model derived for the corrosion in pH 5.4 solution. Instead, it may be possible that the variations in rate are related to changes in the semi-conducting properties of the corrosion product.

The difference between the corrosion behaviour in alkaline solutions and in pH 5.4 has been clearly established from the present results. While it seems likely that this difference in behaviour corresponds to a dissimilarity, either in structure or in composition, between the corrosion films formed in the two environments, it is difficult to reconcile the existence of two distinct species with the data presented in the U-H_2O Pourbaix diagram (Fig. 7). Here, the sole species considered stable, in the pH - potential range of interest, is given as UO_2. However, the diagram has been derived for equilibrium conditions, and it is possible that, during a kinetic process such as studied here, the configuration is significantly altered. As an example of this type of effect, it is interesting that although FeO is thermodynamically unstable, with respect to Fe and Fe_3O_4, below 570°C, a layer of FeO may be found during oxidation at temperatures as low as 400°C [66]. Furthermore, there is considerable evidence which suggests that data from which the diagram is derived does not permit either an accurate or a comprehensive representation of the system. First, the free energy values on which the calculations are based are questionable. Pourbaix and co-workers[12] have chosen values for UO, UO_2, U_3O_8 and UO_3 which were calculated by Brewer[67] using thermodynamic data collected from several sources. The following

values are quoted:

UO = -123 Kcals.

UO_2 = -246.6 Kcals.

U_3O_8 = -804 Kcals.

UO_3 = -273 Kcals.

Latimer[68], on the other hand, reports values for UO_2 and UO_3 which are 3 to 4 per cent greater:

UO_2 = -257 Kcals.

UO_3 = -283 Kcals.

(Note that a relatively small difference in free energy can have a considerable effect on the potential at which a given species is stable). Second, Waber[6] has reported several observations of the presence of the hydroxide $U(OH)_4$, which is not shown in the diagram, in aqueous corrosion films formed on uranium. Katz and Rabinowitch[69] have also commented on the possible formation of hydrated oxides ($U(OH)_4 = UO_2 \cdot 2H_2O$). Moreover, Pourbaix[12] himself is not emphatic in denial of the hydroxide, and states:

"Si la valeur d'enthalpie libre que nous avons admise pour $U(OH)_4$ est exacte, l'hydroxyde est thermodynamiquement moins stable que l'oxyde, et il tend à se déshydrater selon la réaction $U(OH)_4 \longrightarrow UO_2 + 2H_2O$. Nous n'avons pas connaissance d'observations expérimentales qui confirmeraient cette réaction".

Clearly, one possible explanation for the difference between the corrosion in pH 5.4 and in alkaline solutions could be based on the formation of $U(OH)_4$ in one of the two environments and of UO_2 in the other. Third, the two stable phases U_4O_9 and U_3O_7 (identified by Willardson and co-workers[15]) of O/U ratios intermediate to UO_2 and U_3O_8 are not included in the diagram. The importance to the present work of this omission is considerable since the measurements have been conducted within the potential range at which, if they exist in equilibrium in H_2O, these species are likely to be stable.

In view of these possible inadequacies of the Pourbaix diagram, it is not unreasonable to reconstruct the relevant portions to fit the data obtained during the present investigation. However, it is necessary to this intention, first, to discuss the results in greater detail and, second, to make a number of assumptions.

Fig. 46 illustrates the dissimilar trends exhibited during the corrosion of uranium in pH 5.4 and in alkaline solutions. A demarcation between the two hypothetical species has been shown at pH 7 (although there is probably a gradual transition). It is clear that the rate in pH 5.4 solution increases with increasing hydrogen activity between E_{HA} = 0 V and E_{HA} =-0.6 V. A similar increase has also been shown

for both uranium-5 wt % zirconium and uranium-10 wt % zirconium in the same solution (Figs. 29 and 30). This suggests from considerations of electronic conductivity (see sub-section V(c)) that corrosion films formed under these conditions are n-type semi-conductors. The behaviour in alkaline solutions is illustrated for pH 9.7, and is similar for both pH 11.6 and pH 13 (Figs. 36a, 36b and 37). It is shown in Fig. 46 that the rate increases with decreasing potential between E_{HA} = +0.2 V and E_{HA} = 0 V, decreases between E_{HA} = -0.2 V and E_{HA} = -0.5 V, and increases again below E_{HA} = -0.5 V. These two changes in process appear to indicate that the semi-conductivity of the corrosion product is altered from n- to p- to n-type as the potential is decreased*.

The changes in the conductivity mechanism, indicated by the rate changes in Fig. 46, are suggestive of the formation of non-stoichiometric phases. Within the domain of stability of a given species, the oxygen-rich region (positive, with respect to potential) will tend to be p-type while oxygen-deficiency will result

*N.B. It must be stressed that the absence of parabolic growth during corrosion at certain potentials in alkaline solutions does not necessarily imply the total absence of a diffusion process. As pointed out earlier, it is believed that the duration of the process is too short to allow detection by the measuring instrument.

in n-type semi-conduction (e.g. UO_{2+x} ~ p-type, U_4O_{9-x} ~ n-type, U_3O_{7+x} ~ p-type). Note that, since the exact potentials at which the changes in mechanism occur are not known from the results, a division has been made in Fig. 46 at the arbitrarily chosen potentials E_{HA} = -0.1 V and E_{HA} = -0.7 V. These two potentials, hence, bound the domain of stability of one species while immediately below lies the oxygen-rich region of a stable compound of lesser O/U ratio and immediately above is the oxygen-deficient region of the next phase.

The following assumptions have also been made :
(1) that the sequence of stable phases formed in alkaline solutions (in order of increasing O/U ratio) is <u>either</u> UO_2-U_4O_9-U_3O_7-U_3O_8-UO_3 or $U(OH)_4$-U_4O_9-U_3O_7-U_3O_8-UO_3,
(2) that the free energy values quoted by Pourbaix[12] for UO_2, $U(OH)_4$ and UO_3 are acceptable. (Clearly, the assumption that the values for both UO_2 and $U(OH)_4$ are <u>correct</u> appears mutually incompatible for the purposes of this discussion since, if this be the case, then it is implicit that $U(OH)_4$ can never be stable in preference to UO_2. It is emphasised, therefore, that the free energy values of these compounds have been accepted solely in order to calculate the two theoretical sequences, and that their correctness remains open to doubt,

(3) that the stable oxide phase within the potential boundary of $E_{HA} = -0.1\,V$ and $E_{HA} = -0.7\,V$ is U_4O_9. p- and n-type semi-conduction in this domain may then be ascribed to the formation of U_4O_{9+x} and U_4O_{9-x} respectively.

Consider the formation of higher uranium oxides starting from UO_2. Using the expression

$$\frac{\sum_{\gamma}(\nu_{\gamma}\mu^{\circ}_{\gamma})}{23{,}060\ n} = E^{\circ}$$

(where, ν_{γ} is the molar or stoichiometric coefficient of constituent γ, μ°_{γ} is the standard molar chemical potential of constituent γ at 25°C, n is the stoichiometric coefficient of the electrons in the reaction, and E° is the equilibrium potential when the reactants are all in the standard state.)

the free energy of formation for U_4O_9 is calculated as - 1075.3 Kcals. and for U_3O_7 as - 821.8 Kcals. The free energy of formation for U_3O_8 can be obtained by interpolation from a plot of free energy/gm. atom vs. O/U ratio (Fig. 47, curve A) and is shown to be approximately - 857 Kcals.

Similarly, in the sequence $U(OH)_4$ - U_4O_9 - U_3O_7 - U_3O_8 - UO_3 the free energy of formation of U_4O_9 is calculated as - 1041.9 Kcals, and of U_3O_7 as - 796.7 Kcals.

Again, by interpolation (Fig. 47, curve B) the free energy for U_3O_8 is found to be approximately - 833. Kcals.

Since the latter calculated value for the free energy of formation of U_3O_8 (- 833 Kcals) differs by as little as 3.5 per cent from the value quoted by Pourbaix[12] and appears to bear a relationship to the higher values given by Latimer[68],* the sequence from $U(OH)_4$ to UO_3 has been chosen in preference to the sequence from UO_2 to UO_3 for the reconstruction of the pH - potential diagram. The completed list of solid-solid equilibrium reactions and potentials is given below:

$$U + 4\,H_2O = U(OH)_4 + 4\,H^+ + 4\,e^- \qquad E_{HA} = -1.353$$

$$4\,U(OH)_4 = U_4O_9 + 7\,H_2O + 2\,H^+ + 2\,e^- \qquad E_{HA} = -0.7$$

$$3\,U_4O_9 + H_2O = 4\,U_3O_7 + 2\,H^+ + 2\,e^- \qquad E_{HA} = -0.1$$

$$U_3O_7 + H_2O = U_3O_8 + 2\,H^+ + 2\,e^- \qquad E_{HA} = +0.45$$

$$U_3O_8 + H_2O = 3\,UO_3 + 2\,H^+ + 2\,e^- \qquad E_{HA} = +1.53$$

Fig. 48a illustrates a reconstruction of the Pourbaix diagram. The broken lines 1 to 5 represent

*N.B. It is interesting that if the free energy of formation of UO_2 (- 257 Kcals.) quoted by Latimer is employed in calculating the UO_2 - U_3O_8 oxidation reaction[12]

$$3\,UO_2 + 2\,H_2O = U_3O_8 + 4H^+ + 4e^- \qquad E = +0.533 - 0.0591\ pH$$

then the free energy value obtained for U_3O_8 (-835 Kcals.) is in excellent agreement with the value obtained theoretically in the present work.

the equilibrium activities of the various ionic species in solution; these remain unaffected by the incorporation of $U(OH)_4$, U_4O_9 and U_3O_7 into the diagram. The values of the redox potentials which correspond to these lines have been taken from Pourbaix[12].

Equilibrium potentials between the solid species (underlined) are represented by the heavy horizontal lines. Equilibrium activities between solid and ionic species are calculated from the general expression:

$$E = E^{o} - 0.0591 \frac{m}{n} pH + \frac{0.0591a}{n} \log (C)$$

(where, E is the potential of the electrode in equilibrium with oxidized and reduced species in the reaction, E^{o} is the equilibrium potential when the reactants are all in the standard state, m is the stoichiometric coefficient of H^{+} ion, n is the stoichiometric coefficient of electrons, and a is the stoichiometric coefficient of the ionic species of which (C) is the concentration).

and are shown on the diagram by the set of lines marked A to I. The following type of reaction was considered :

A. $U = U^{3+} + 3\,e^{-}$ $\qquad E_{HA} = -1.798 + 0.0197 \log (U^{3+})$

D. $4UOH^{3+} + 5H_2O = U_4O_9 + 14H^{+} + 2e^{-}$ $\qquad E_{HA} = +0.348 - 0.355\ pH + 0.118 \log (UOH^{3+})$

I. $UO_2^{2+} + H_2O = UO_3 + 2H^{+}$ $\qquad \log (UO_2^{2+}) = 14.74 - 2pH$

It is possible now from Fig. 48a to consider the corrosion behaviour of uranium in alkaline solutions in terms of the formation of non-stoichiometric derivatives of the species U_3O_7, U_4O_9 and $U(OH)_4$. It has been shown (Figs. 35a and 35b) that the changes in the corrosion process of the 10 weight per cent alloy in pH 9.7 solution occur at more negative potentials than those of the pure metal. It is believed that this effect can be ascribed to the difference between the free energies of formation of the pure oxides and those of the mixed oxides which result from the corrosion of the alloy.

However, it is seen from the figure that, in the potential range of interest (E_{HA} = 0 V to E_{HA} = -0.6 V) the solid species U_4O_9 and U_3O_7 are stable in both alkaline solutions and in pH 5.4 It is still difficult, therefore, to account for the difference between the corrosion behaviour in the two environments in terms of the formation of distinct species. Nevertheless, since no other explanation for this phenomenon seems rational, it may be concluded that although the reconstructed Pourbaix diagram provides a fuller representation of the U - H_2O system than the previous one (Fig. 7), it is by no means either entirely complete or accurate, and that it is possible, for example, that the lines representing ionic activity (A to I) should be shifted a number of pH units to the right.

Consider the activity lines D representing the reaction

$$4\ UOH^{3+} + 5\ H_2O = U_4O_9 + 14\ H^+ + 2e^- \quad \text{(Fig.48a)}$$

If these are moved two pH units to the right, then the continuation of the unit activity line (marked 0) will cut the vertical axis of the diagram at $E_{HA} = +0.92$ V, which value will correspond to E° in the equation $E = E^\circ - 0.0591 \frac{m}{n}\ pH + \frac{0.0591a}{n} \log (C)$. Assuming that no change is involved in the free energy of formation of the solid species U_4O_9, the free energy of the ionic species UOH^{3+} may be recalculated by use of the expression

$$\frac{\sum_x (\nu_x \mu^\circ_x)}{23{,}060\ n} = E^\circ$$

Since it may be assumed further that the potentials of the redox reactions 1 to 5 are accurately established and not liable to change, it is possible to re-estimate the free energies of formation of all ionic species on the basis of the value thus deduced for UOH^{3+}. Table 5 shows both the values quoted by Pourbaix and the new values which follow from a two pH unit shift to the right of the ionic-solid equilibria in Fig. 48a.

TABLE FIVE

	Pourbaix values	Recalculated values
U^{3+}	124.4 Kcals	131.1 Kcals.
U^{4+}	138.4 "	145.1 "
UOH^{3+}	193.5 "	200.2 "
UO^{2+}	236.4 "	243.1 "

Clearly, the 'new' values are not significantly different from the figures given by Pourbaix.

Fig. 48b illustrates the Pourbaix diagram, using the recalculated free energies of formation for the ionic species, derived to fit the data obtained during the present work. Although it would appear from the equilibria that the formation of a solid compound is impossible in the region to the left of the ionic-solid activity lines, the kinetic data do not agree. Experimentation has shown film growth on uranium cathodically-polarised in sulphuric acid solutions of unit pH. It is probable, however, that the solid species formed under such conditions differ fundamentally from the compounds stable under equilibrium conditions, and it is suggested, therefore, that Fig.48b can be used to provide a satisfactory explanation for the difference between the corrosion behaviour of uranium in pH 5.4 and in alkaline solutions in terms of the formation of dissimilar species in the two environments.

V(h) Electrode Measurements

Detailed discussions of electrode measurements on pure uranium and an uranium-molybdenum alloy have already been published elsewhere[4,9]. It was concluded from these reports (i) that the very high values of capacity and conductivity which are recorded for these metals at less negative potentials are evidence of a valency change occurring in the oxide formed, and (ii) that the mechanism of the increase in conductivity with current density at very cathodic potentials is difficult to explain.

The formation, in alkaline solutions, of higher oxides of uranium, associated with a change in valency from 4^+ to 6^+ of some fraction of the metal ions, has been predicted from theoretical considerations. Therefore, it is interesting that the peak in the capacity and conductivity of the pure uranium electrode in pH 9.7 solution (Fig. 22) is found at approximately E_{HA} = +0.4 V, which corresponds to the potential at which a change occurs in oxide species from U_3O_7 to U_3O_8 (Fig. 48b). According to the same theory, similar peaks in capacity and conductivity should be observed at the equilibrium potentials between other oxide phases. Some recent research[70] has, in fact, shown the existence of a further peak at a potential positive to +0.4 E_{HA},

and it is believed that this corresponds to the equilibrium between U_3O_8 and UO_3. The absence of the two peaks which should be associated with the U_4O_9 - U_3O_7 and $U(OH)_4$ - U_4O_9 equilibria at more cathodic potentials, however, requires to be explained. Possible explanations appear to be (1) that the oxide-oxide reactions at these potentials are highly irreversible and occur so slowly that the capacity effect is not observed; (2) that the definition of the peaks may be impaired by the non-stoichiometry of the oxide present on the metal, and, thus, in the case of the U_4O_9 - U_3O_7 equilibrium the associated "peak" may be incorporated in the broad "peak" ascribed to the U_3O_7 - U_3O_8 equilibrium; (3) that the hydrogen evolution reaction can, in some way, mask the changes in the measured capacity of the system.

Two other points are relevant to the discussion. First, it can be seen from Figs. 22, 23 and 24 that the addition of zirconium to uranium appears to lower the potentials at which the peaks in capacity and conductivity occur. It is believed that this confirms the previous observation, ascribed to the difference between the free energies of formation of the pure oxides and those of the mixed oxides which result from the corrosion of alloys, that alloying causes the changes in corrosion process to

occur at more negative potentials (compare Figs. 34a, 34b with Figs. 35a, 35b). Second, it has been reported[70] that the values of capacity and conductivity measured for U/UO_2 electrodes in pH 5.4 solution are significantly lower than in alkaline solutions, and that "peaks" do not occur. This may be taken as an independent illustration of the difference between the oxides formed during corrosion in the two types of solutions.

With regard to the increase in conductivity and current density at very cathodic potentials, it would appear that for the oxides of metals such as zirconium, aluminium and tantalum, where the capacity bears an inverse relationship to the thickness (i.e. the oxide behaves as a dielectric), this is caused by a real decrease in the resistance of the oxide due to the entry of hydrogen as can be shown[55] by measurements at more positive potentials immediately after cathodic polarisation. Under these conditions of low imposed current and, hence, low Faradaic admittance, the measured resistance of the oxide remains low for a short time. In the case of pure uranium and the uranium-molybdenum alloy, however, this experiment is not possible since at the more positive potentials the reaction in the oxide produces a large Faradaic admittance which masks the relatively small effect on the resistance due to the hydrogen. Here, although this simple explanation has yet to be confirmed, it is believed that the increase in the

conductivity and the current may be ascribed to a combination of both Faradaic and oxide effects. As a result of these complexities, it does not seem possible to relate the capacities at these cathodic potentials either to the double-layer capacity or, simply, to the oxide thickness.

The hysteresis effect which was observed for all impedance and current density curves has been previously discussed by several workers[4,9,55] who obtained similar results. The present work does not add to the explanations offered. The effect of oxygen in solution on the electrode properties of uranium has been studied in detail by Isaacs[9] and it is not proposed to discuss these results here.

SECTION VI.

SUMMARY AND CONCLUSIONS

VI(a) Summary.

The following list summarises the major observations made during the course of the present work:-

(1) The room-temperature corrosion of uranium in non-alkaline solution (pH 5.4) follows the kinetic sequence: parabolic-linear$_1$-linear$_2$. The kinetics at higher temperatures and in alkaline solutions can be more complex.

(2) Cathodic polarisation of uranium and its alloys in non-alkaline solution increases the corrosion rate. It is found that the corrosion rate is directly related to the square of the hydrogen activity.

(3) For given conditions, an increase in cathodic polarisation does not significantly alter the thickness of the protective oxide formed on uranium and the alloys during corrosion.

(4) Alloy additions of zirconium to uranium are found to increase both the diffusion rates in the protective oxide and the thickness of the film.

(5) Although the rate of parabolic growth is increased by zirconium additions to uranium, the overall corrosion rate is reduced due to the greater thickness of the protective film.

(6) The activation energy for the aqueous corrosion of uranium is much lower than the activation energy both

for atmospheric oxidation and for oxygen self-diffusion in UO_2, and is reduced further both by the addition of zirconium as an alloying constituent and, for both the pure metal and the alloy, by cathodic polarisation.

(7) The uranium-water pH-potential diagram due to Pourbaix and co-workers[12] does not appear to provide a comprehensive representation of the system for the conditions employed in the present research.

(8) The overall corrosion rate of uranium and uranium-zirconium alloys in alkaline solutions is increased by increasing solution pH.

(9) The corrosion products formed in non-alkaline solution are believed to differ significantly from those formed in alkaline solutions.

(10) The corrosion rate of uranium is a sensitive function of the oxygen concentration in the test solution.

(11) The measured capacities and conductivities of those metal-oxide systems in which the metal can display two or more valencies are difficult to interpret in conventional terms.

VI(b) Conclusions

The following conclusions have been drawn from the results obtained in the present research :-

(1) Hydrogen increases the corrosion rate of uranium and its alloys in non-alkaline solutions without disrupting the protective oxide. This conclusion does not support

the view held by Draley and Ruther[3] that the deleterious effects of hydrogen can be explained on the basis either of physical changes in the oxide or the formation of a hydride or gas phase at the metal-oxide interface, but suggests rather that the higher rates follow from a change in the electrical properties of the protective oxide due to the increase in the activity of hydrogen ions. A similar argument has been proposed by Wagner[11] to account for the dependence on the electronic conductivity of the rate of sulphidation in the system Ag - Ag_2S - S.

(2) Alloying with zirconium has a marked effect on both the ionic diffusion rates in and the thickness of the protective oxide. The increase in diffusion is difficult to explain in terms of the conventional 'Hauffe Valency Rule', but may result from an increase in disorder in the oxide lattice due to the presence of zirconium ions. The increase in thickness has been interpreted to imply a change in the mechanical properties of the oxide due to alloying. It seems likely that such changes are associated with an increase in the plasticity of the oxide rather than in the strength.

(3) The energy requirements for the aqueous corrosion of uranium are significantly different from those for atmospheric oxidation. This may imply that the presence of water (or H^+ ions) can cause a considerable change in

the corrosion process involving, perhaps, very high mobility of the metal ions. McNamara[63] has recently shown that small additions of zirconia to urania increase the mobility of uranium ions in the solid mixture. This observation supports the present results which have shown that the activation energy for the corrosion of uranium is reduced by alloy additions of zirconium.

(4) The corrosion behaviour of uranium and uranium-zirconium alloys in alkaline solutions has been shown to be markedly different from the behaviour in pH 5.4 solution. Alkalinity appears to influence not only the corrosion rate but the nature of the protective film. The effect of cathodic polarisation in alkaline solutions has been discussed in terms of changes in the stoichiometry of the corrosion product.

(5) The corrosion of uranium is a process of some complexity. Clearly, further work is necessary both to clarify and to establish many of the effects which have been observed in this investigation. An evaluation of the relative importance of these effects has led to the following proposals for future work :

(a) That corrosion rate measurements be conducted over a period of time which comprises both protective and non-protective oxide growth, and, further, that during measurement such variables as potential, pH, temperature and oxygen content of the solution be strictly controlled.

(b) That the effect of surface preparation on the corrosion rate be investigated.

(c) That rate measurements be extended to include other alloys of uranium in order to establish whether, as in the case of uranium-zirconium alloys, an improvement in corrosion resistance is again associated with an increase in the thickness of the protective oxide.

(d) That an independent study of the deformation of uranium oxides be conducted in order to establish whether alloying of the base metal leads to greater strength or to greater plasticity of the mixed oxide.

(e) That high temperature measurements be extended to cover a wider range both of temperature and of solution pH in order to establish, among other things, whether the higher corrosion rates observed in alkaline solutions are accompanied by a change in activation energy.

(f) That the semi-conduction of uranium oxides be investigated as a function of hydrogen content and O/U ratio.

(g) That the difference between the structure and composition of corrosion products formed in non-alkaline and alkaline solutions be established by an independent technique such as electron diffraction.

ACKNOWLEDGEMENTS

The author is deeply indebted to his supervisor Dr. J.S.Ll.Leach, without whose advice and unfailing encouragement this thesis might never have been conceived and certainly would not have been delivered. He is also grateful to the other members of the Corrosion Research Group at the Royal School of Mines with whom he had many valuable discussions, and, in particular, to Mr. J.C.Brunel for the technical assistance he rendered in times of difficulty. The author thanks also Mrs. Spiddal who produced the typescript of this thesis at such high speed.

The author expresses his gratitude to Professor J.G.Ball in whose department this work was carried out for permission to use the laboratory facilities. The financial support of the U.K.A.E.A. is also gratefully acknowledged.

REFERENCES.

1. R.K.Geary. U.S.A.E.C. Rept. Westinghouse Electric Corporation. WAPD - 127 Part I (1955).
   M.W.Burkart. U.S.A.E.C. Rept. Westinghouse Electric Corporation. WAPD - 127 Part III (1956).
2. J.E.Draley and W.E.Ruther. Corrosion (1956) 12, 441t, 480t.
3. J.E.Draley and W.E.Ruther. J.E.C.S. (1957) 104, 329.
4. J.S.L.Leach. J.I.M. (1959) 88, 24.
5. T.P.Hoar and U.R.Evans. J.E.C.S. (1952) 99, 212.
6. J.T.Waber. Aqueous Corrosion of Uranium and its Alloys, Brussels Conference on Aqueous Corrosion of Reactor Materials (1959).
7. J.T.Waber. U.S.A.E.C. Rept. Los Alamos Scientific Laboratory LA-1381 (1948).
8. E.F.Losco. U.S.A.E.C. Rept. Westinghouse Electric Corporation WAPD-PMM-238 (1955).
9. H.S.Isaacs. D.I.C. Thesis (1960) Imperial College, London.
10. G.D.Fawkes. Private communication (1961).
11. C.Wagner. J.Chem.Phys. (1953) 21, 1819.
12. E.Deltombe, N.de Zoubov and M.Pourbaix. Cebelcor, Rapport Technique No.31 (1956).
13. F.Gronvald. J.Inorg.Nucl.Chem. (1955) 1, 897.
14. P.E.Blackburn. J.Phys.Chem. (1958) 62, 897.

15. R.K.Willardson, J.W.Moody and H.L.Goering. U.S.A.E.C. Rept. Battelle Memorial Institute, BMI-1135 (1956).

16. J.Belle and B.Lustman. U.S.A.E.C. Rept. Westinghouse Electric Corporation. WAPD-184 (1957).

17. C.Wagner. J.Chem.Phys. (1950), 18, 62.

18. D.Grahame. J.E.C.S. (1952), 99, 370C.

19. L.Young. Trans. Faraday Soc. (1955) 51, 1250.

20. J.V.Petrocelli. J.E.C.S. (1959) 106, 566.

21. A.Charlesby. U.K.A.E.A. Rept. AERE M/R (1953) 1176.

22. J.N.Wanklyn and D.R.Silvester. J.E.C.S. (1958) 105,647.

23. J.J.McMullen and N.Hakerman. J.E.C.S. (1959) 106, 341.

24. J.N.Wanklyn. Colloque sur la Corrosion, Saclay (1959).

25. W.T.Denholm. Priv. Comm. (1958) Imperial College, London.

26. N.Cabrera and N.F.Mott. Rep. Progr.Phys. (1948-49) 12, 163.

27. U.R.Evans. Rev. pure and appl. Chem. (Melbourne 1955) 5, 1.

28. J.F.Dewald. J.E.C.S. (1956) 103, 690.

29. N.F.Mott. Trans.Faraday Soc. (1939) 35, 1175.

30. C.Wagner. Z.Phys.Chem. (1933) B21, 25, reported in O.Kubaschewski and B.E.Hopkins 'Oxidation of Metals and Alloys', London (Butterworth 1953) and reference 33.

31. T.P.Hoar and L.E.Price. Trans.Faraday Soc. (1938) 34, 714.

32. W.B.Pilling and R.E.Bedworth. J.I.M. (1923) 29, 529.

33. U.R.Evans. The Corrosion and Oxidation of Metals, London (Arnold 1960).

34. J.E.Antill. Communicated at lecture (Jan.1961) Imperial College, London.

35. A.A.Pray and W.E.Berry. U.S.A.E.C. Rept. Battelle Memorial Institute BMI-893 (1953).

36. J.E.Draley et al. U.S.A.E.C. Rept. Argonne National Laboratory ANL-5030 (1953).

37. M.Hansen. Constitution of Binary Alloys, New York (McGraw-Hill 1958).

38. J.E.Draley, S.Greenberg and W.E.Ruther. U.S.A.E.C. Rept. Argonne National Laboratory ANL-5530 (1957).

39. A.A.Bauer, S.Kass and K.M.Goldman. Phys.Met. and Props. of Zr-U Alloys. Paper 1785, Proc. 2nd Int. Conf. on Peaceful Uses of Atomic Energy (Geneva 1958).

40. F.A.Rough. U.S.A.E.C. Rept. Battelle Memorial Institute BMI-1030 (1955) reported in reference 6.

41. F.A.Rough and A.A.Bauer. U.S.A.E.C. Rept. Battelle Memorial Institute BMI-1300 (1958).

42. J.N.Chirigos. U.S.A.E.C. Rept. Westinghouse Electric Corporation WAPD-T-985 (1959).

43. D.Cubiciotti. Illinois Institute of Technology, Technical Rept. NP-3208 (1951) reported in reference 6.

44. M.Roberts. Brit. J. Appl.Phys. (1954) 3, 351.

45. C.Edeleanu. Nature (1954) 173, 739.

46. A.E.Stebbens and L.L.Shrier. J.E.C.S. (1961) 108, 30.

47. A.E.Stebbens. Ph.D. Thesis (1959) London University.

48. J.T.Waber. U.S.A.E.C. Rept. Los Alamos Scientific Laboratory LA-2035 (1958).

49. D.Cubiciotti. J.Amer.Chem.Soc. (1952) 74, 1079.

50. J.E.Antill and K.A.Peakall. J.Less Common Metals, (1961) 3, 239.

51. A.A.Griffith. Phil.Trans.Roy.Soc. (1920) A221, 163.

52. J.N.Wanklyn and B.E.Hopkinson. J.Appl.Chem. (1958) 8, 496.

53. A.R.Bray, P.W.M.Jacobs and L.Young. J.Nucl.Materials (1959) 1, 359.

54. N.J.M.Wilkins. Private communication (1962).

55. G.D.Fawkes. M.Sc. Thesis (1963) London University.

56. K.Hauffe. Progr. in Metal Phys. Vol.4, London (Pergamon 1953).

57. R.W.Nichols and C.Tyzack. U.K.A.E.A. Industrial Group Rept. IGR-TN/C.639.

58. W.D.Kingery. Introduction to Ceramics, New York, (Wiley, 1960).

59. G.Christie and J.Williams. J.Nucl.Materials (1962),5,1.

60. R.Scott, A.R.Hall and J.Williams. J.Nucl.Materials (1959), 1, 39.

61. C.O.Hulse and J.A.Pask.J.Am.Ceramic Soc. (1960) 43,373.

62. A.E.Gorum, W.J.Luhman and J.A.Pask. J.Am.Ceramic Soc. (1960), 43.

63. P.McNamara. Private communication (1962).

64. D.E.Thomas. U.S.A.E.C. Rept. Westinghouse Electric Corporation WAPD-T-186 (1954).

65. E.C.Potter and G.M.W.Mann. Contribution to 1st International Congress on Metallic Corrosion, London (1961).

66. E.A.Gulbransen and R.Ruka. J.Metals, New York (1950) 188, 1500.

67. L.Brewer. Chem. Rev. (1953), 52, 1.

68. W.M.Latimer. Oxidation Potentials, New York. (Prentice-Hall 1952).

69. J.J.Katz and E.Rabinowitch. The Chemistry of Uranium. Nat. Nucl. Eng. Series. Div. VIII - 5 New York (McGraw-Hill 1951).

70. H.S.Isaacs. Private communication (1962).

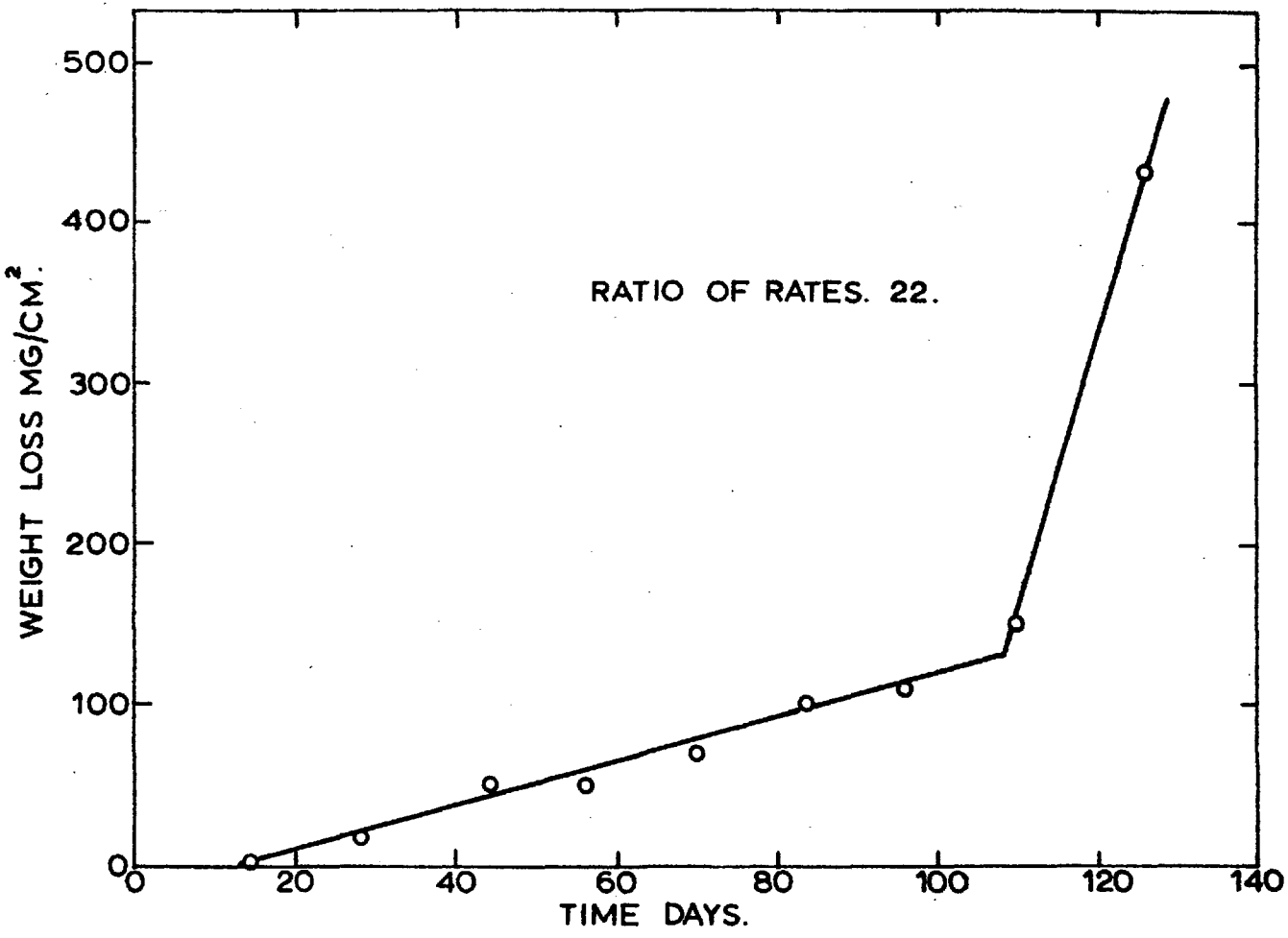

FIG. 1. CORROSION-RATE OF AN URANIUM ALLOY. IN HIGH TEMPERATURE WATER.(1)

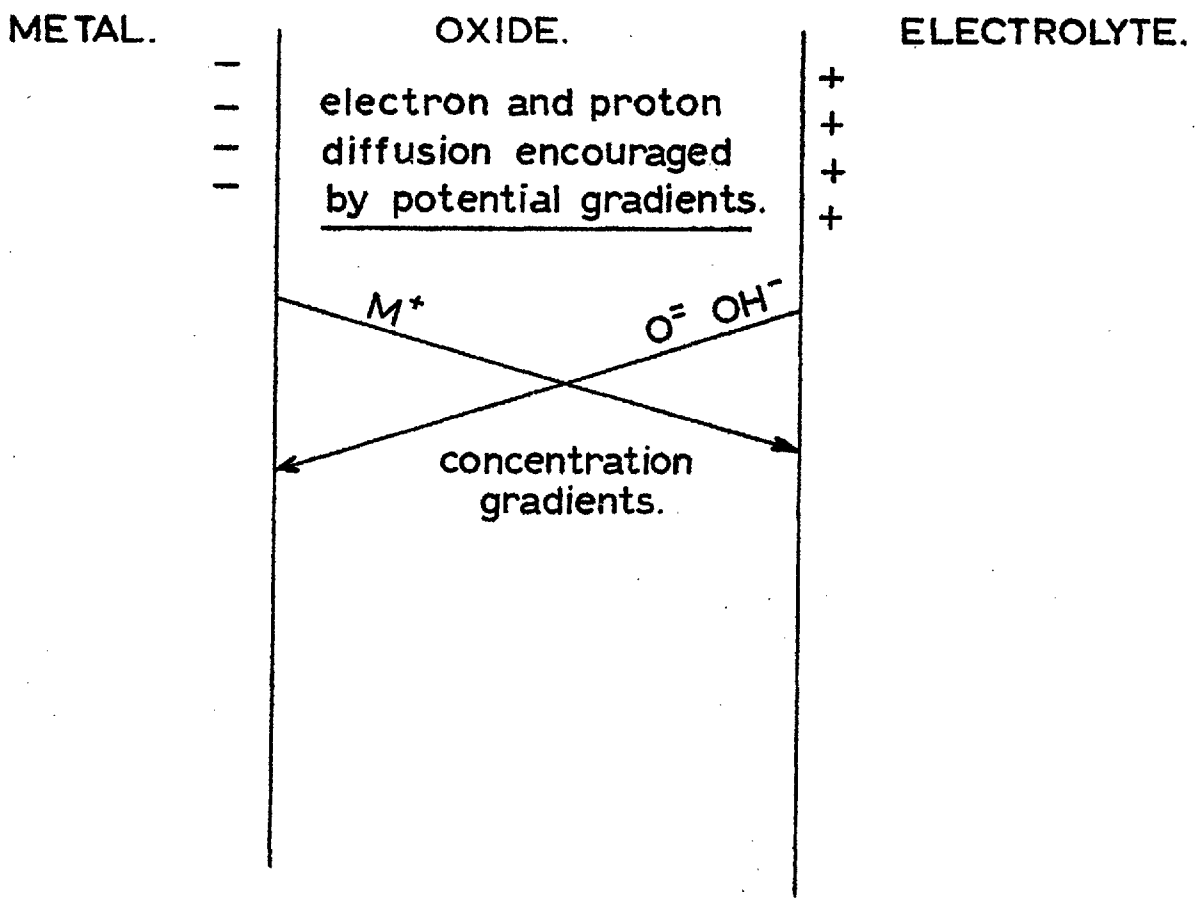

FIG. 2.

GRADIENTS ENCOUNTERED WITHIN GROWING OXIDE.

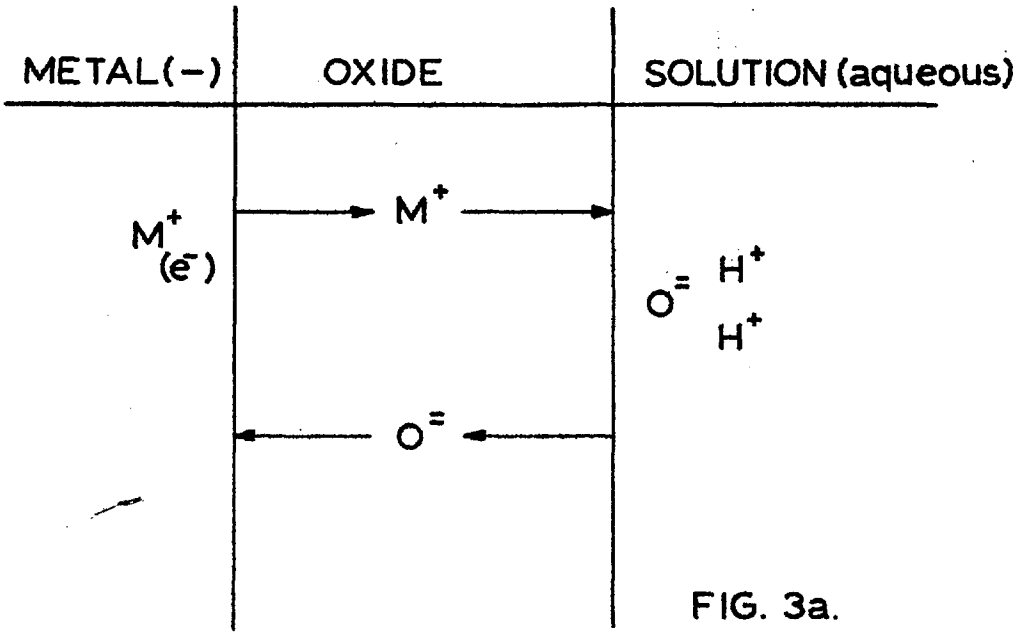

FIG. 3a.
ANODIC.

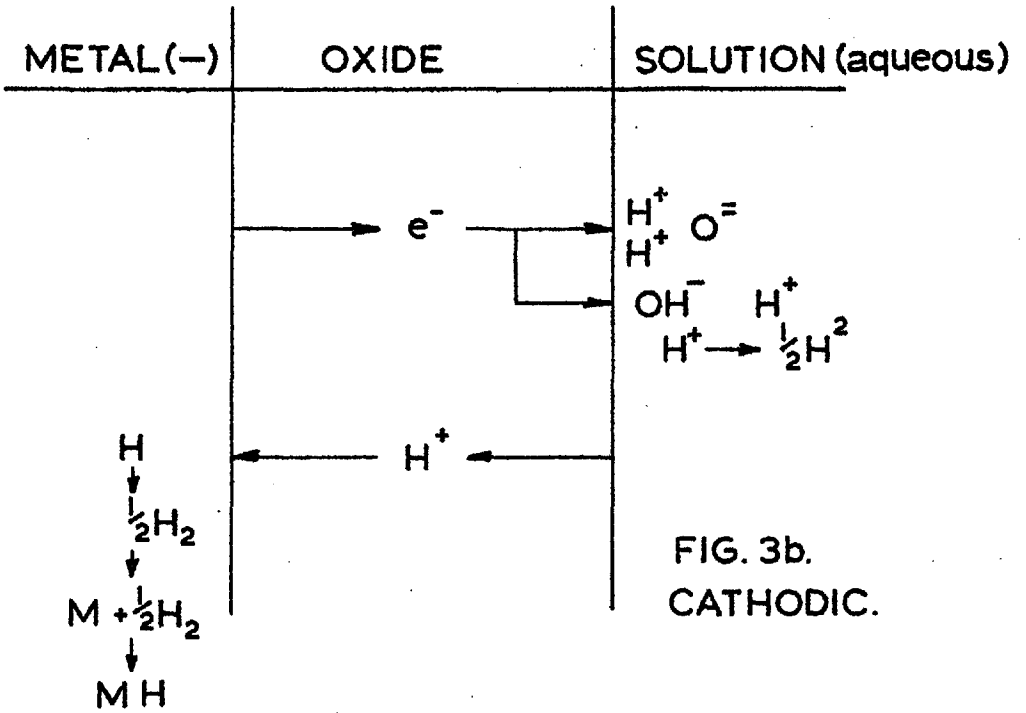

FIG. 3b.
CATHODIC.

ANODIC AND CATHODIC PROCESSES IN AN OXIDE. (3)

DISCHARGE OF SOLVATED PROTON.

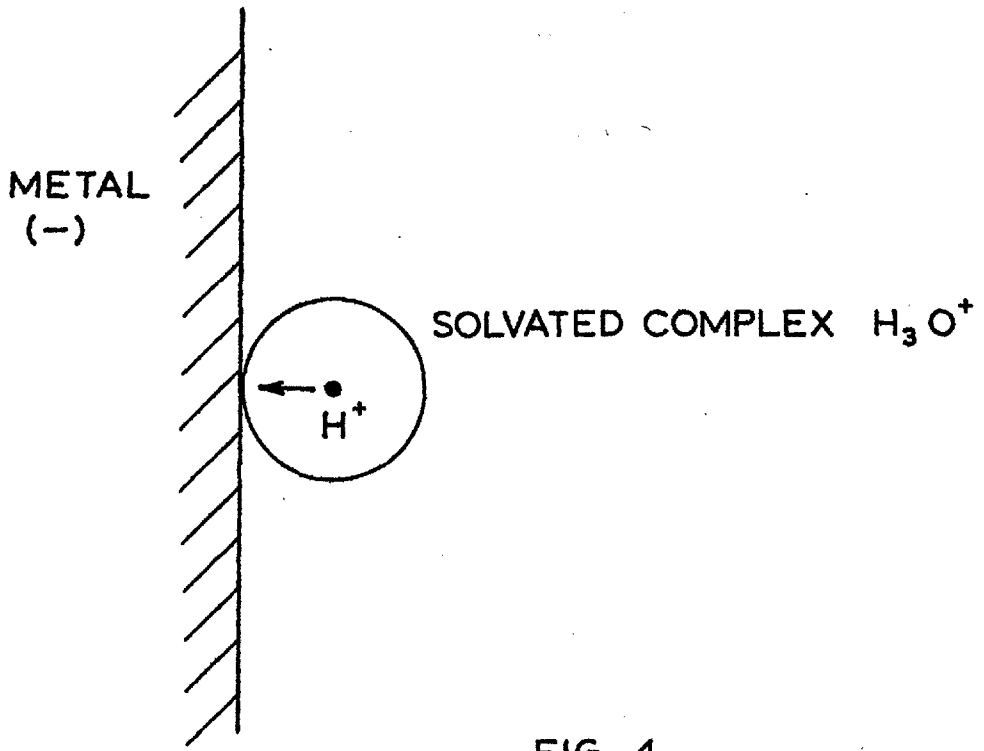

FIG. 4.

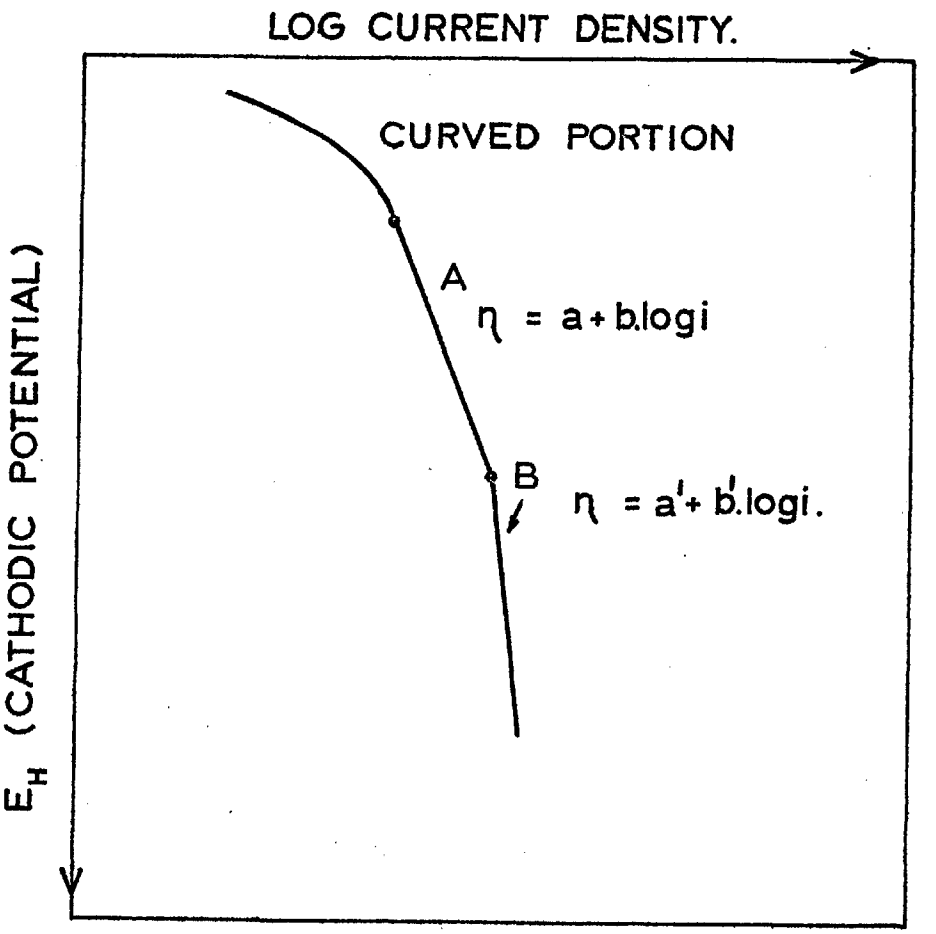

FIG. 5. CURRENT vs POTENTIAL BEHAVIOUR OF OXIDE-FREE CATHODE.

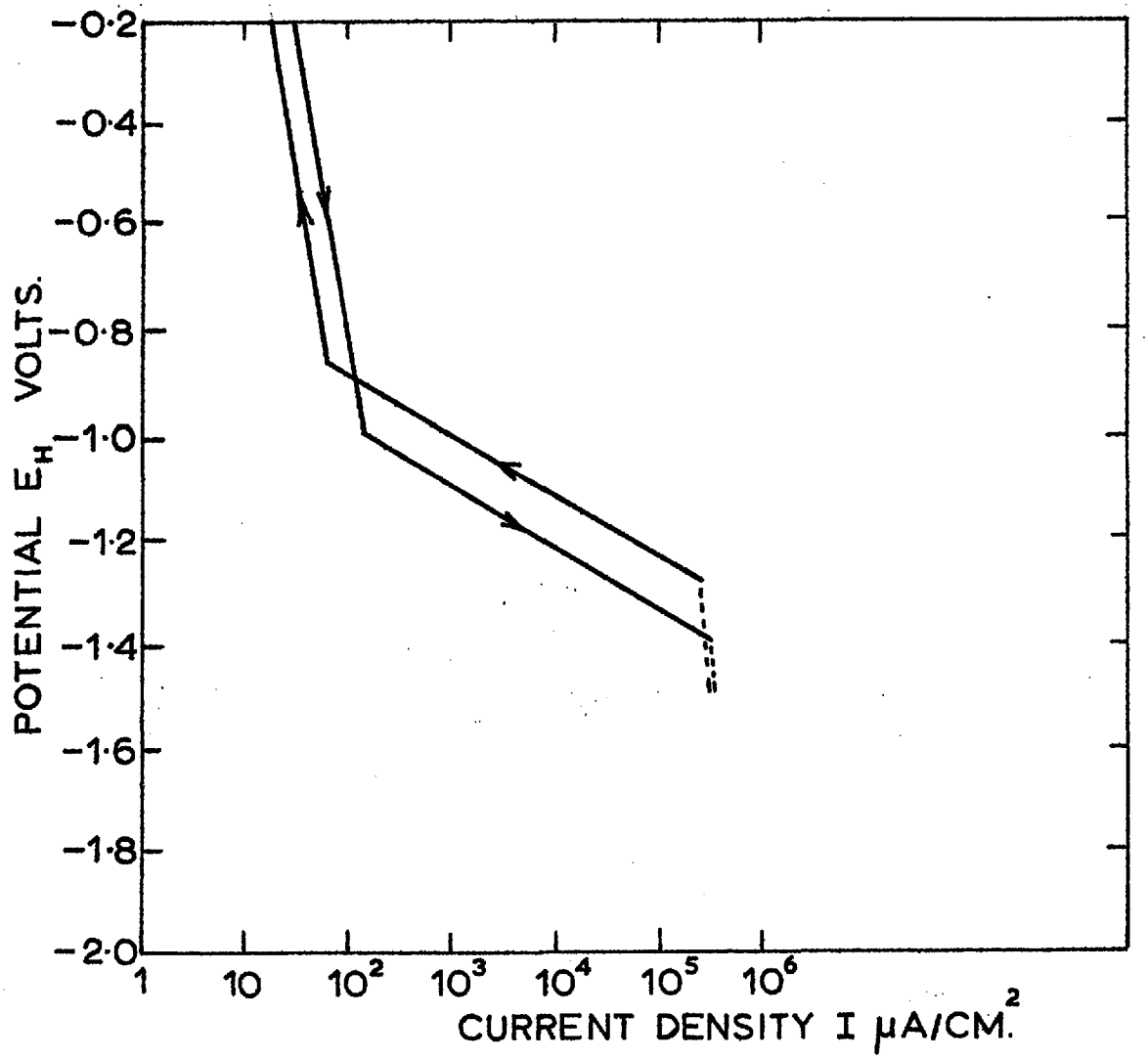

FIG. 6. GENERAL CURRENT-POTENTIAL RELATIONSHIPS FOR AN URANIUM ALLOY.

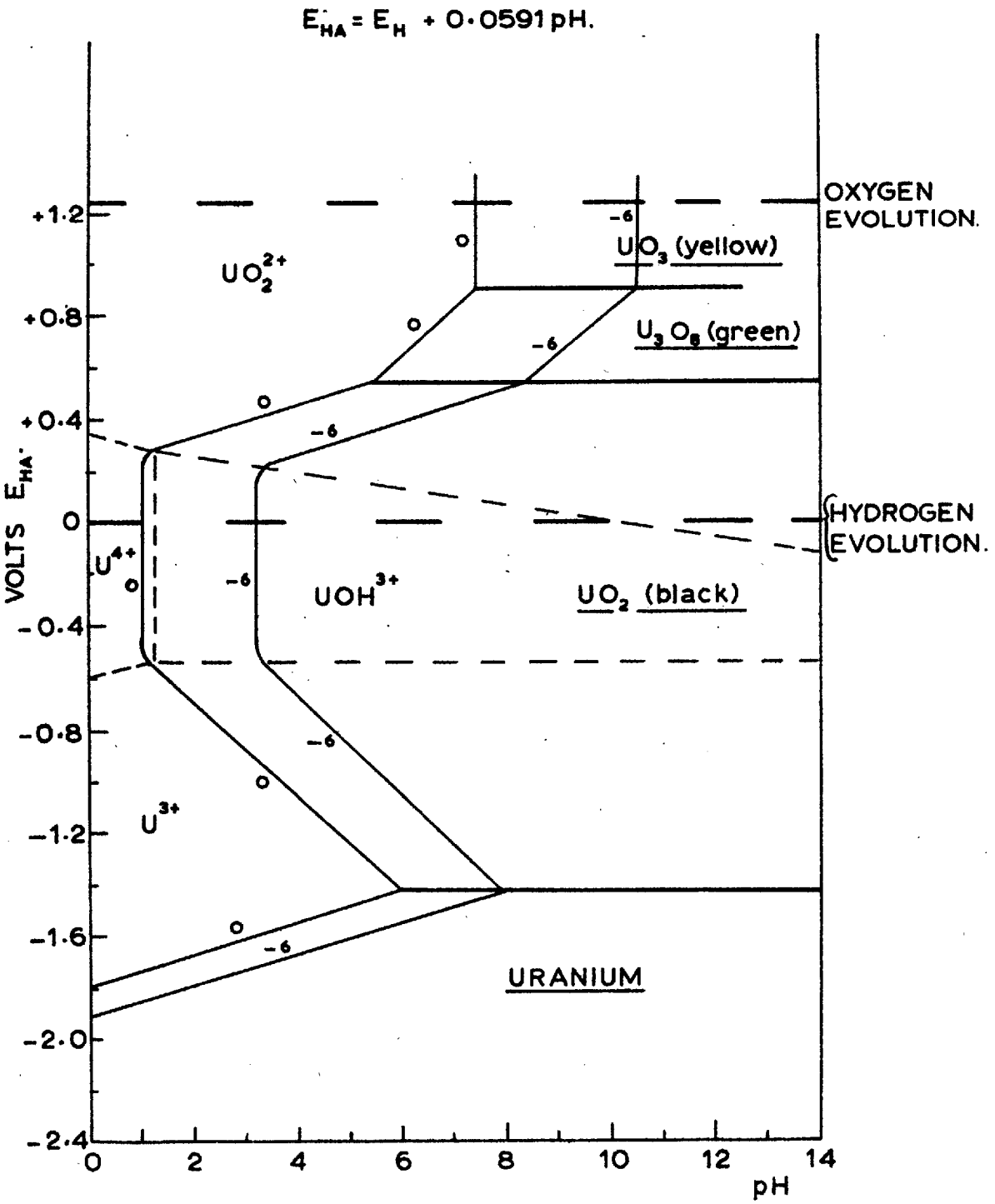

pH – POTENTIAL DIAGRAM FOR U – H_2O SYSTEM.
(AFTER POURBAIX)

FIG. 7.

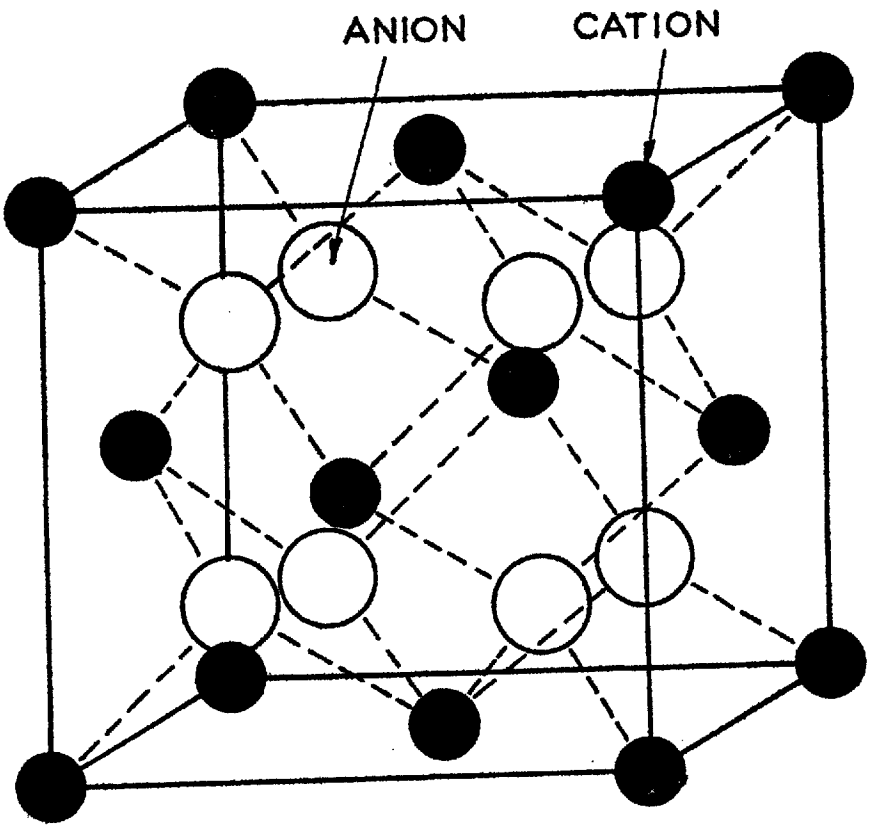

FLUORITE TYPE CRYSTAL LATTICE.

FIG. 8.

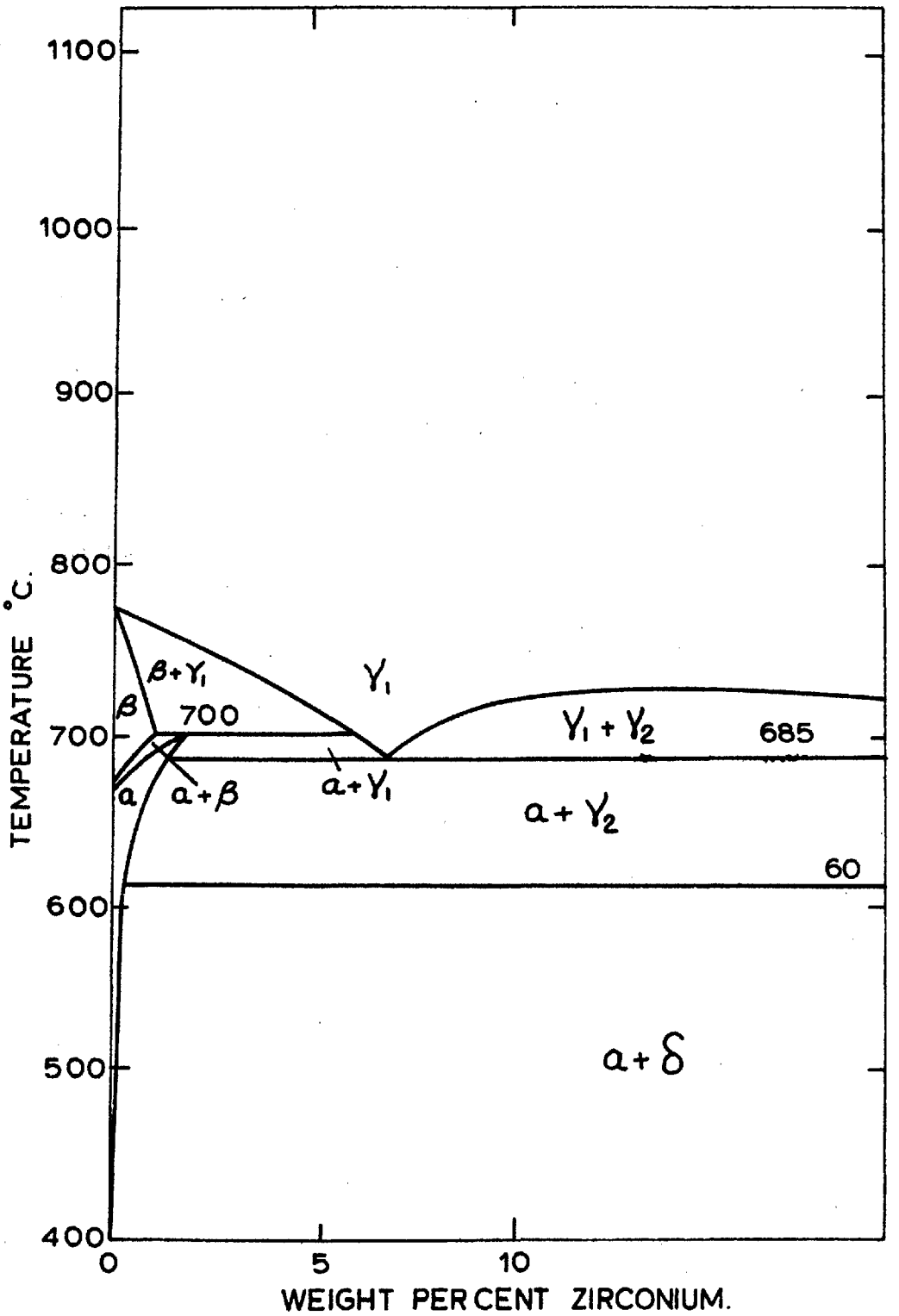

FIG.9. PHASE DIAGRAM OF URANIUM-RICH URANIUM-ZIRCONIUM ALLOY SYSTEM.(41)

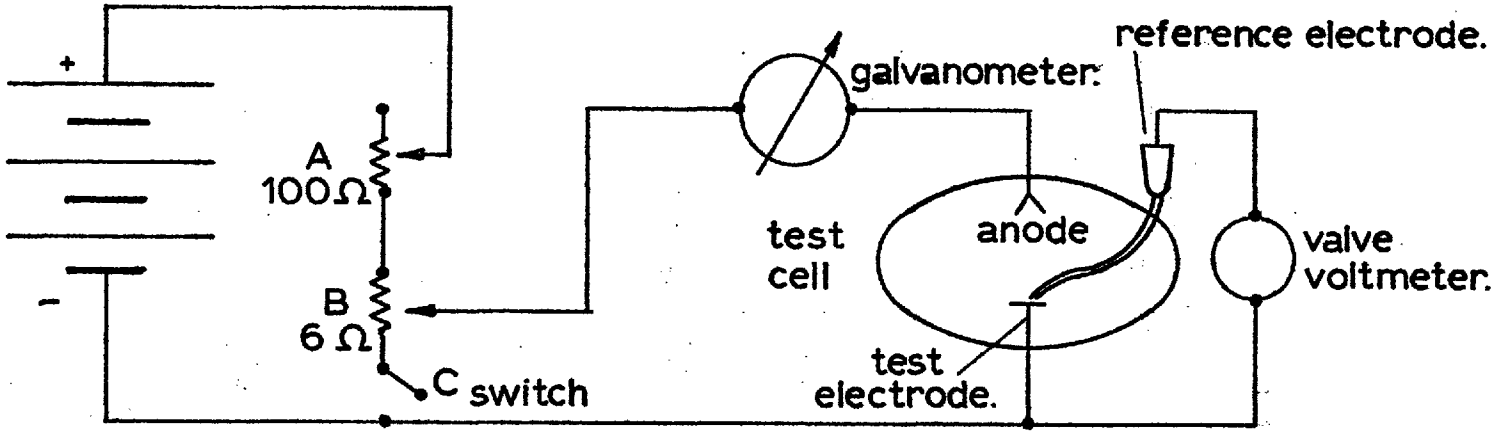

FIG.10. CIRCUIT DIAGRAM FOR OVERPOTENTIAL MEASUREMENTS.

FIG. 11. CELL USED FOR OVERPOTENTIAL MEASUREMENTS

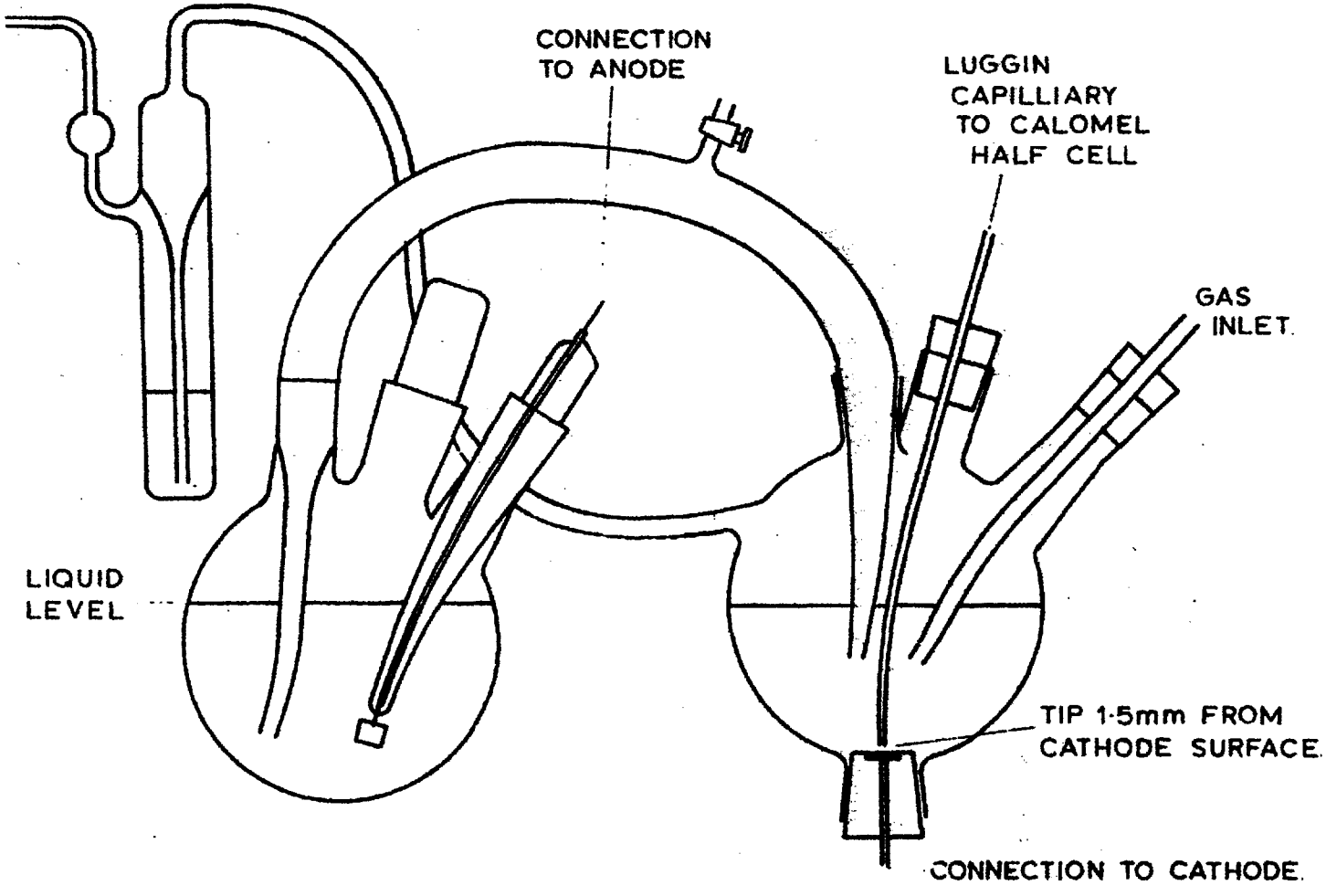

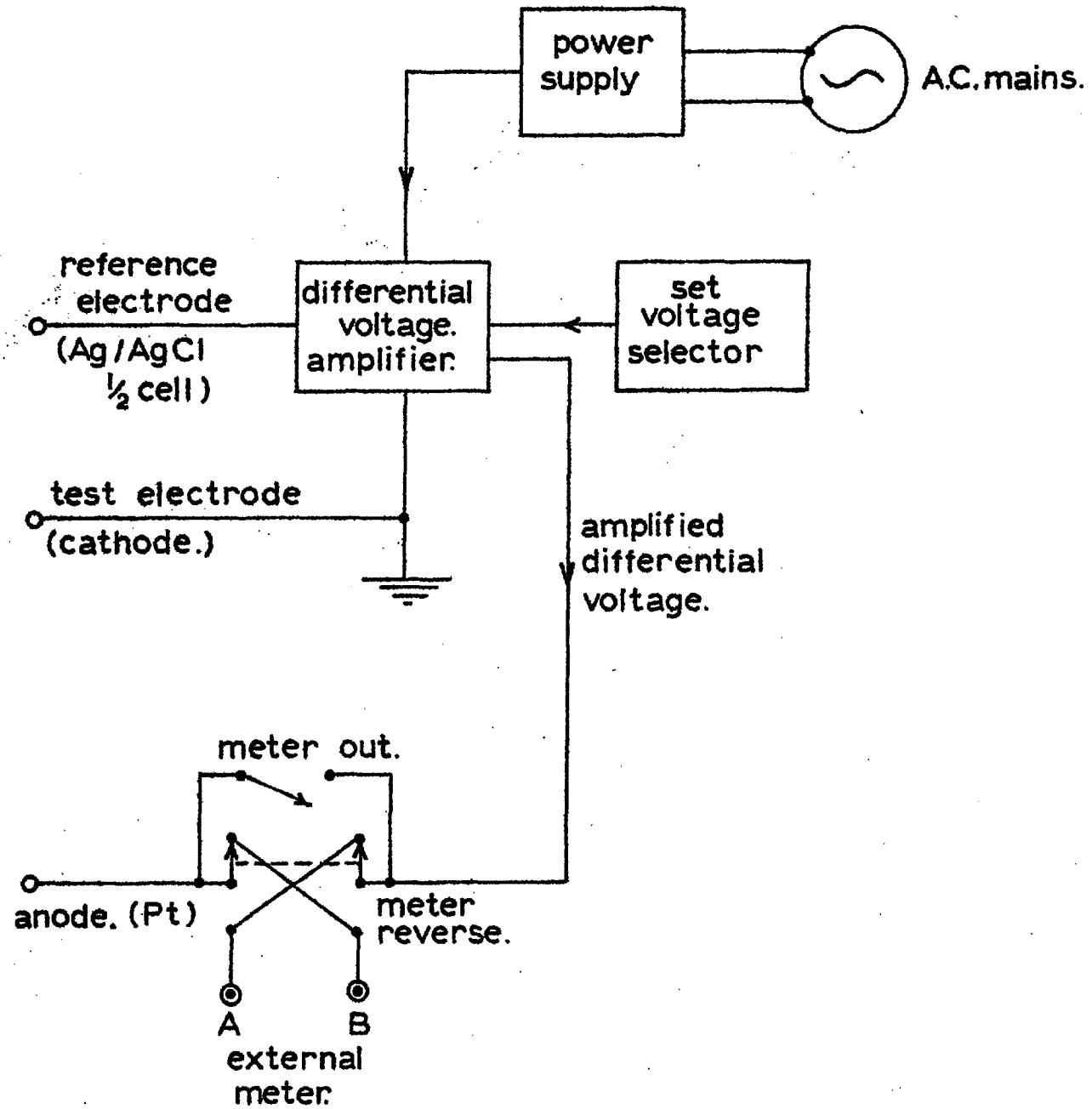

(44)(45)

FIG. 12. SCHEMATIC DIAGRAM OF POTENTIOSTAT.

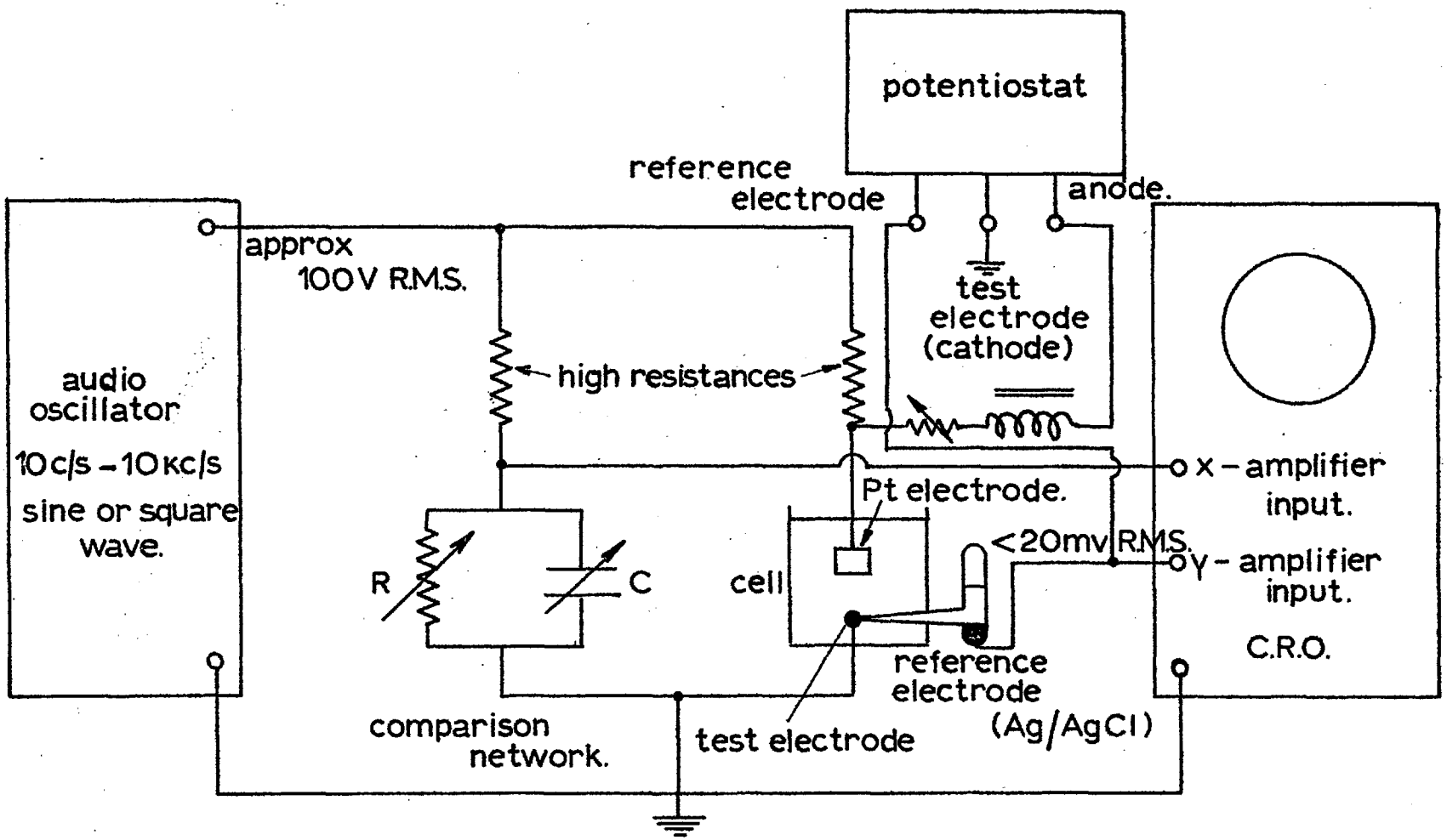

FIG. 13. SCHEMATIC DIAGRAM OF IMPEDANCE-MEASURING EQUIPMENT.

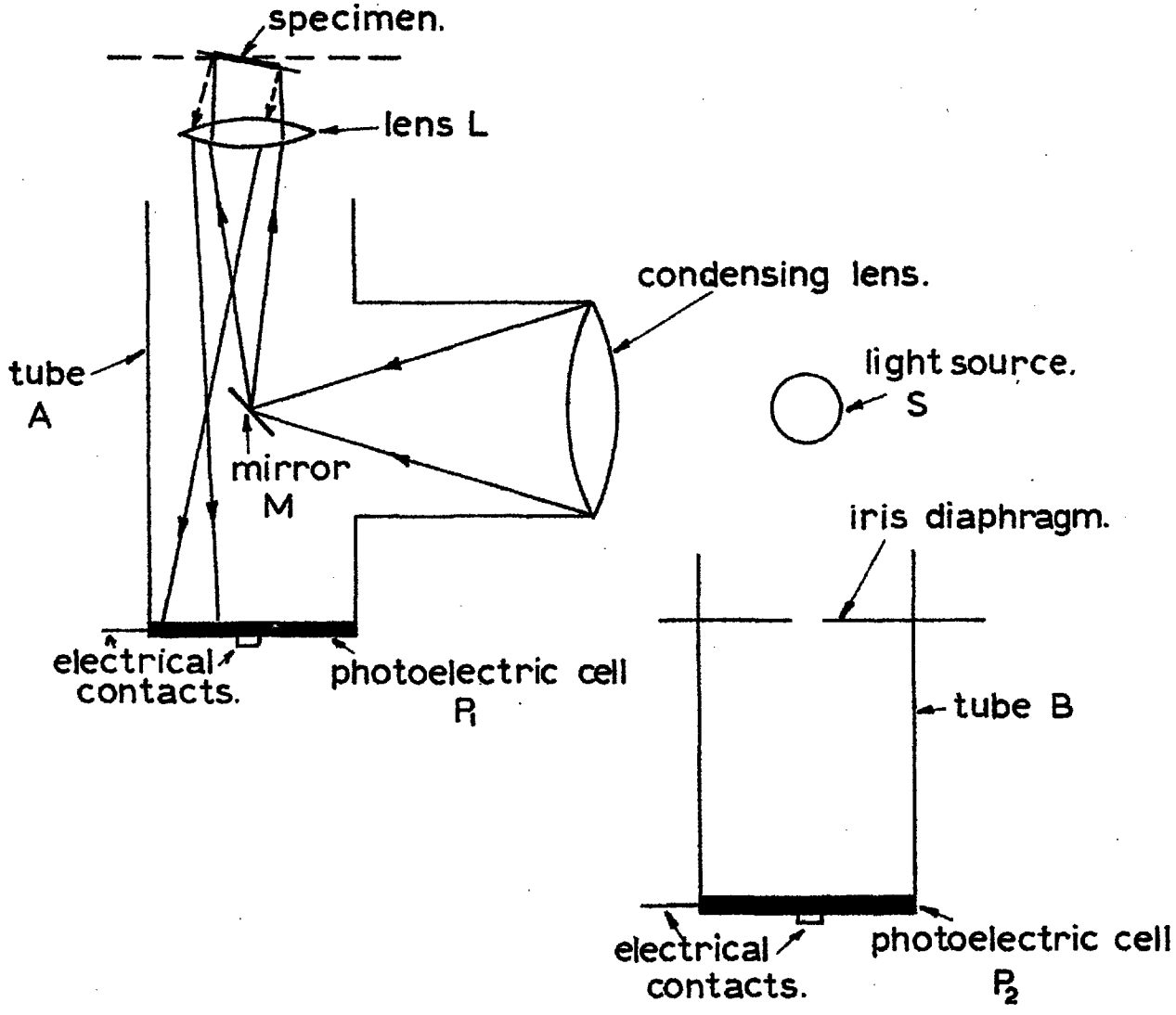

FIG. 14. SCHEMATIC DIAGRAM OF OPTICAL EQUIPMENT FOR MEASURING CORROSION RATES.

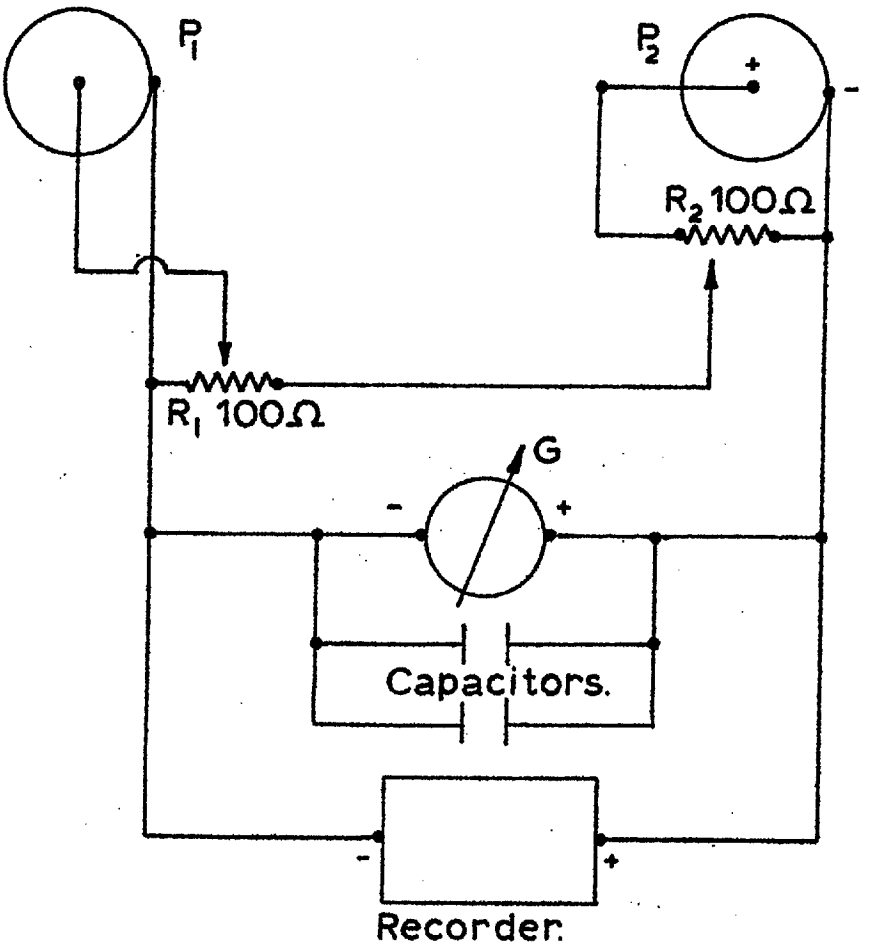

FIG. 15.

ELECTRICAL CIRCUITRY OF THE OPTICAL EQUIPMENT

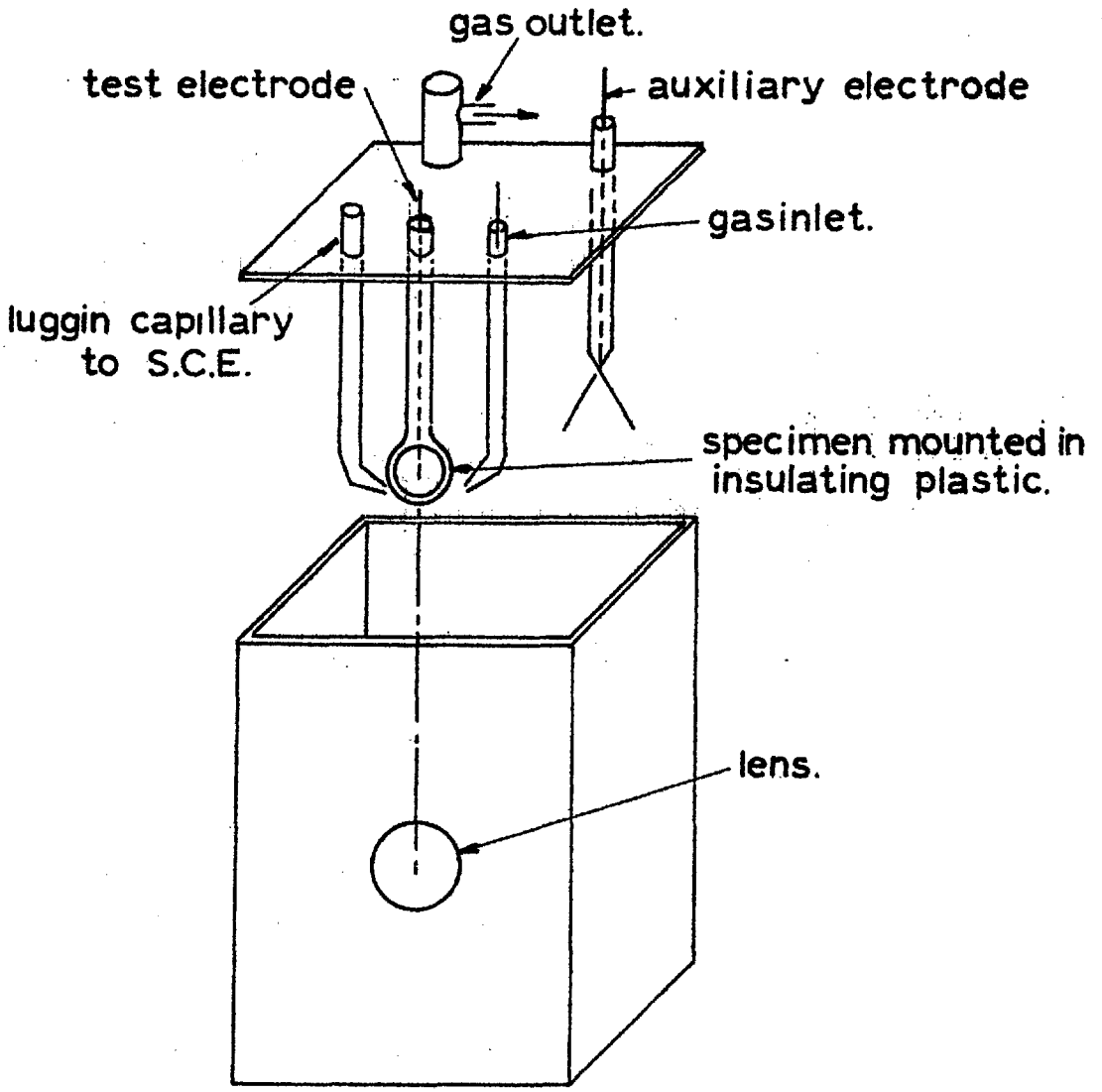

FIG. 16.

CELL USED IN CORROSION RATE MEASUREMENTS.

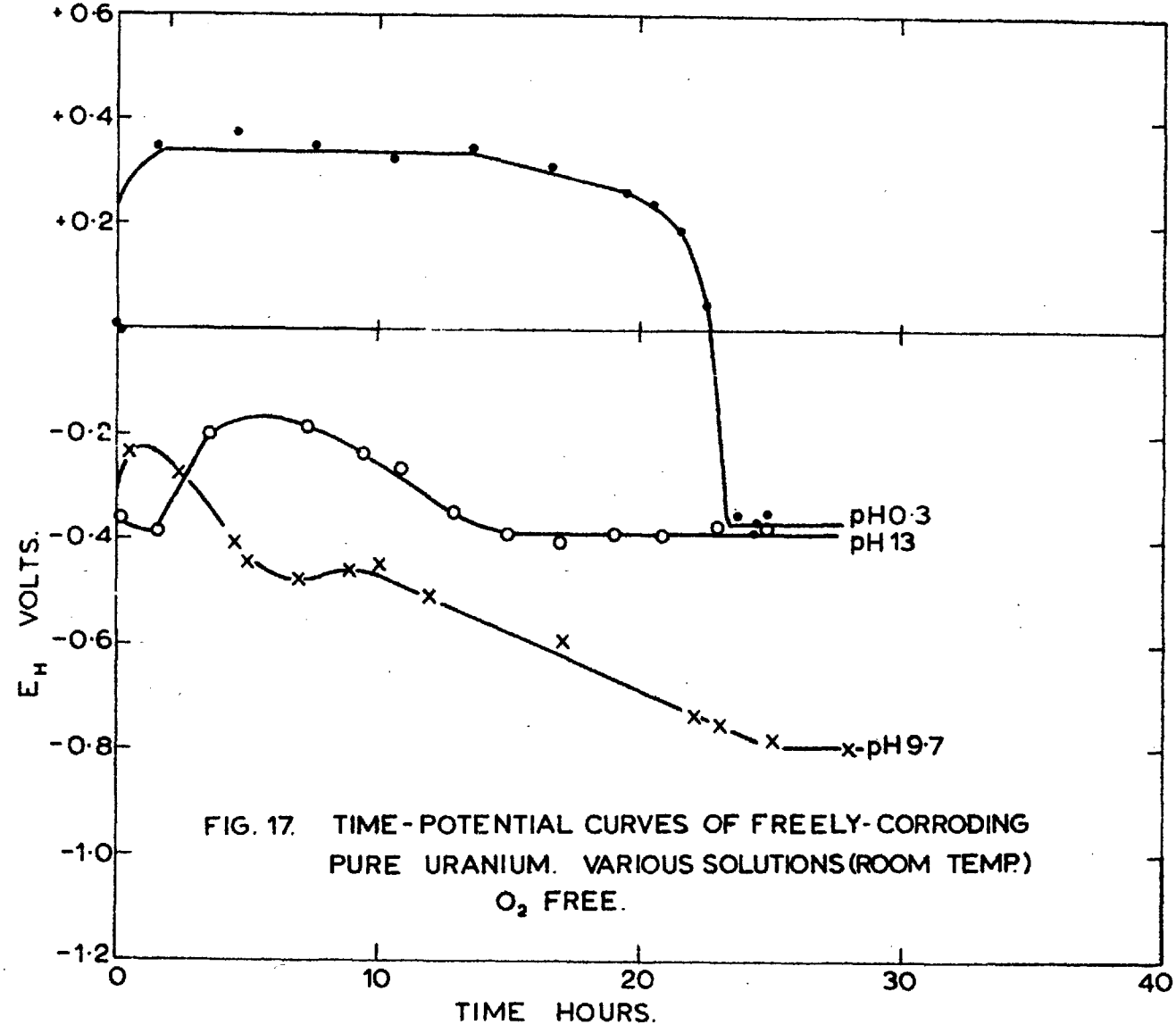

FIG. 17. TIME-POTENTIAL CURVES OF FREELY-CORRODING PURE URANIUM. VARIOUS SOLUTIONS (ROOM TEMP.) O_2 FREE.

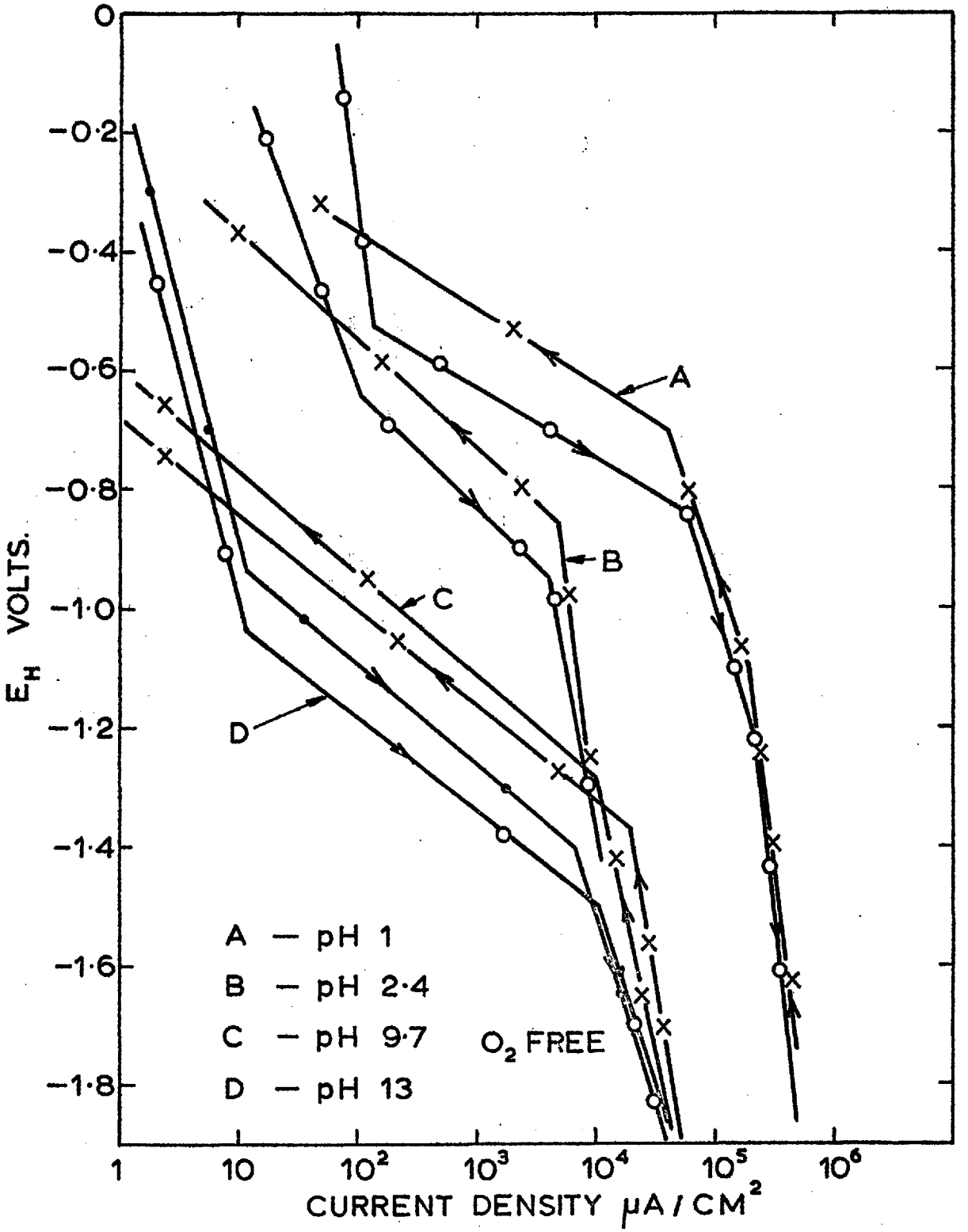

FIG. 18. POLARISATION CURVES FOR U − 12wt°/₀ Mo IN SOLUTIONS OF DIFFERENT pH.

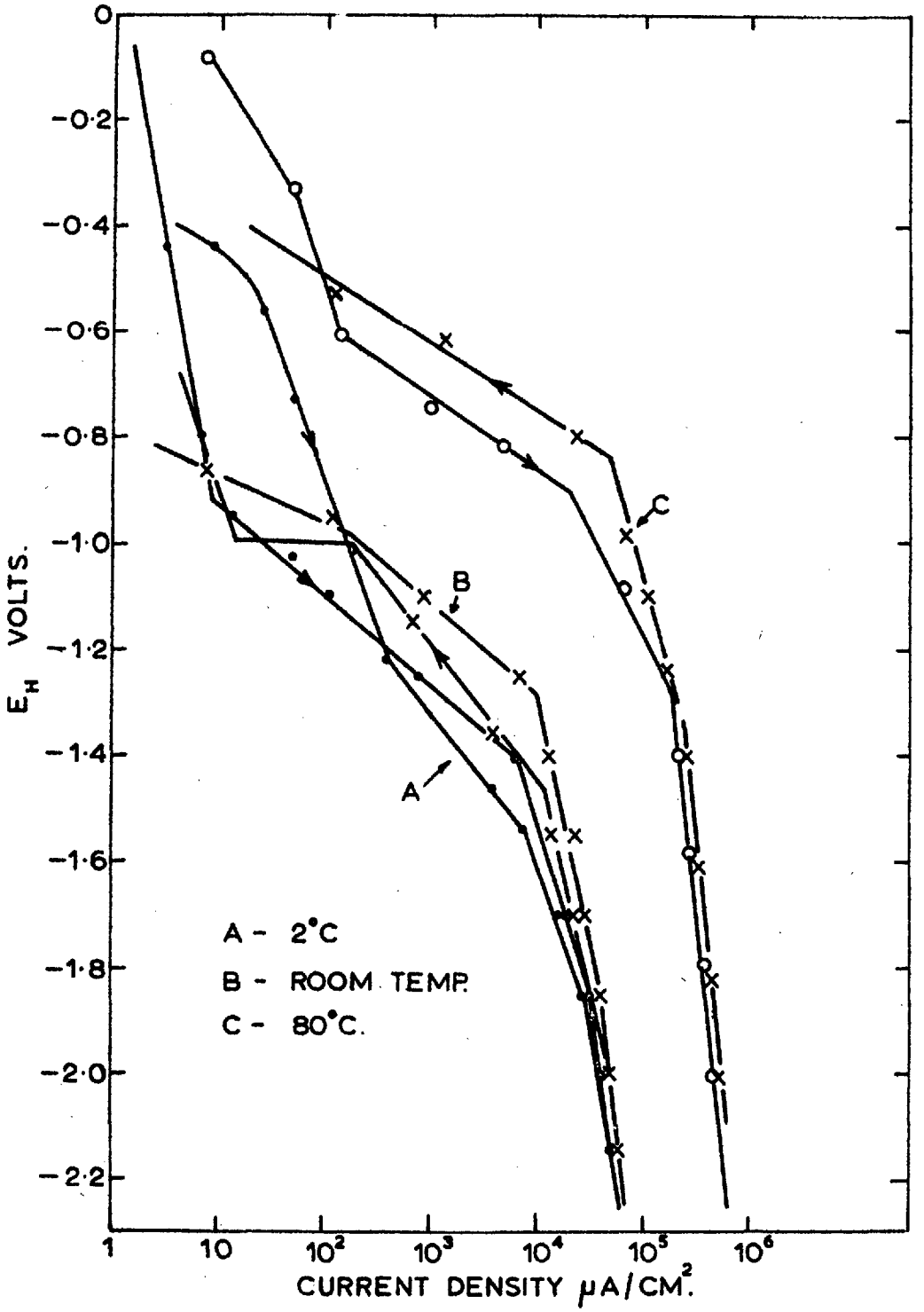

FIG. 19. POLARISATION CURVES FOR U–12wt °/₀ Mo IN SOLUTIONS AT DIFFERENT TEMPERATURES.
pH 9·7 SOLUTION.
O_2 FREE.

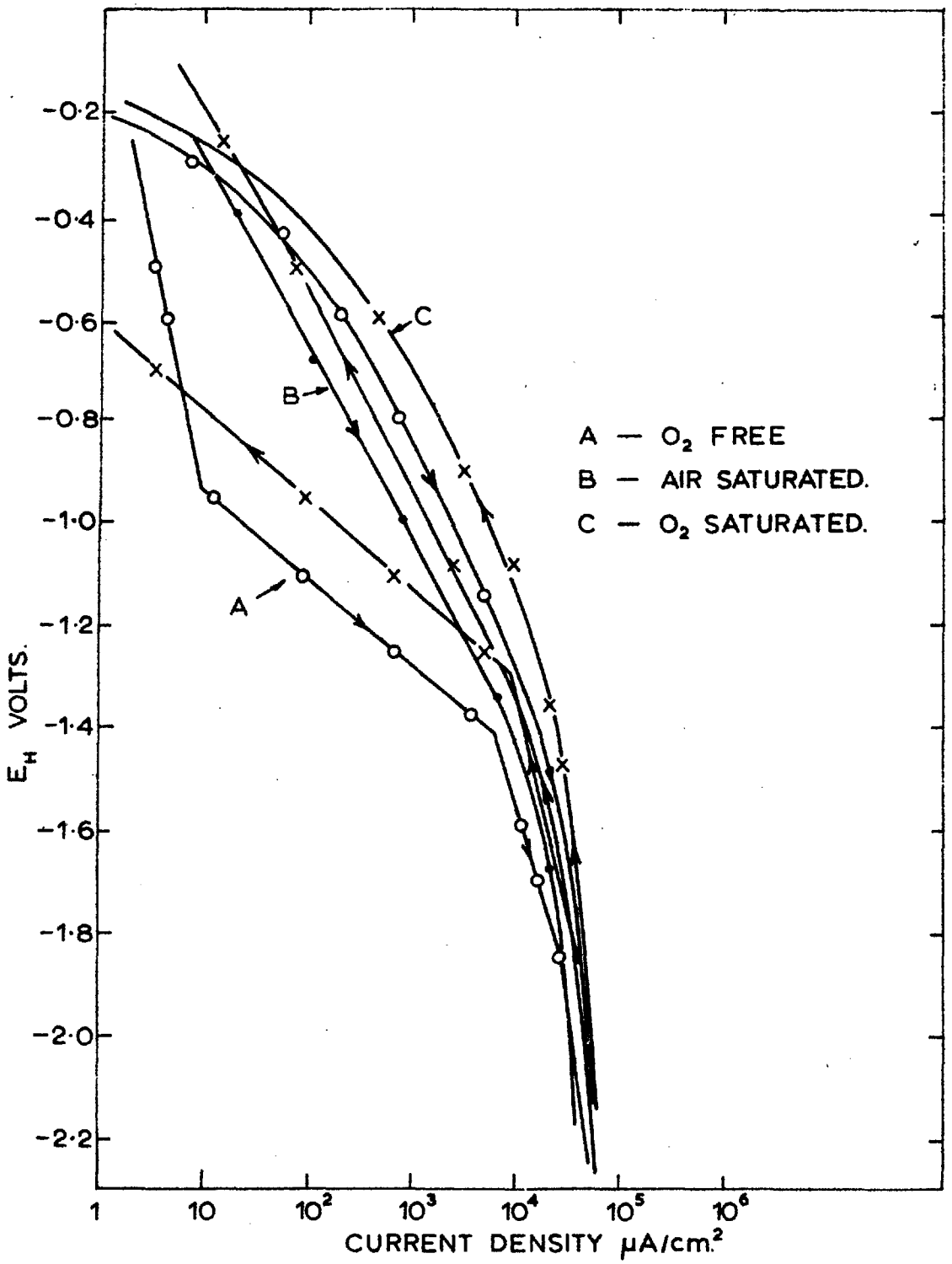

FIG. 20. POLARISATION CURVES FOR U-12wt°/₀Mo IN SOLUTIONS OF DIFFERENT OXYGEN CONTENT.

pH 9·7 SOLUTION.

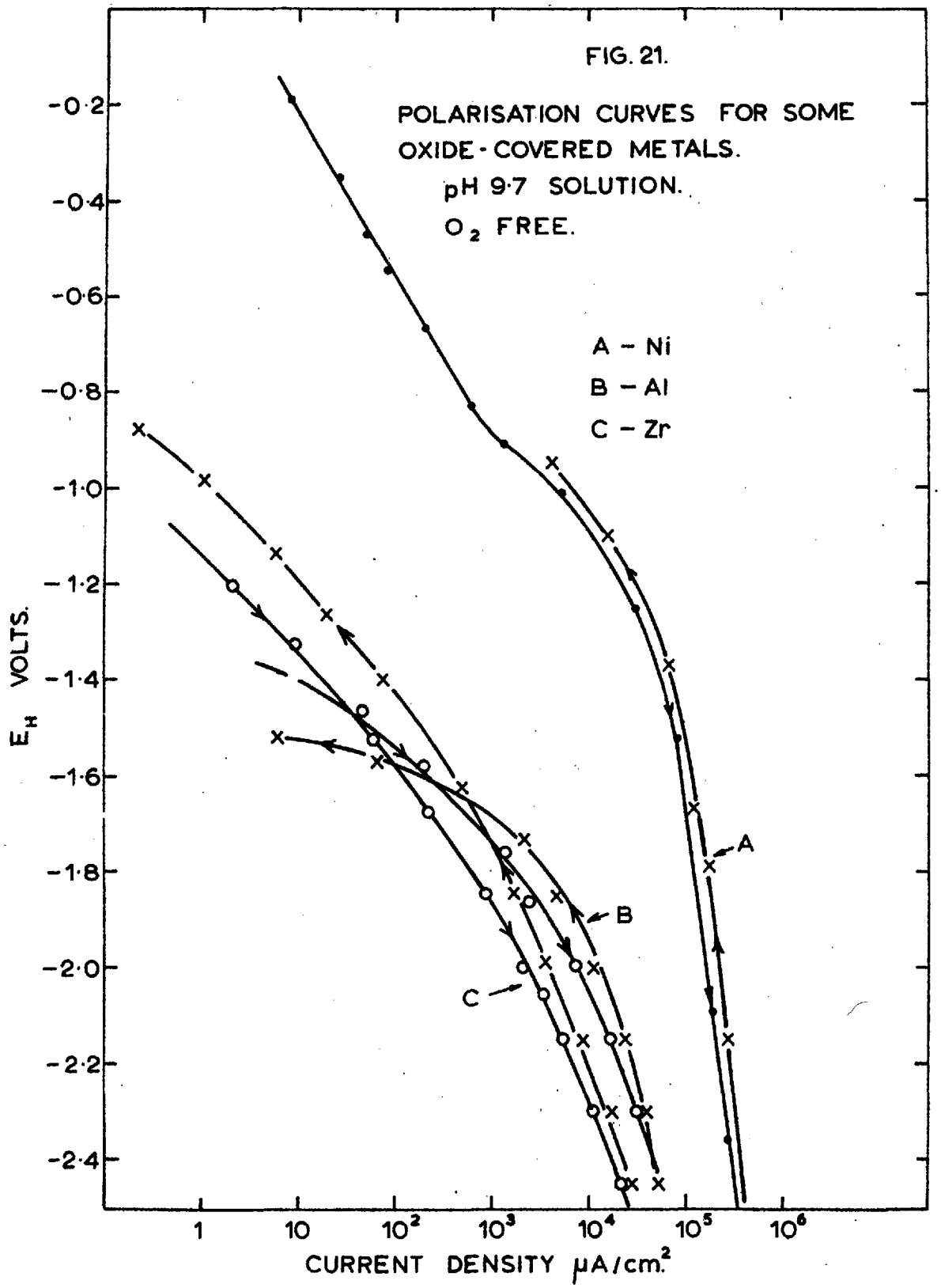
FIG. 21.
POLARISATION CURVES FOR SOME OXIDE-COVERED METALS.
pH 9·7 SOLUTION.
O2 FREE.
A – Ni
B – Al
C – Zr
A
B
C
-0·2
-0·4
-0·6
-0·8
-1·0
-1·2
-1·4
-1·6
-1·8
-2·0
-2·2
-2·4
EH VOLTS.
1
10
10²
10³
10⁴
10⁵
10⁶
CURRENT DENSITY μA/cm²

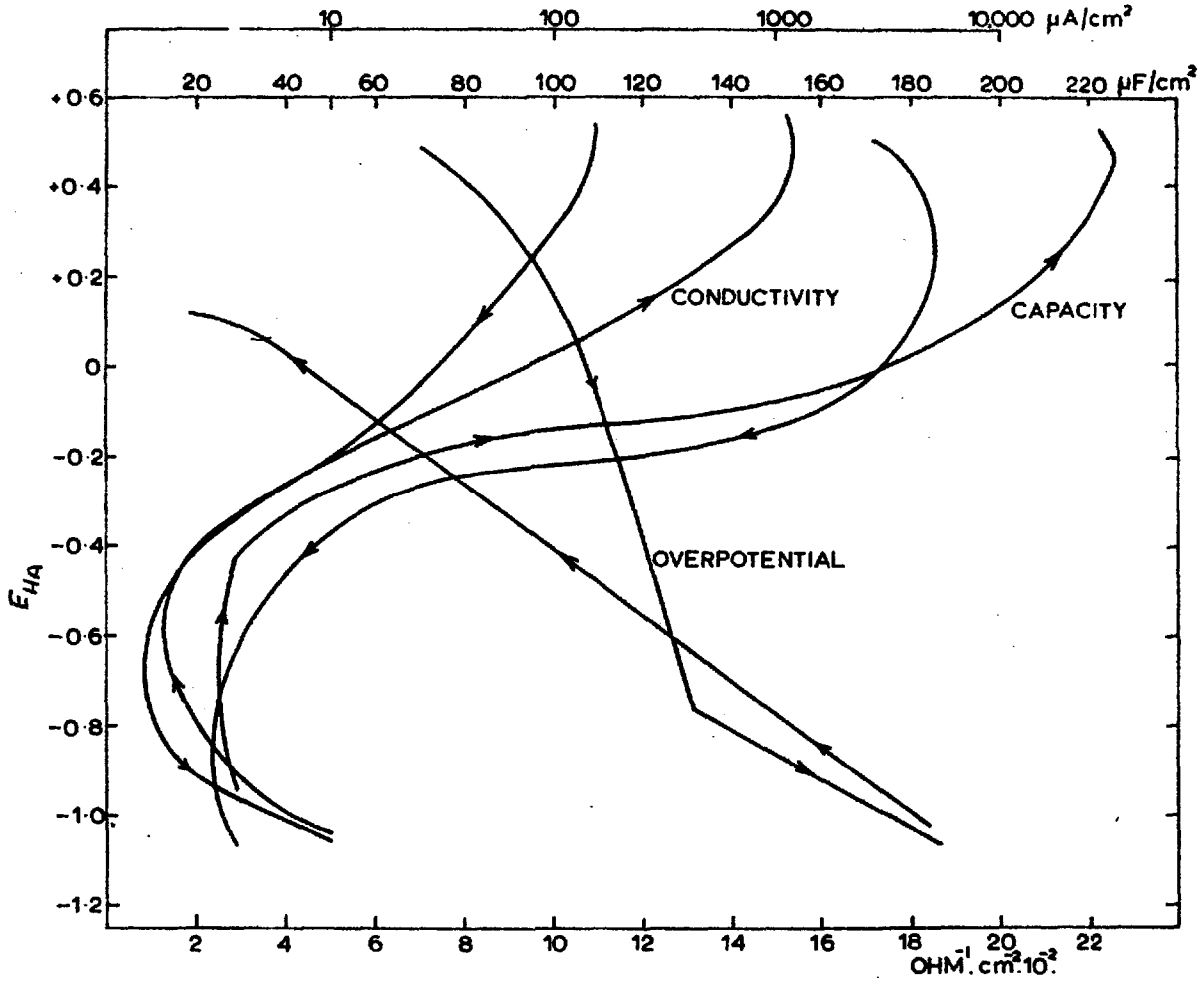

FIG. 22. OVERPOTENTIAL AND IMPEDANCE CURVES.
PURE URANIUM.
pH 9·7 SOLUTION.
O_2 FREE.

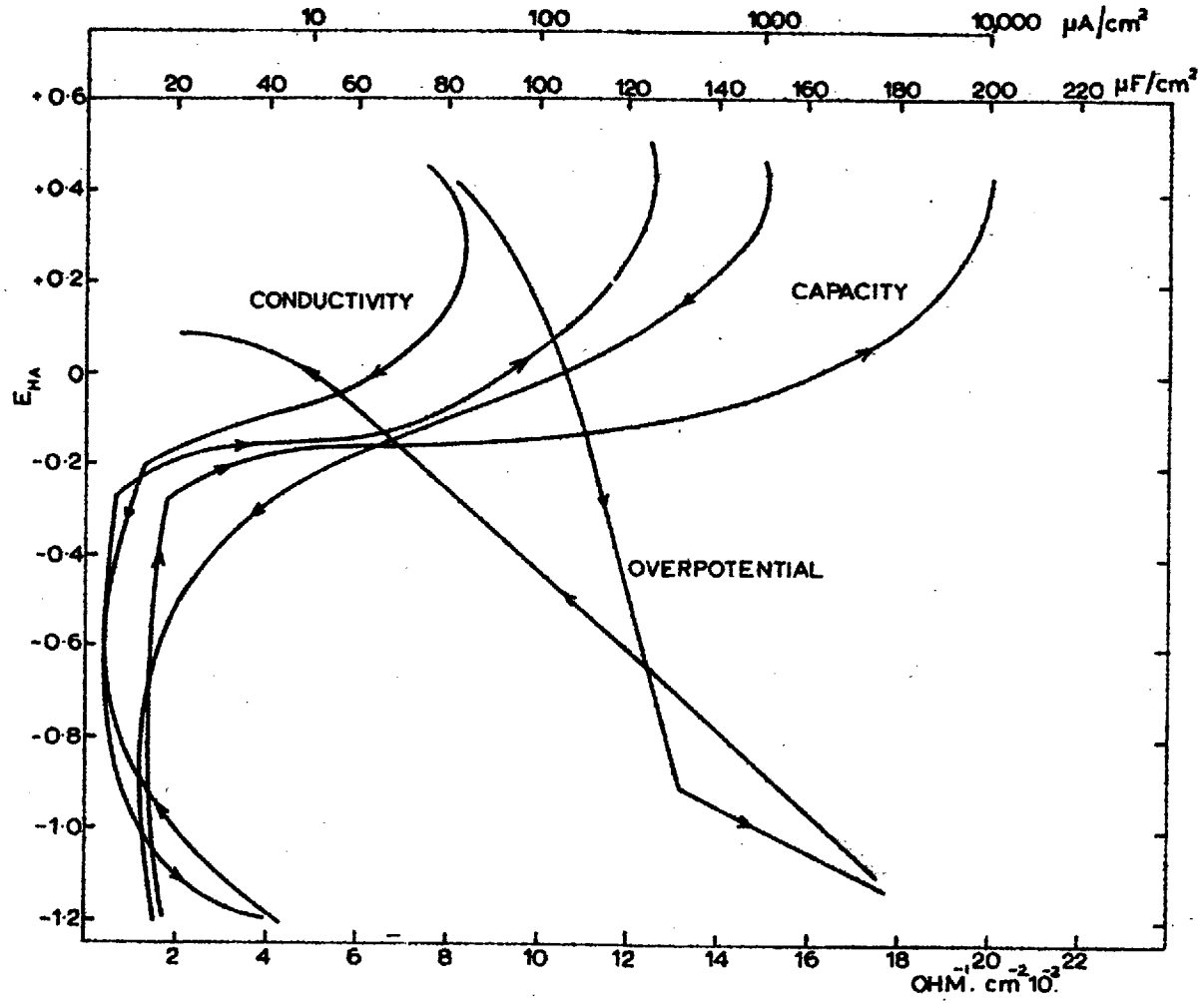

FIG. 23. OVERPOTENTIAL AND IMPEDANCE CURVES.
U - 5wt% Zr.
pH 9·7 SOLUTION.
O_2 FREE.

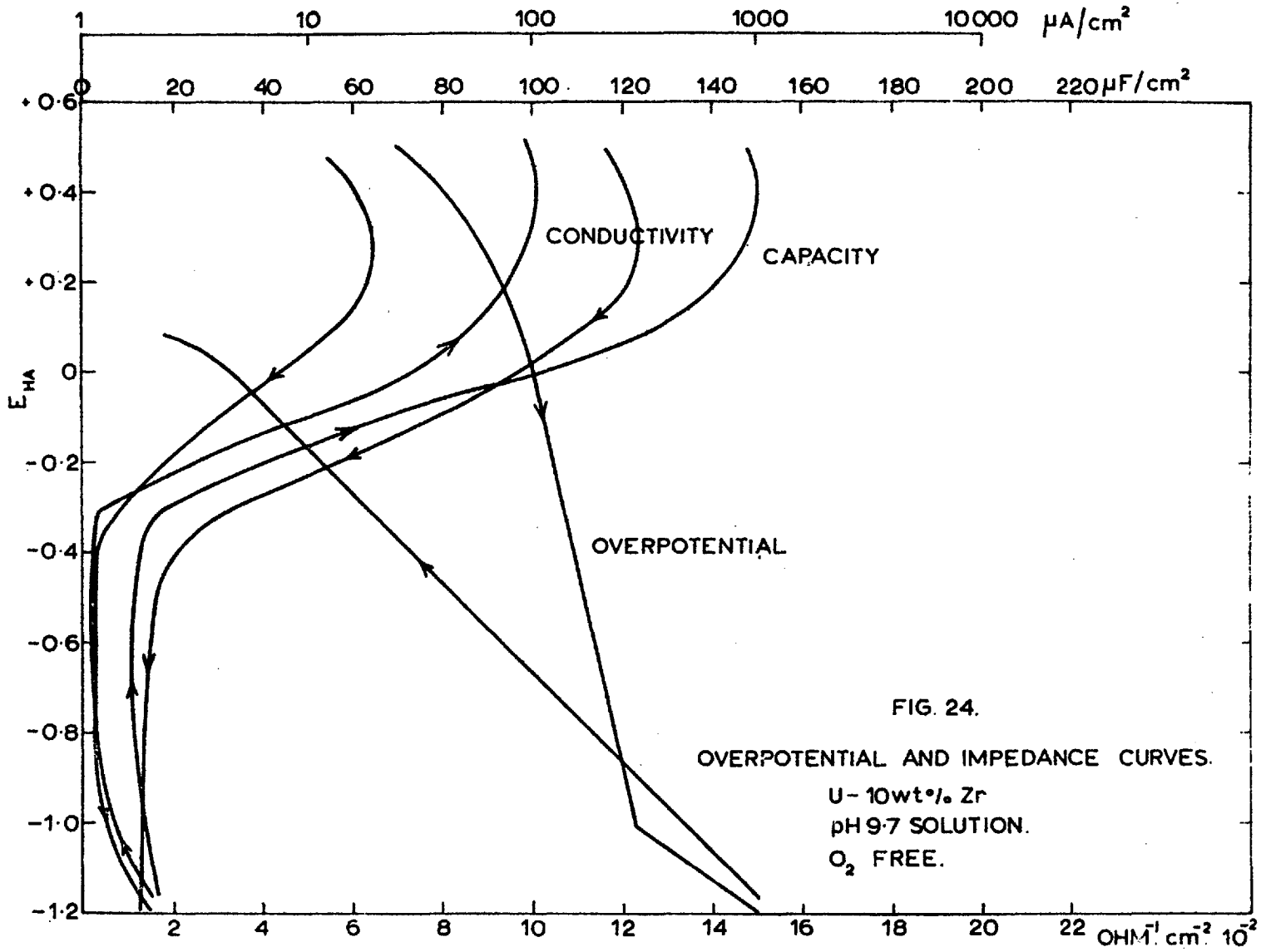

FIG. 24.

OVERPOTENTIAL AND IMPEDANCE CURVES.

U - 10wt% Zr

pH 9·7 SOLUTION.

O_2 FREE.

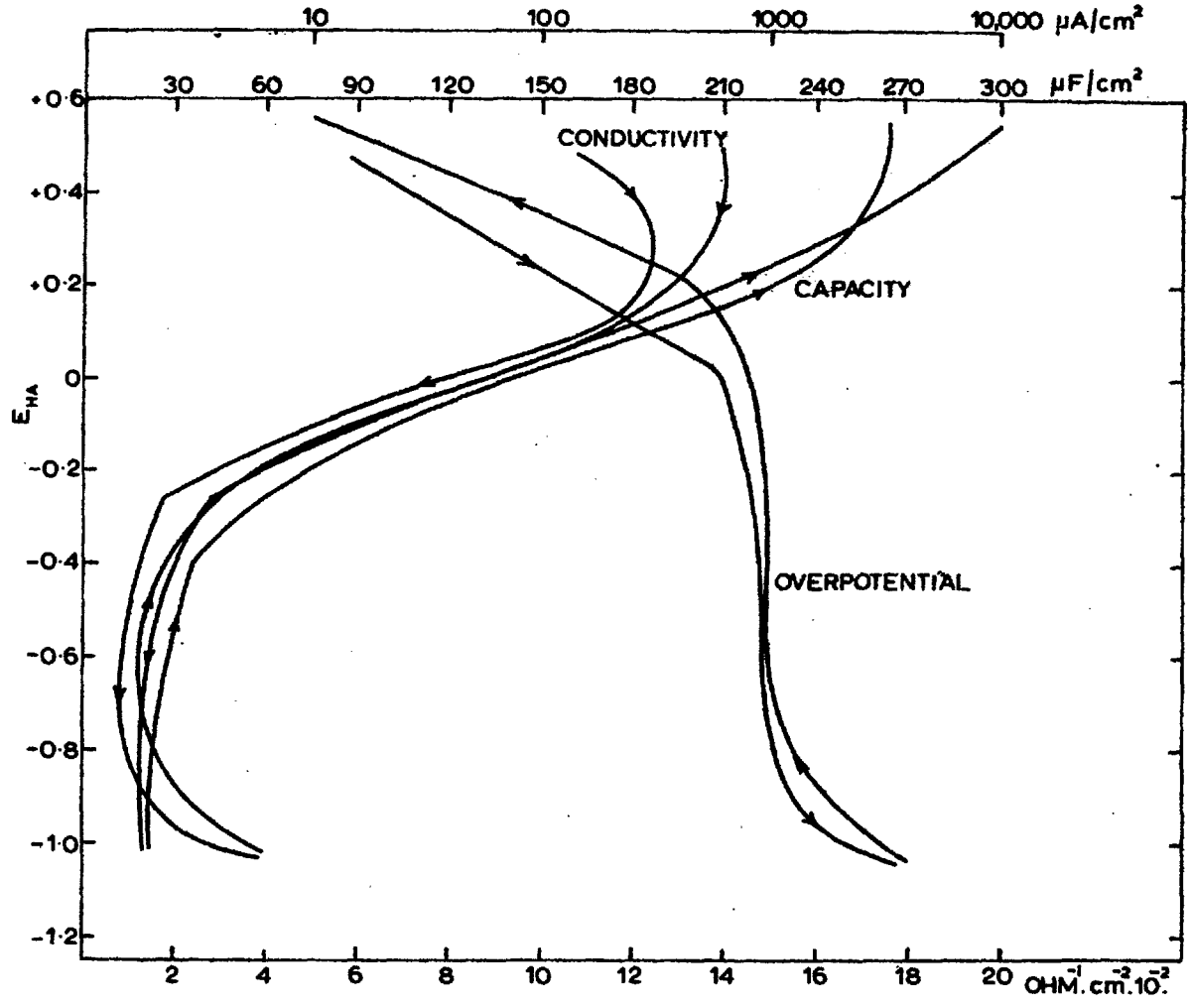

FIG. 25. EFFECT OF OXYGEN ON OVERPOTENTIAL AND IMPEDANCE. PURE URANIUM.
pH 9·7 SOLUTION.
O_2 - SATURATED.

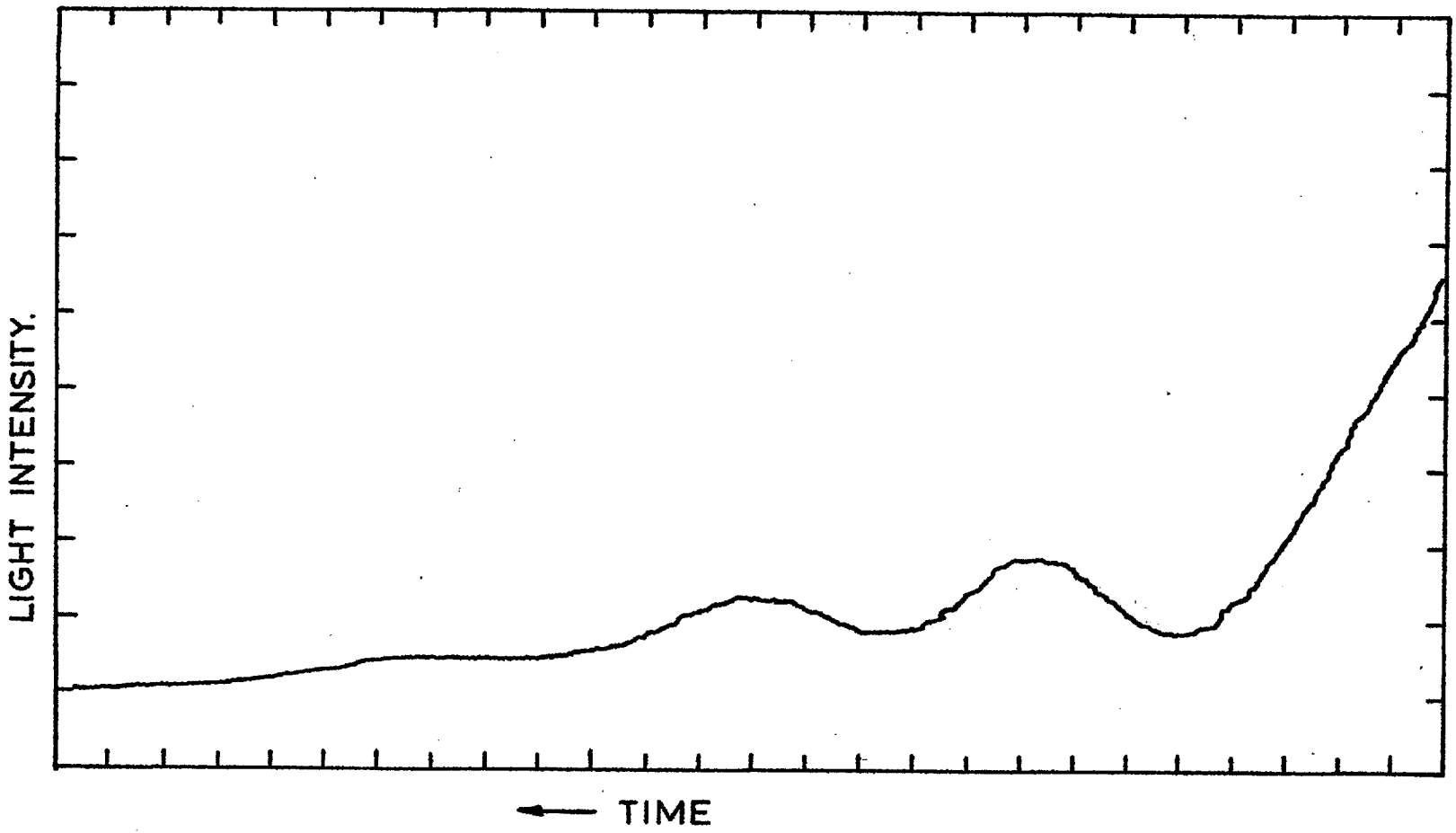

FIG. 26a. MONOCHROMATIC LIGHT MEASUREMENT OF CORROSION.

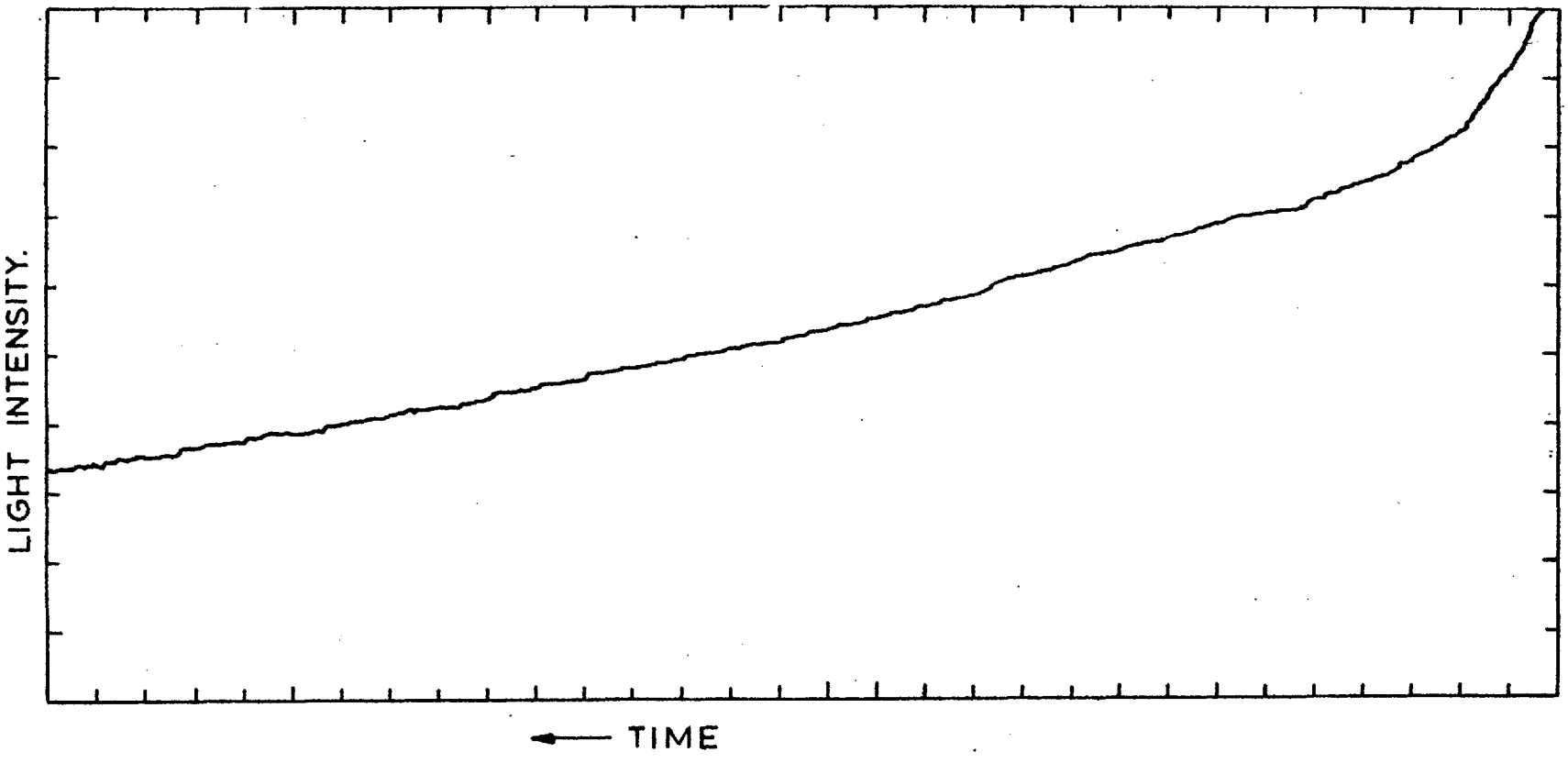

FIG. 26b. "WHITE" LIGHT MEASUREMENT OF CORROSION.

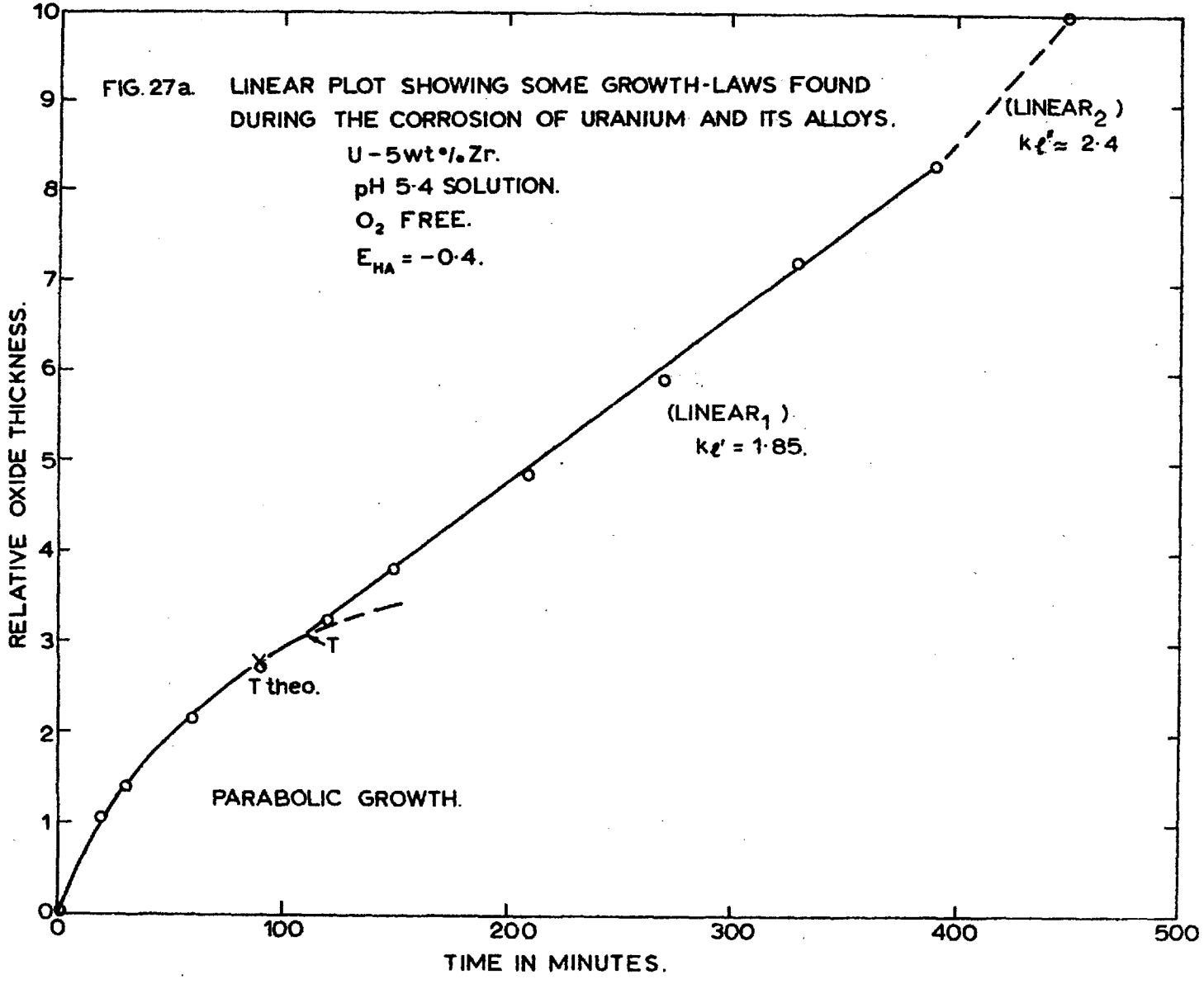
FIG. 27a. LINEAR PLOT SHOWING SOME GROWTH-LAWS FOUND DURING THE CORROSION OF URANIUM AND ITS ALLOYS.
U - 5 wt % Zr.
pH 5·4 SOLUTION.
O_2 FREE.
E_{HA} = -0·4.
(LINEAR$_2$)
$k\ell'$ ≈ 2·4
(LINEAR$_1$)
$k\ell'$ = 1·85.
T
T theo.
PARABOLIC GROWTH.
RELATIVE OXIDE THICKNESS.
TIME IN MINUTES.
0
1
2
3
4
5
6
7
8
9
10
0
100
200
300
400
500

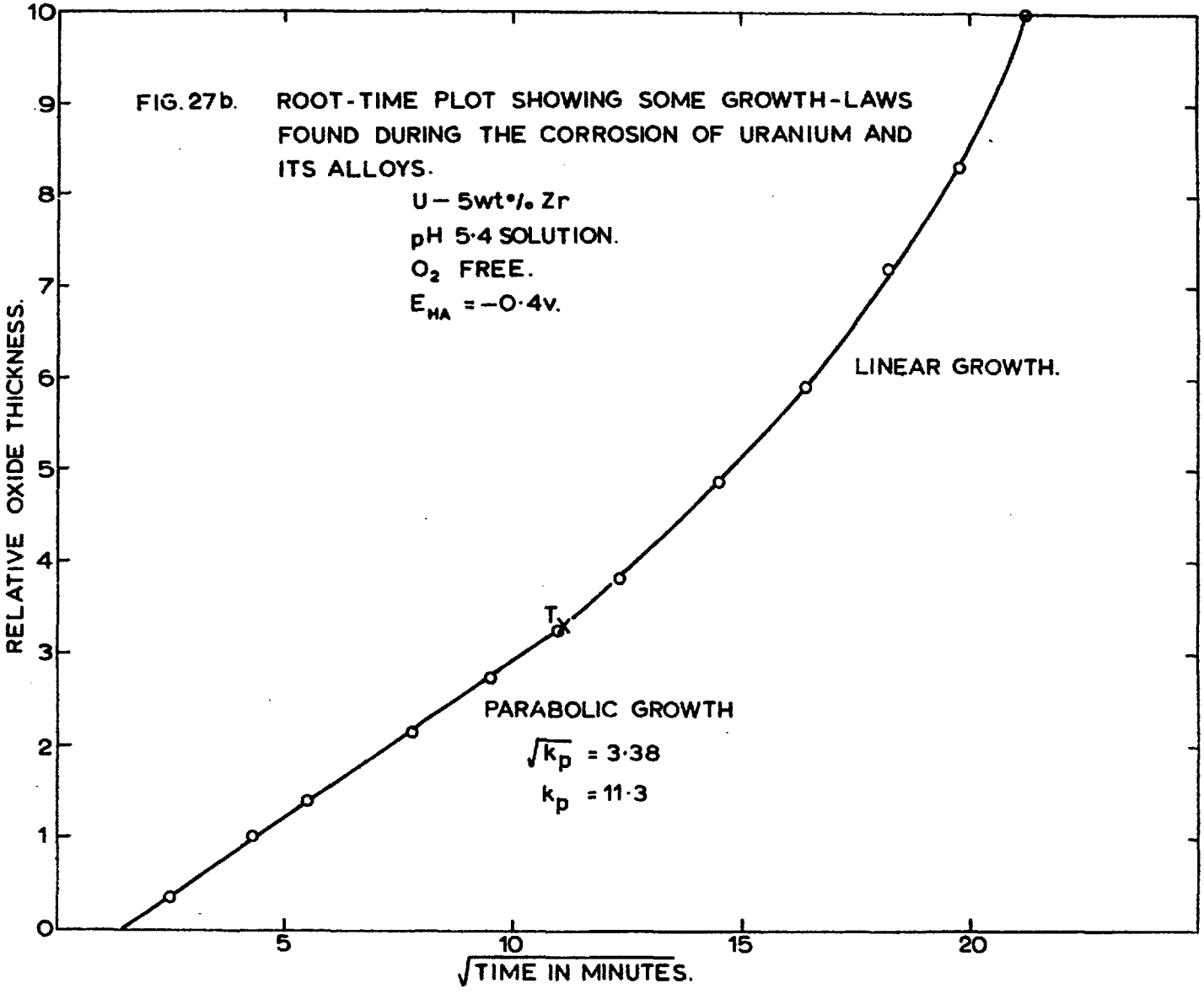

FIG. 27b. ROOT-TIME PLOT SHOWING SOME GROWTH-LAWS FOUND DURING THE CORROSION OF URANIUM AND ITS ALLOYS.

U – 5wt% Zr

pH 5·4 SOLUTION.

O_2 FREE.

E_{HA} = –0·4v.

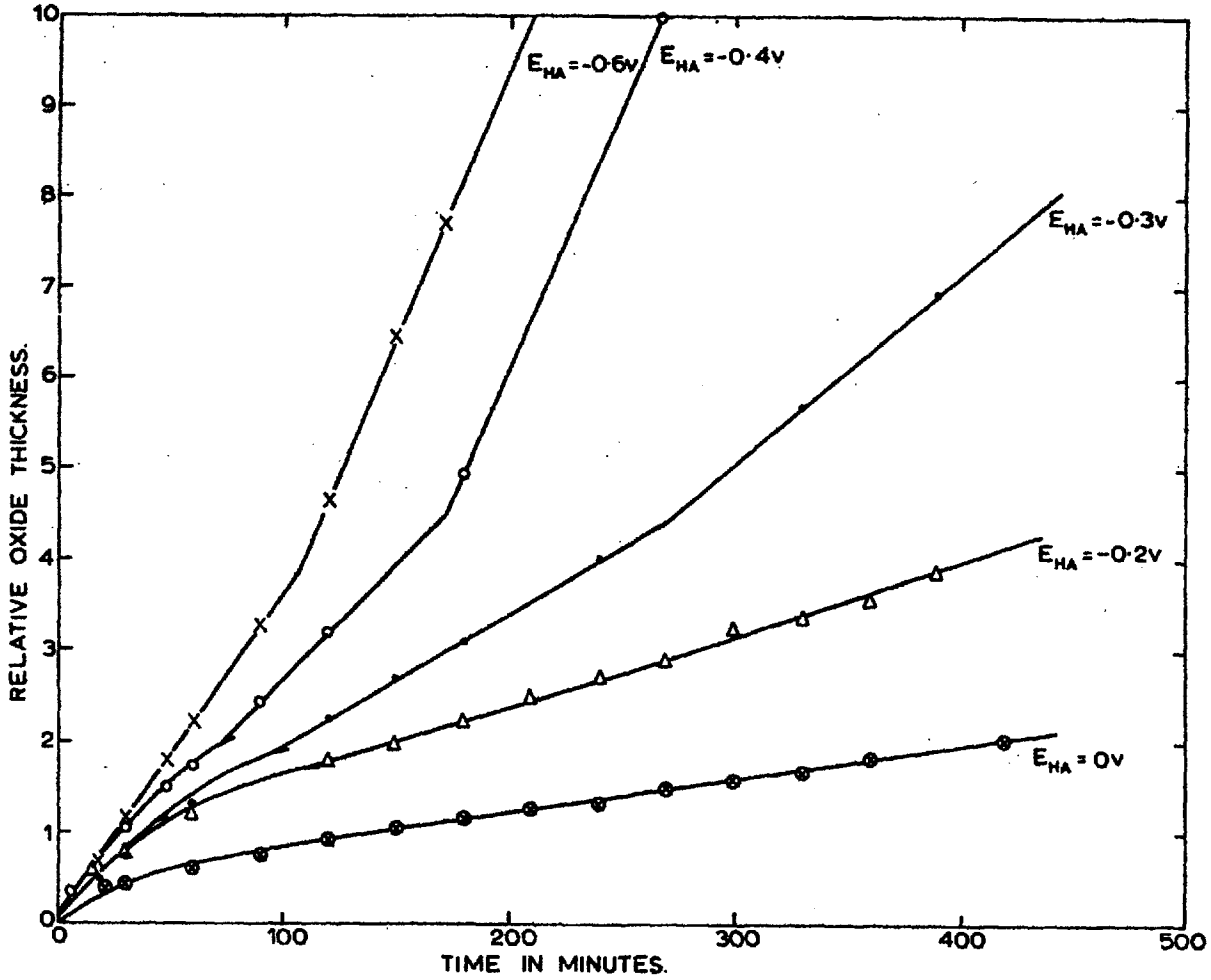

FIG. 28. EFFECT OF CATHODIC POLARISATION
CORROSION OF PURE URANIUM
pH 5·4 SOLUTION.
O_2 FREE.

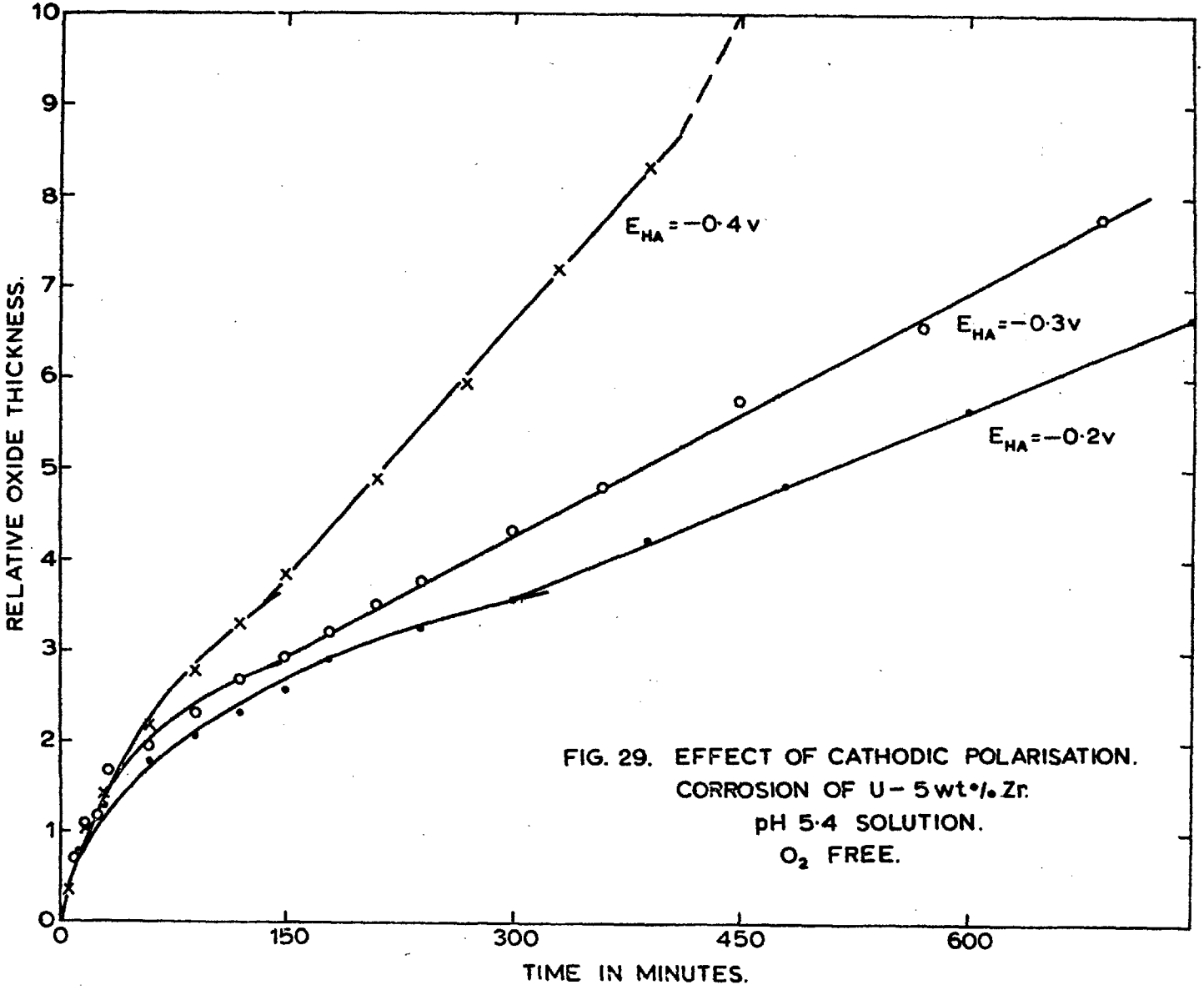

FIG. 29. EFFECT OF CATHODIC POLARISATION.
CORROSION OF U – 5 wt% Zr.
pH 5·4 SOLUTION.
O_2 FREE.

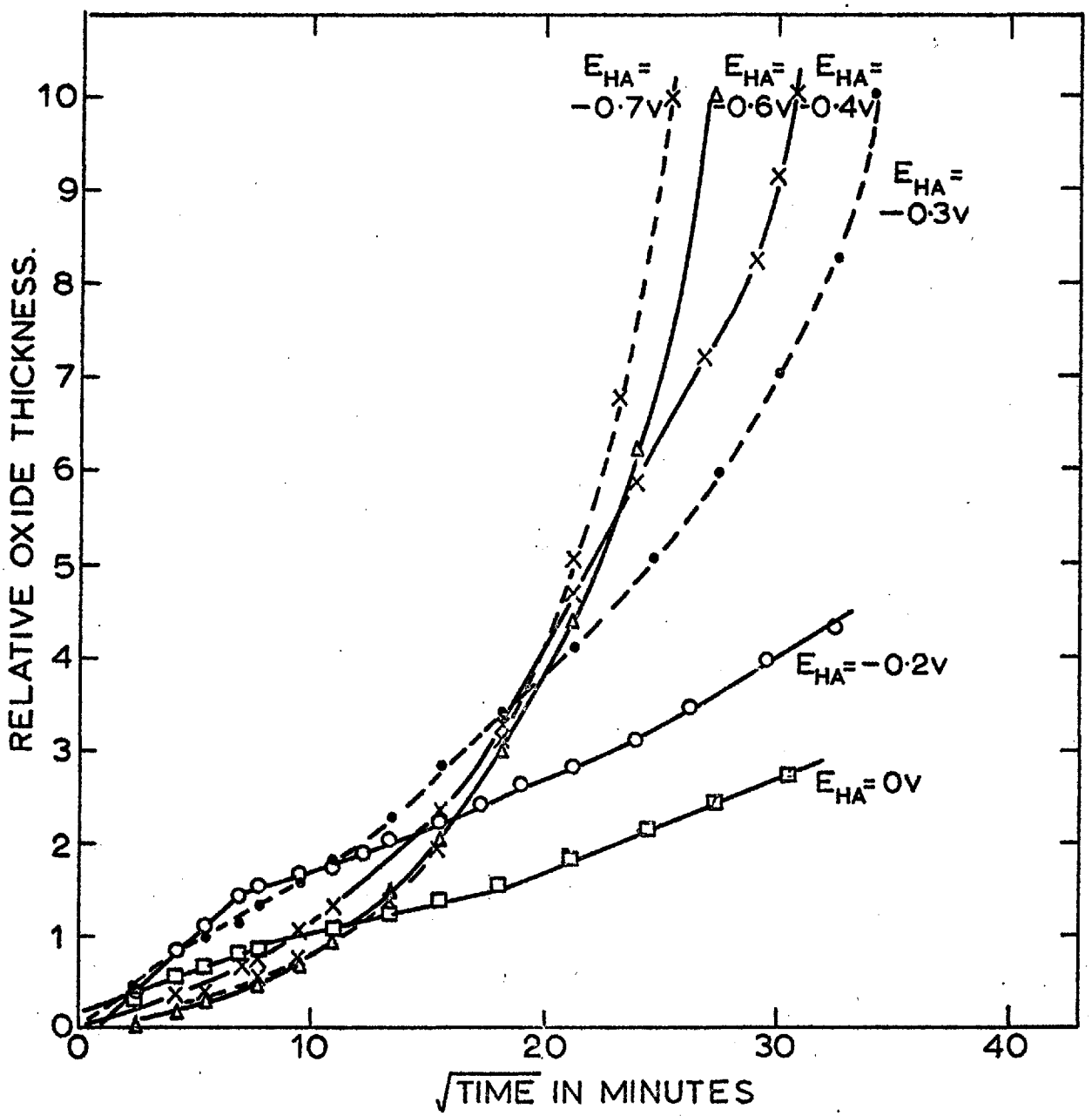

FIG. 30. EFFECT OF CATHODIC POLARISATION.
CORROSION OF U -10wt°/₀Zr
AS A FUNCTION OF √TIME.
pH 5·4 SOLUTION.
O_2 FREE.

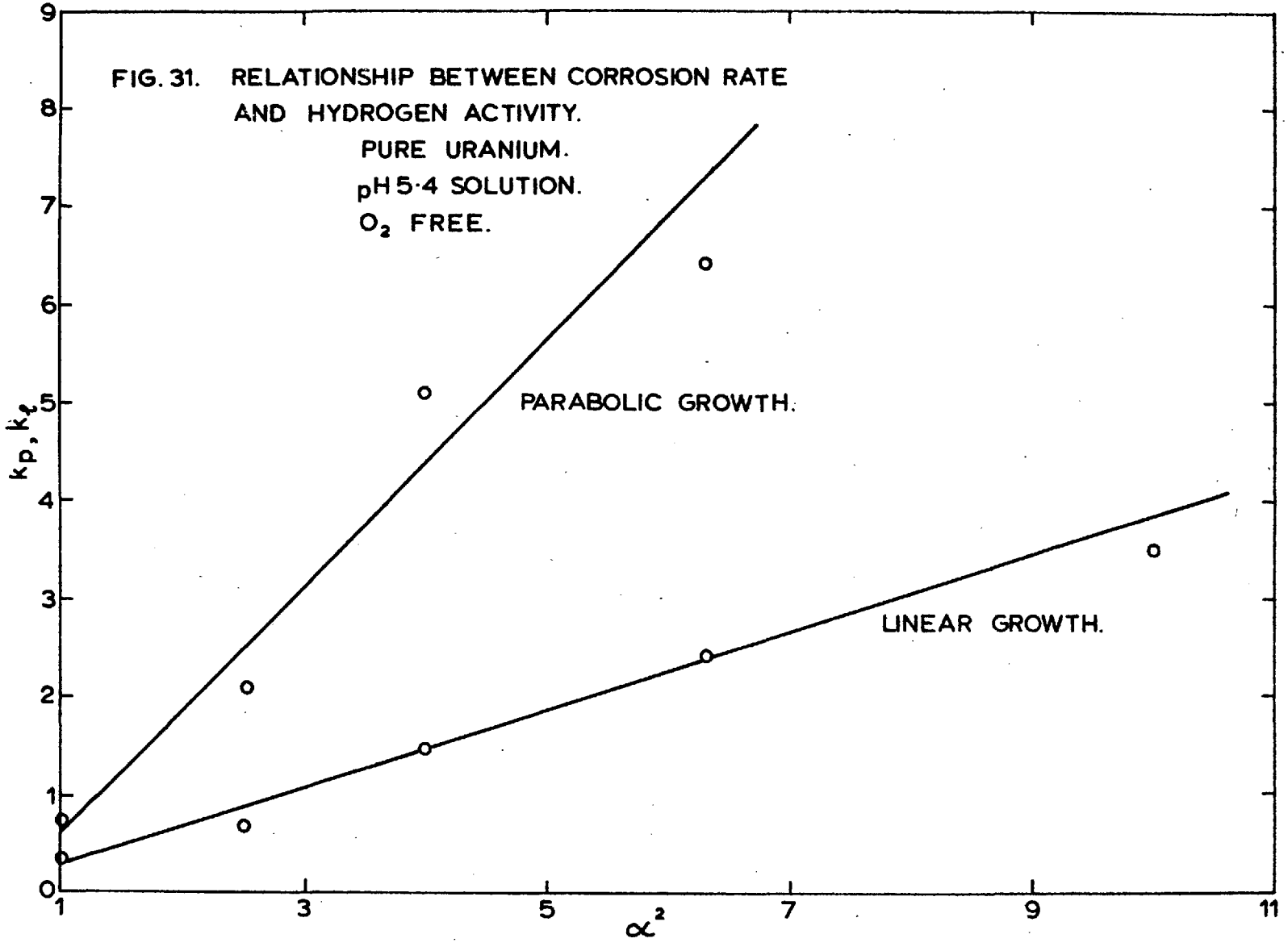
FIG. 31. RELATIONSHIP BETWEEN CORROSION RATE AND HYDROGEN ACTIVITY.
PURE URANIUM.
pH 5·4 SOLUTION.
O_2 FREE.
PARABOLIC GROWTH.
LINEAR GROWTH.
k_p, k_ℓ
α^2
0
1
2
3
4
5
6
7
8
9
1
3
5
7
9
11

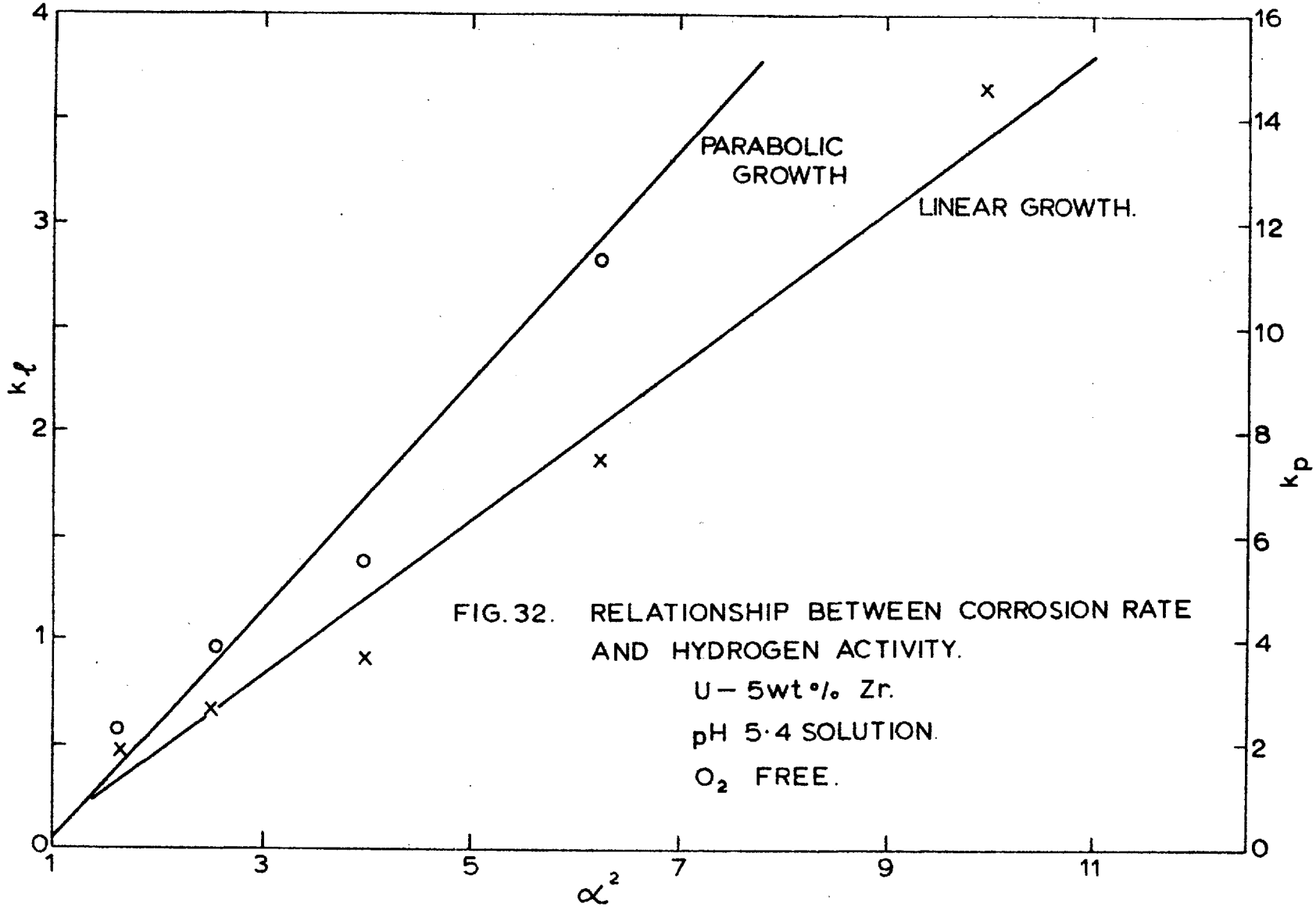

FIG. 32. RELATIONSHIP BETWEEN CORROSION RATE AND HYDROGEN ACTIVITY.
U – 5wt% Zr.
pH 5·4 SOLUTION.
O_2 FREE.

EFFECT ON THE CORROSION RATE OF URANIUM OF ALLOYING WITH ZIRCONIUM.

FIG. 33.

pH 5·4 SOLUTION O_2 FREE.

$E_{HA} = -0{\cdot}2$ V.

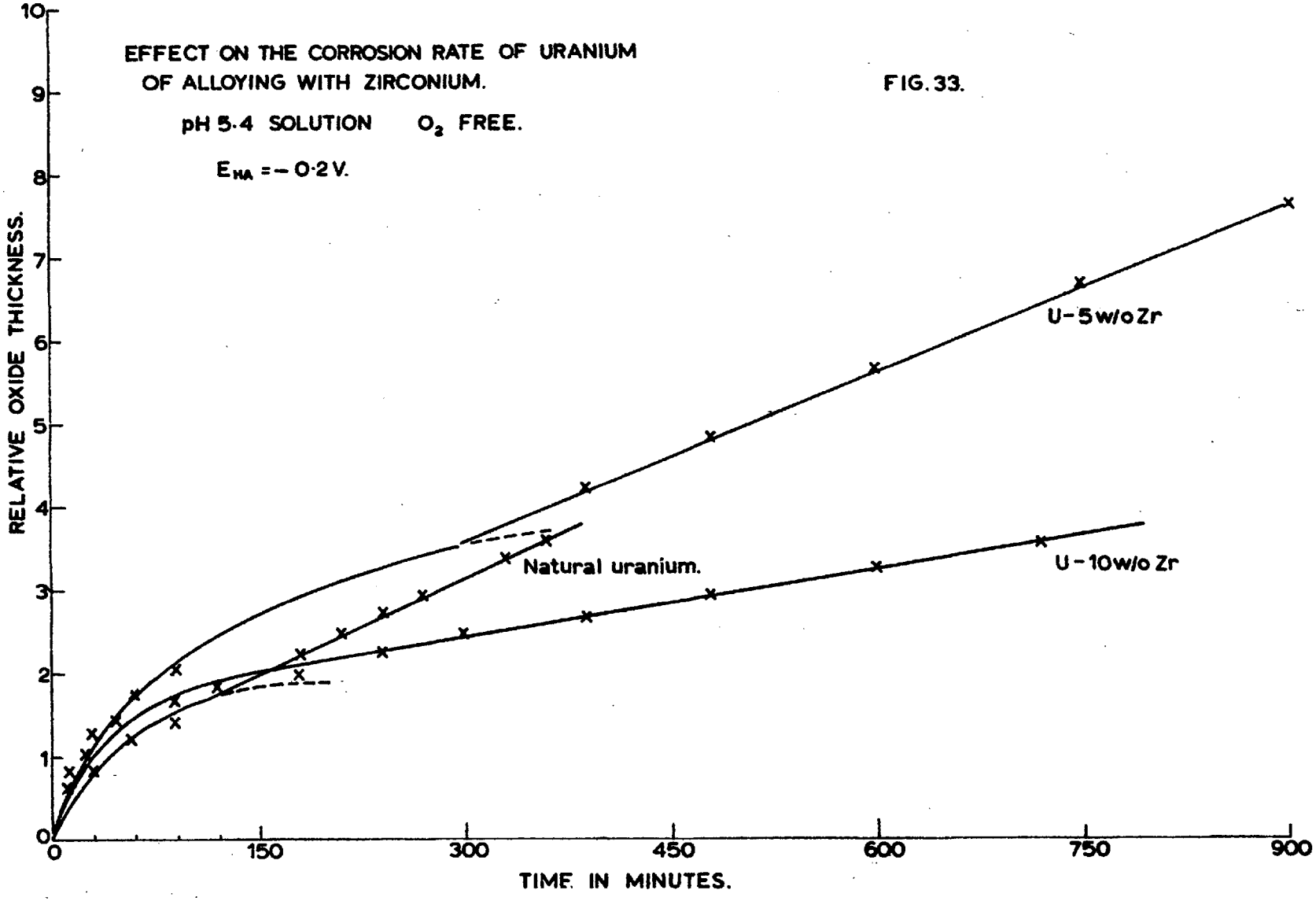

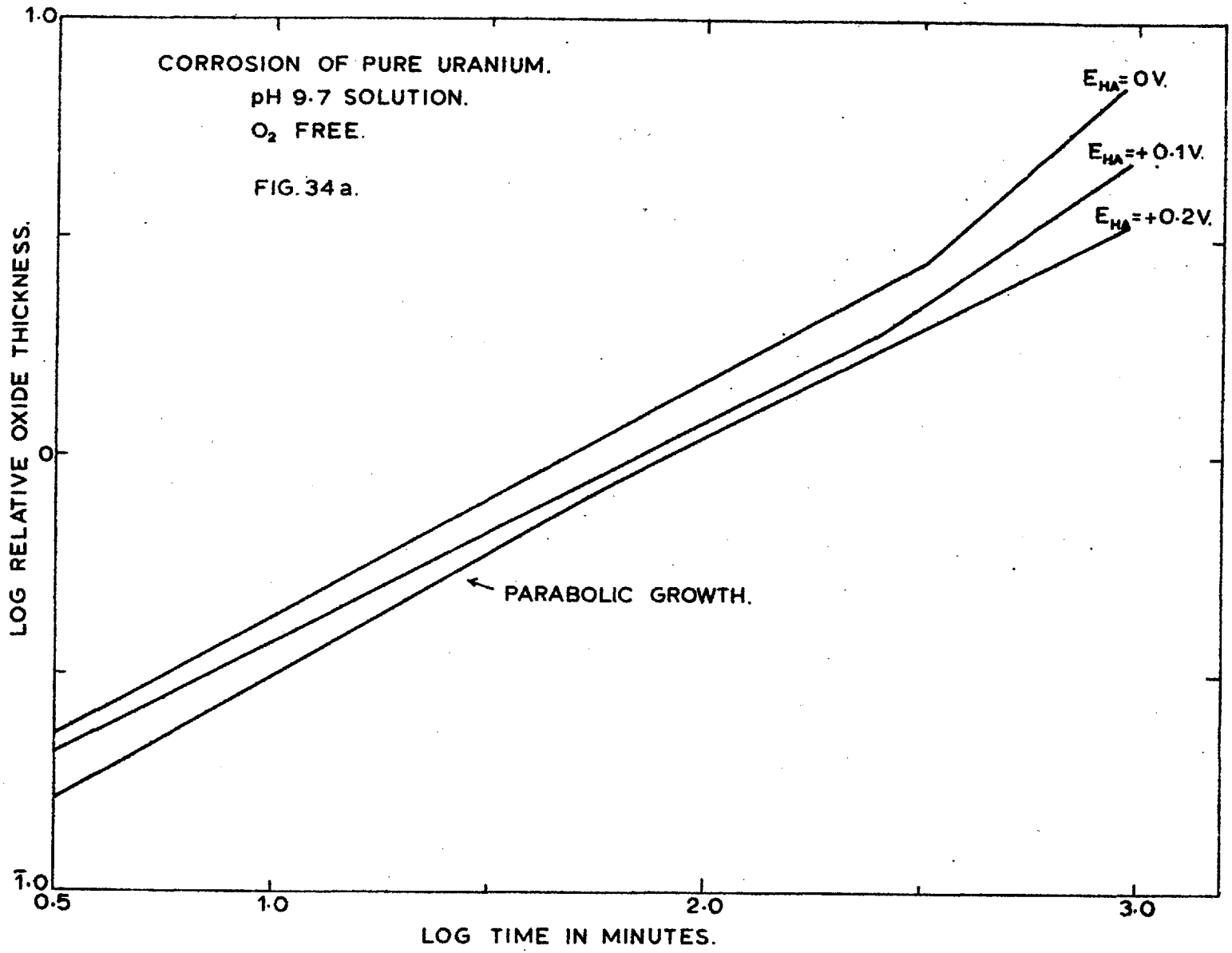
CORROSION OF PURE URANIUM.
pH 9·7 SOLUTION.
O_2 FREE.
FIG. 34 a.
E_{HA} = 0 V.
E_{HA} = + 0·1 V.
E_{HA} = + 0·2 V.
PARABOLIC GROWTH.
LOG RELATIVE OXIDE THICKNESS.
1·0
0
1·0
0·5
1·0
2·0
3·0
LOG TIME IN MINUTES.

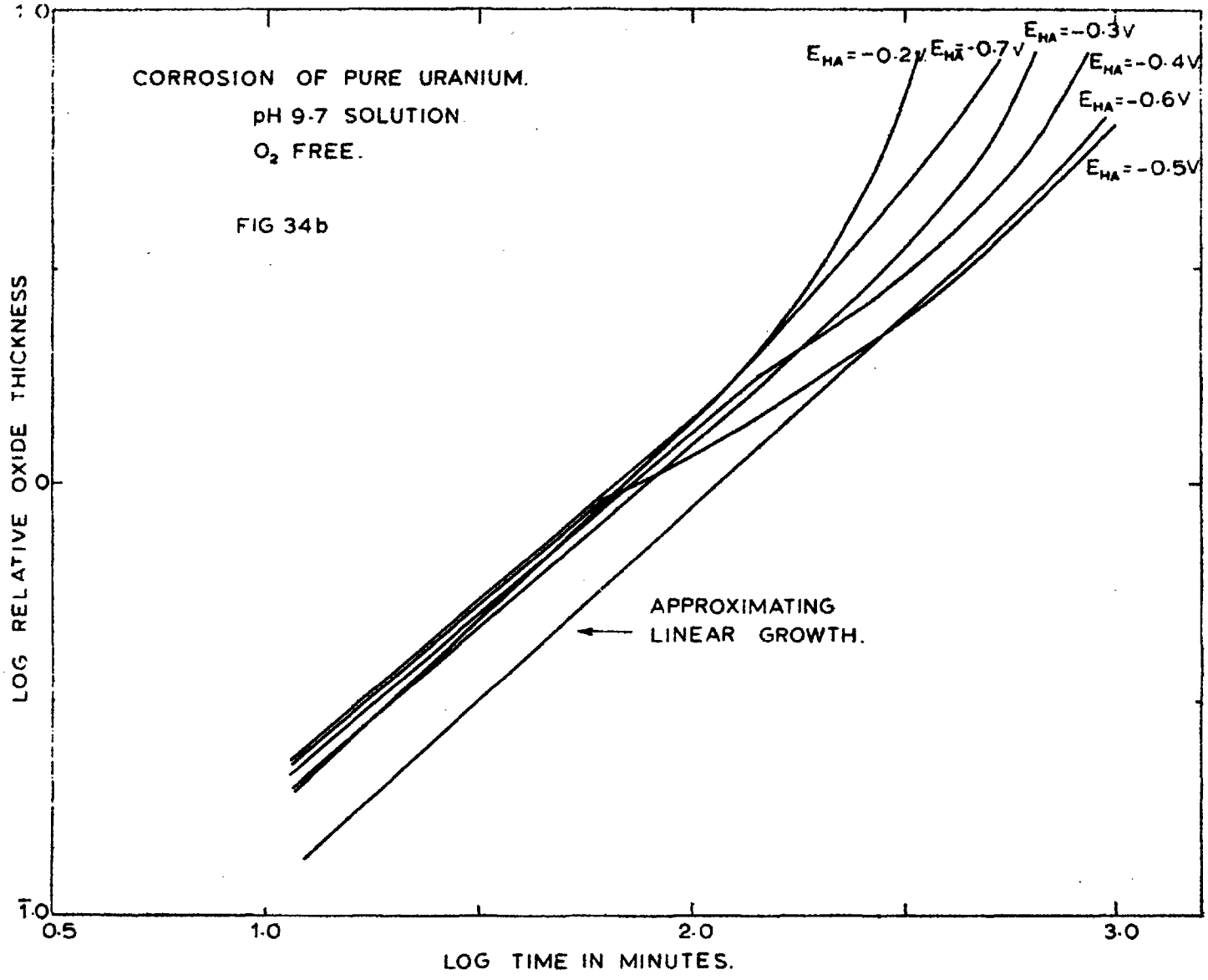
CORROSION OF PURE URANIUM.
pH 9·7 SOLUTION
O_2 FREE.
FIG 34b
E_{HA} = -0·2V
E_{HA} = -0·7V
E_{HA} = -0·3V
E_{HA} = -0·4V
E_{HA} = -0·6V
E_{HA} = -0·5V
APPROXIMATING
LINEAR GROWTH.
LOG RELATIVE OXIDE THICKNESS
1·0
0
1·0
0·5
1·0
2·0
3·0
LOG TIME IN MINUTES.

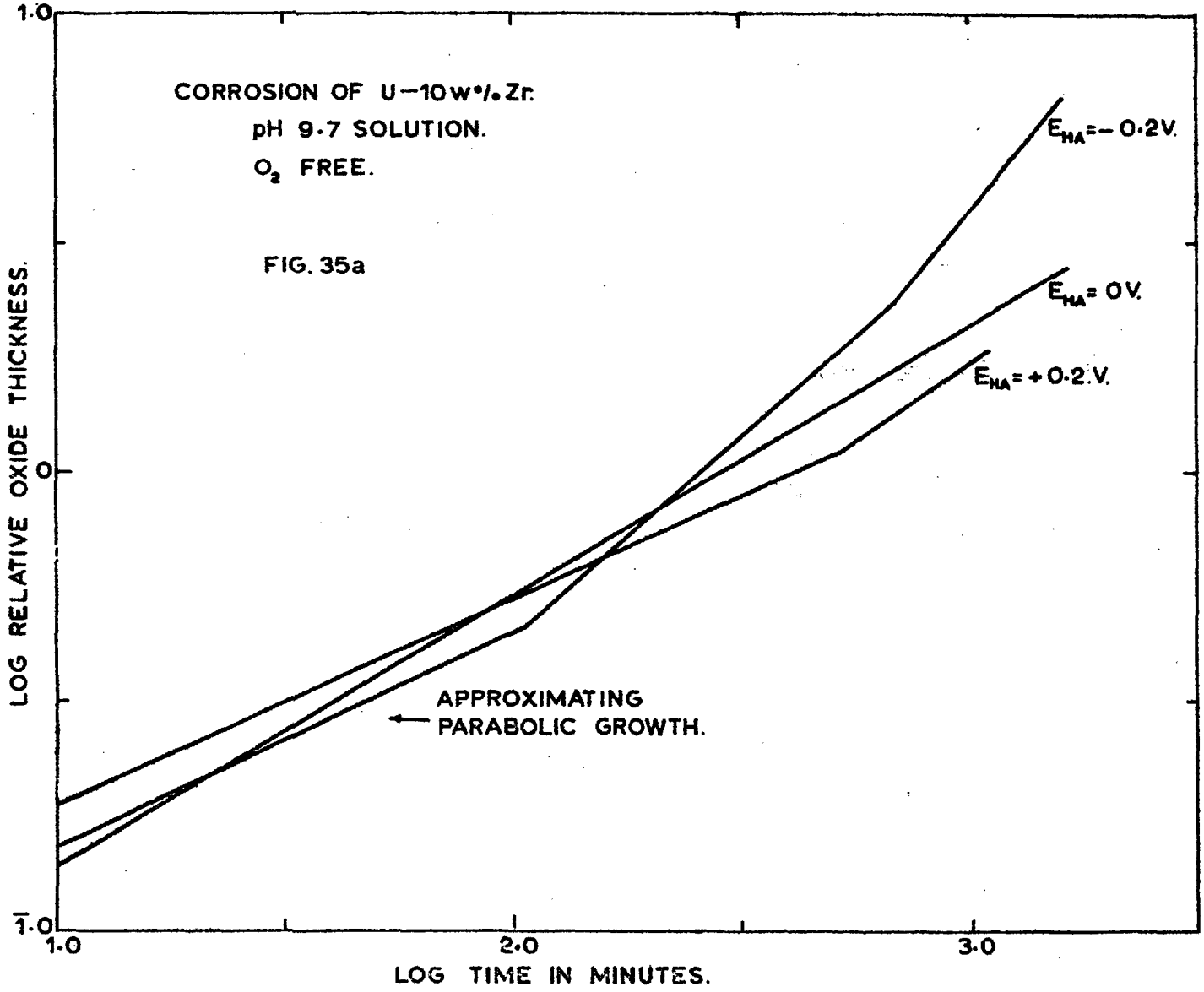
CORROSION OF U—10 w°/o Zr.
pH 9·7 SOLUTION.
O_2 FREE.
FIG. 35a
E_{HA} = – 0·2 V.
E_{HA} = 0 V.
E_{HA} = + 0·2 V.
APPROXIMATING
PARABOLIC GROWTH.
LOG RELATIVE OXIDE THICKNESS.
1·0
0
1·0
1·0
2·0
3·0
LOG TIME IN MINUTES.

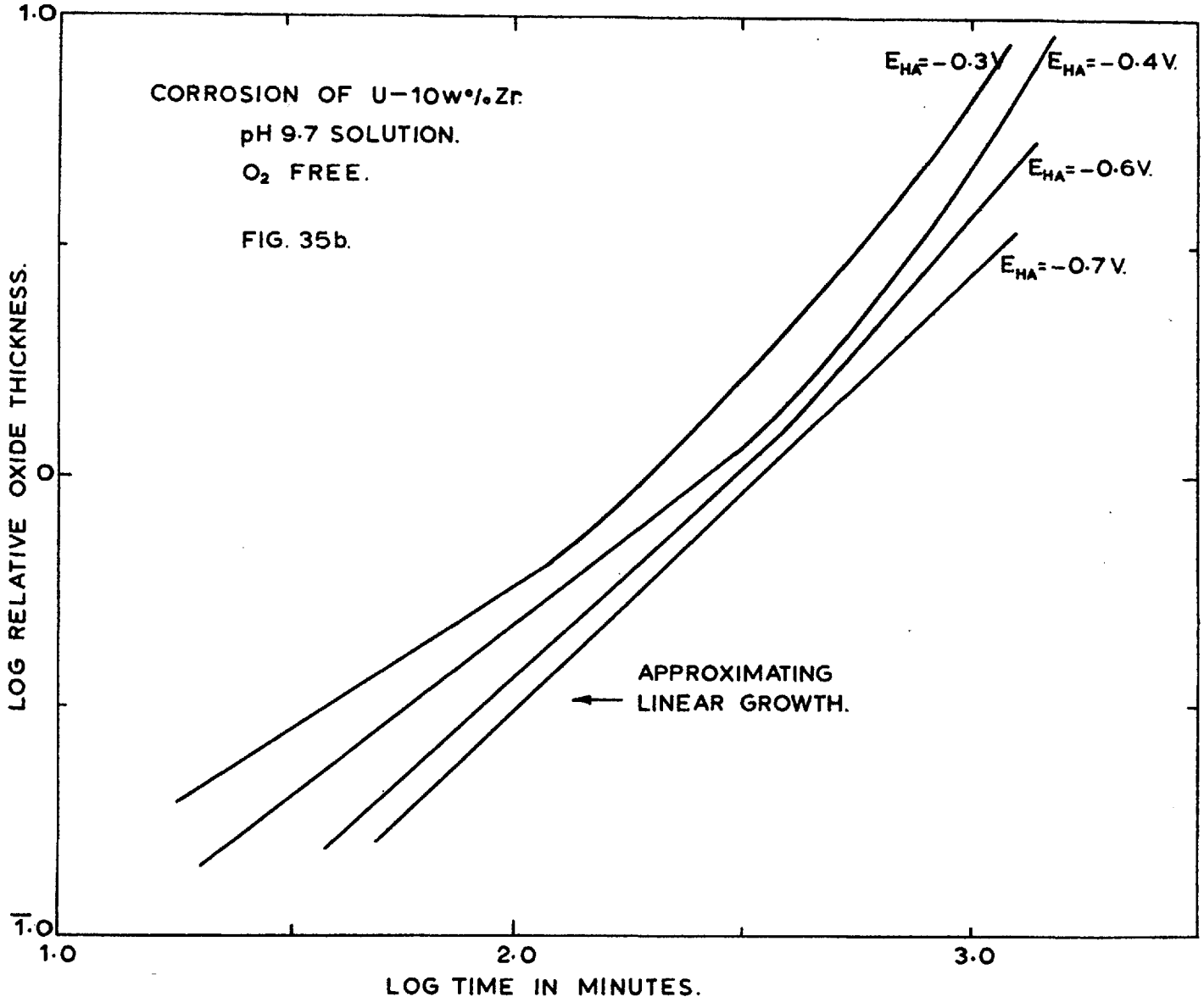
CORROSION OF U–10w°/₀Zr.
pH 9·7 SOLUTION.
O₂ FREE.
FIG. 35b.
E_HA = –0·3V.
E_HA = –0·4V.
E_HA = –0·6V.
E_HA = –0·7V.
APPROXIMATING
LINEAR GROWTH.
LOG RELATIVE OXIDE THICKNESS.
1·0
0
1·0
1·0
2·0
3·0
LOG TIME IN MINUTES.

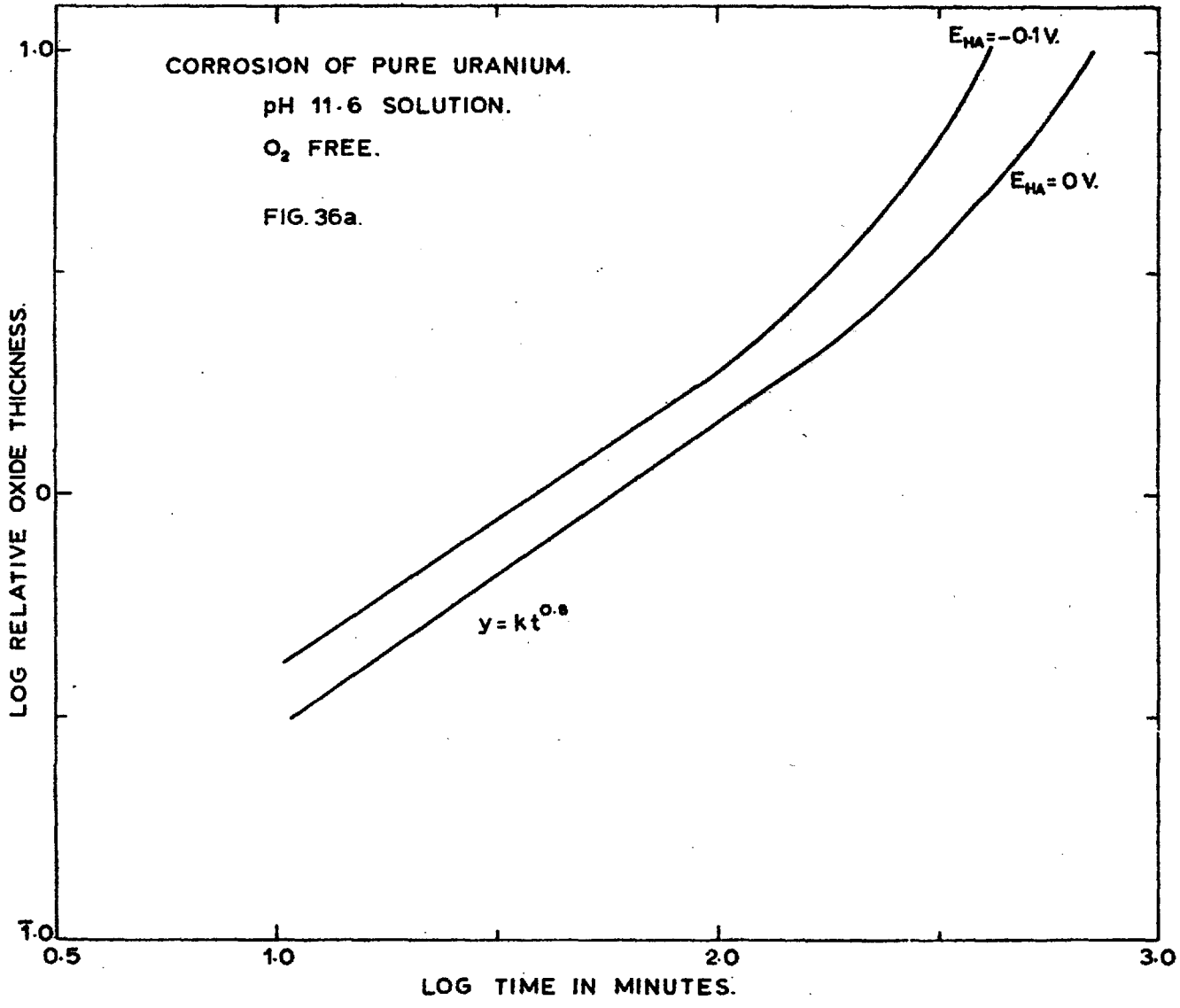
CORROSION OF PURE URANIUM.
pH 11·6 SOLUTION.
O_2 FREE.
FIG. 36a.
E_{HA} = −0·1 V.
E_{HA} = 0 V.
$y = kt^{0.8}$
LOG RELATIVE OXIDE THICKNESS.
1·0
0
1·0
0·5
1·0
2·0
3·0
LOG TIME IN MINUTES.

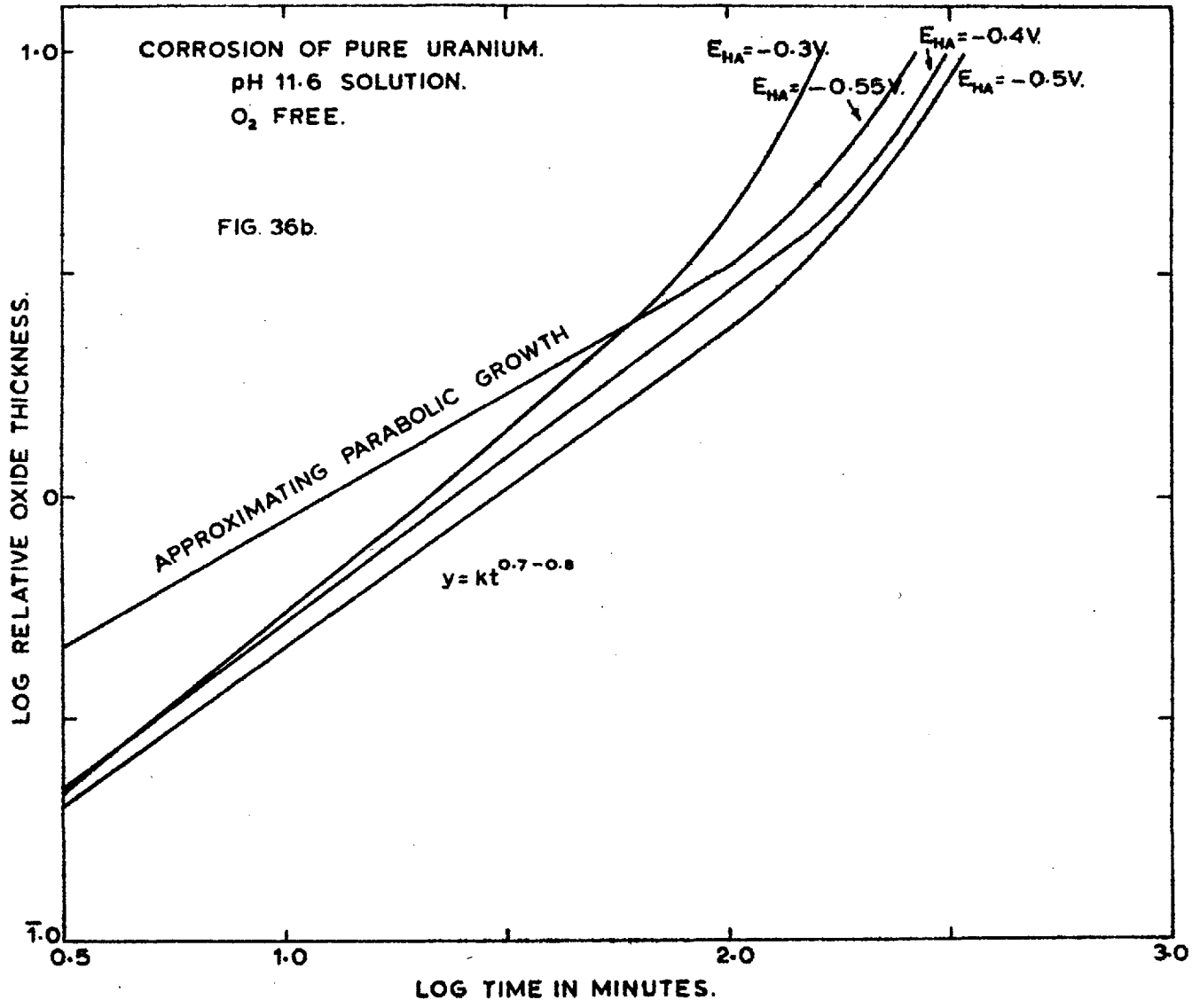
CORROSION OF PURE URANIUM.
pH 11·6 SOLUTION.
O2 FREE.
FIG. 36b.
E_HA = −0·3V.
E_HA = −0·4V.
E_HA = −0·55V.
E_HA = −0·5V.
APPROXIMATING PARABOLIC GROWTH
y = kt^0.7−0.8
LOG RELATIVE OXIDE THICKNESS.
1·0
0
1·0
0·5
1·0
2·0
3·0
LOG TIME IN MINUTES.

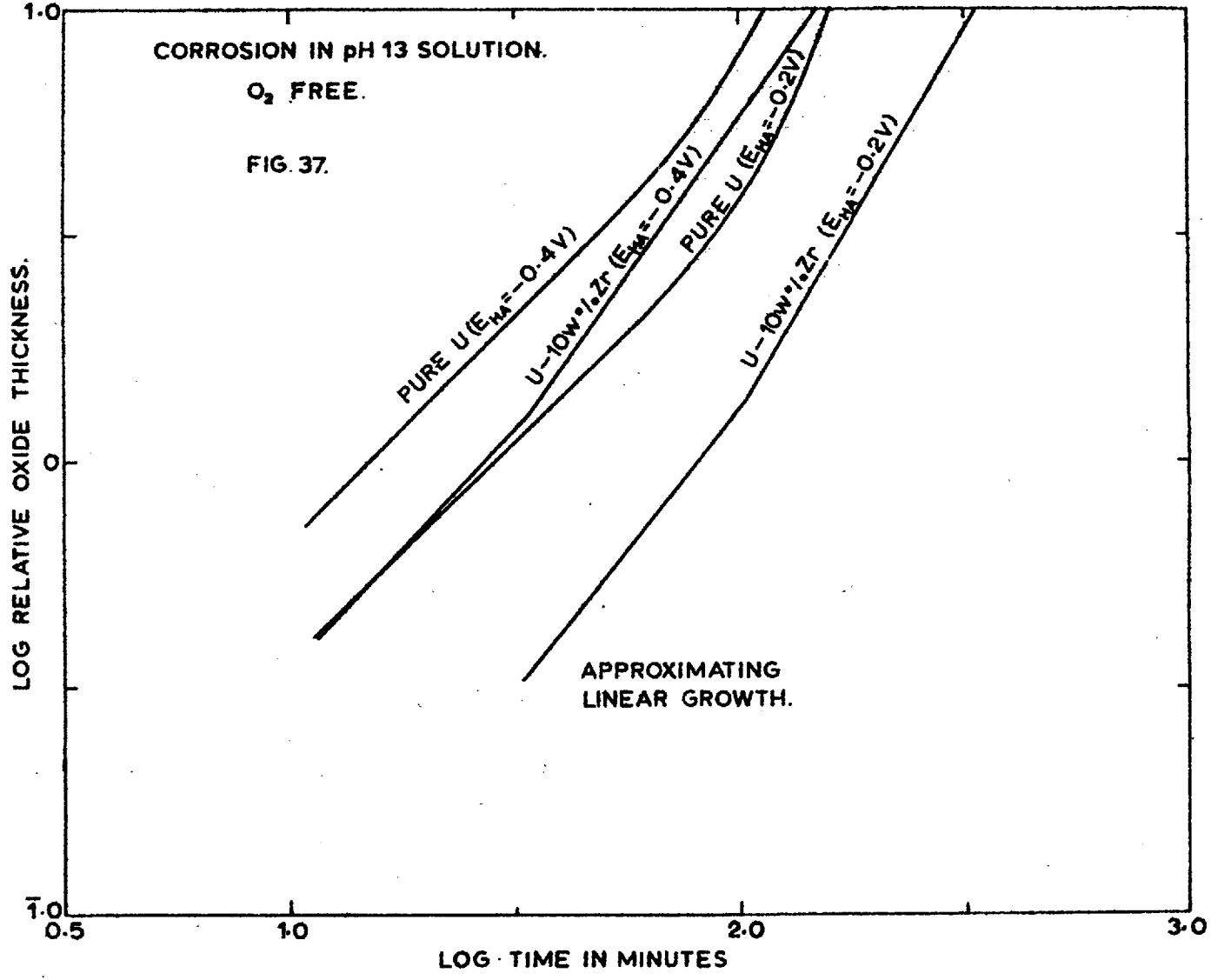
CORROSION IN pH 13 SOLUTION.
O_2 FREE.
FIG. 37.
PURE U (E_{RHE} = −0.4V)
U−10W%Zr (E_{RHE} = −0.4V)
PURE U (E_{RHE} = −0.2V)
U−10W%Zr (E_{RHE} = −0.2V)
APPROXIMATING LINEAR GROWTH.
LOG RELATIVE OXIDE THICKNESS.
1·0
0
1·0
0·5
1·0
2·0
3·0
LOG · TIME IN MINUTES

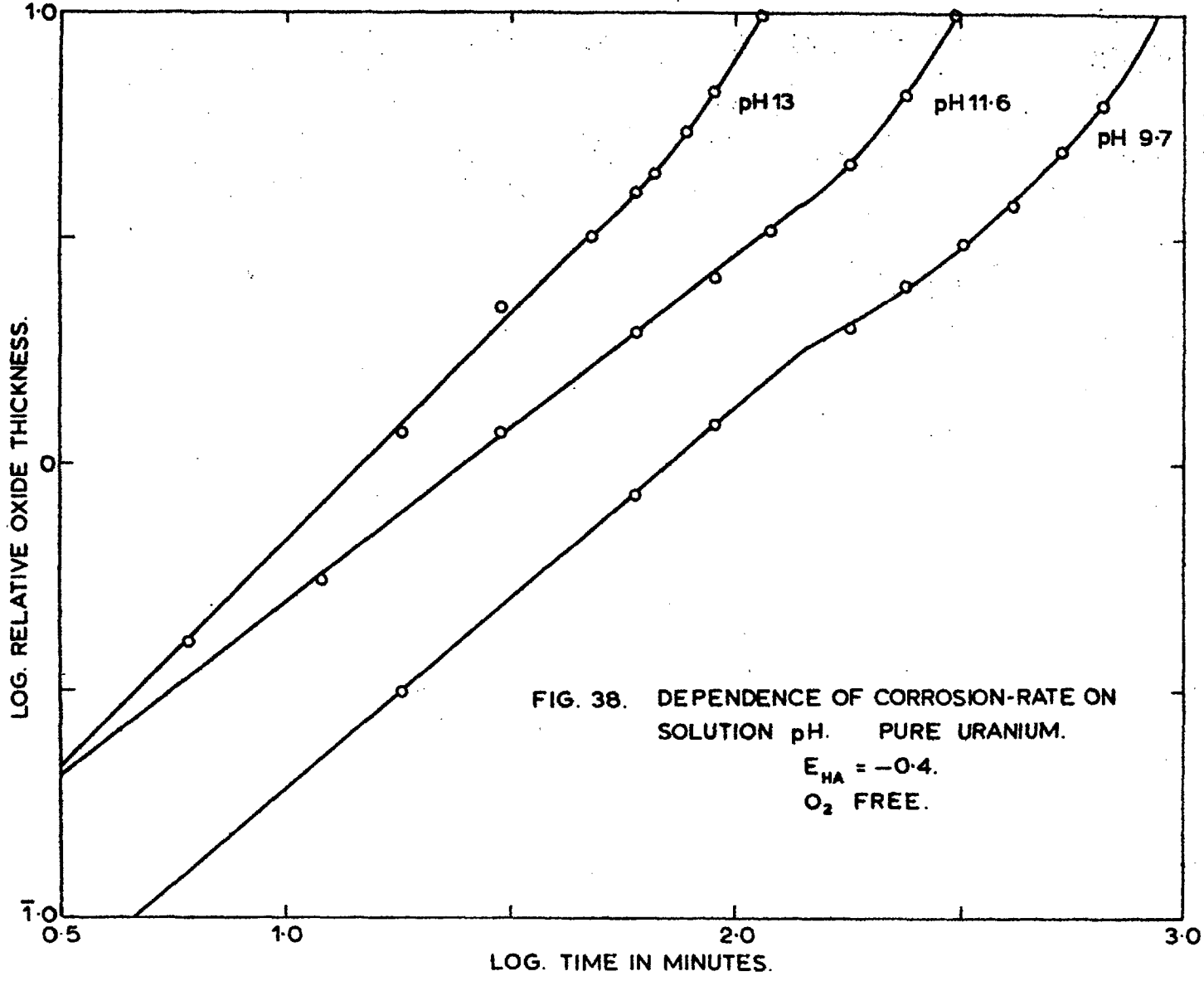

FIG. 38. DEPENDENCE OF CORROSION-RATE ON SOLUTION pH. PURE URANIUM.
$E_{HA} = -0{\cdot}4$.
O_2 FREE.

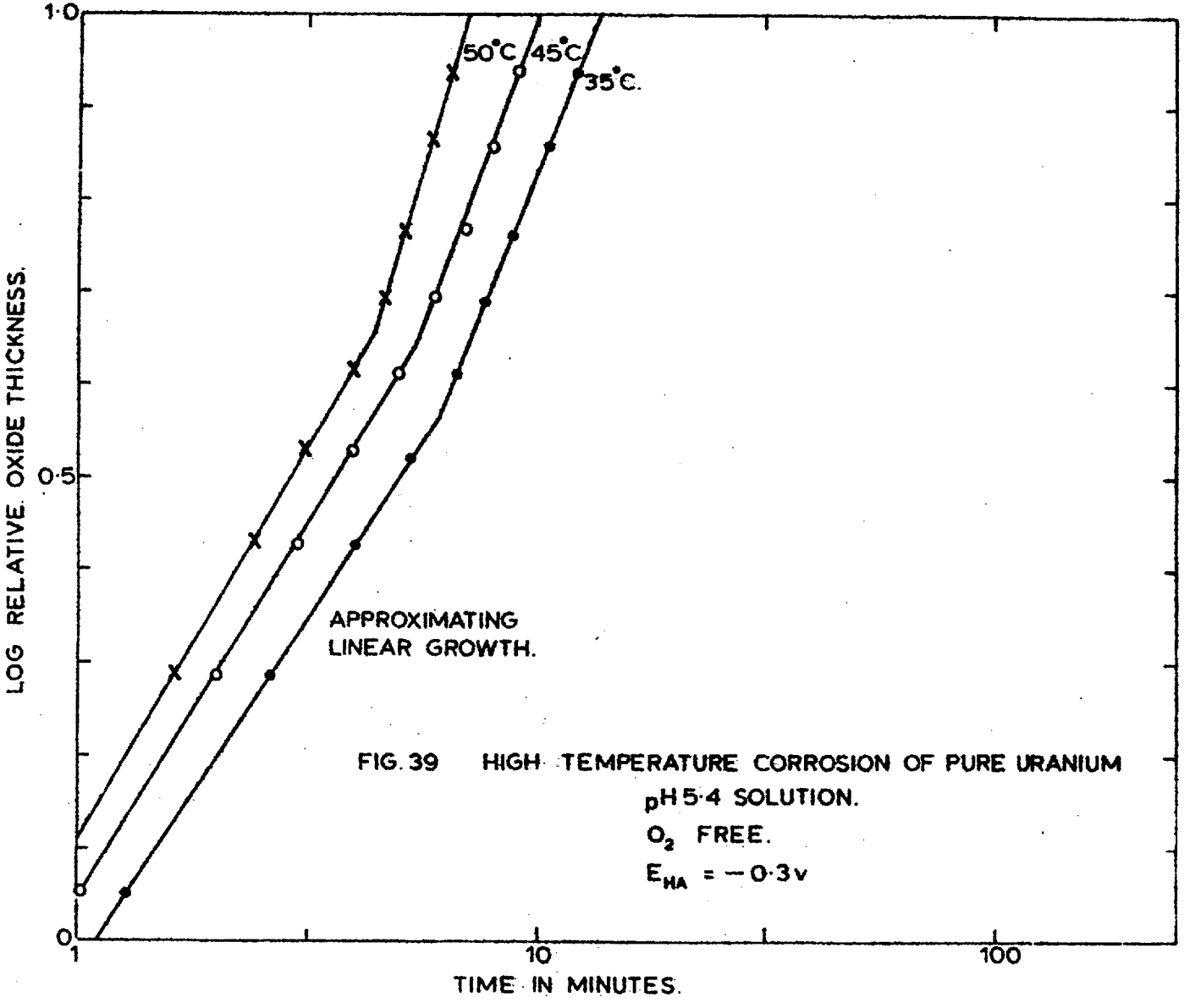

FIG. 39 HIGH TEMPERATURE CORROSION OF PURE URANIUM
pH 5·4 SOLUTION.
O_2 FREE.
$E_{HA} = -0{\cdot}3v$

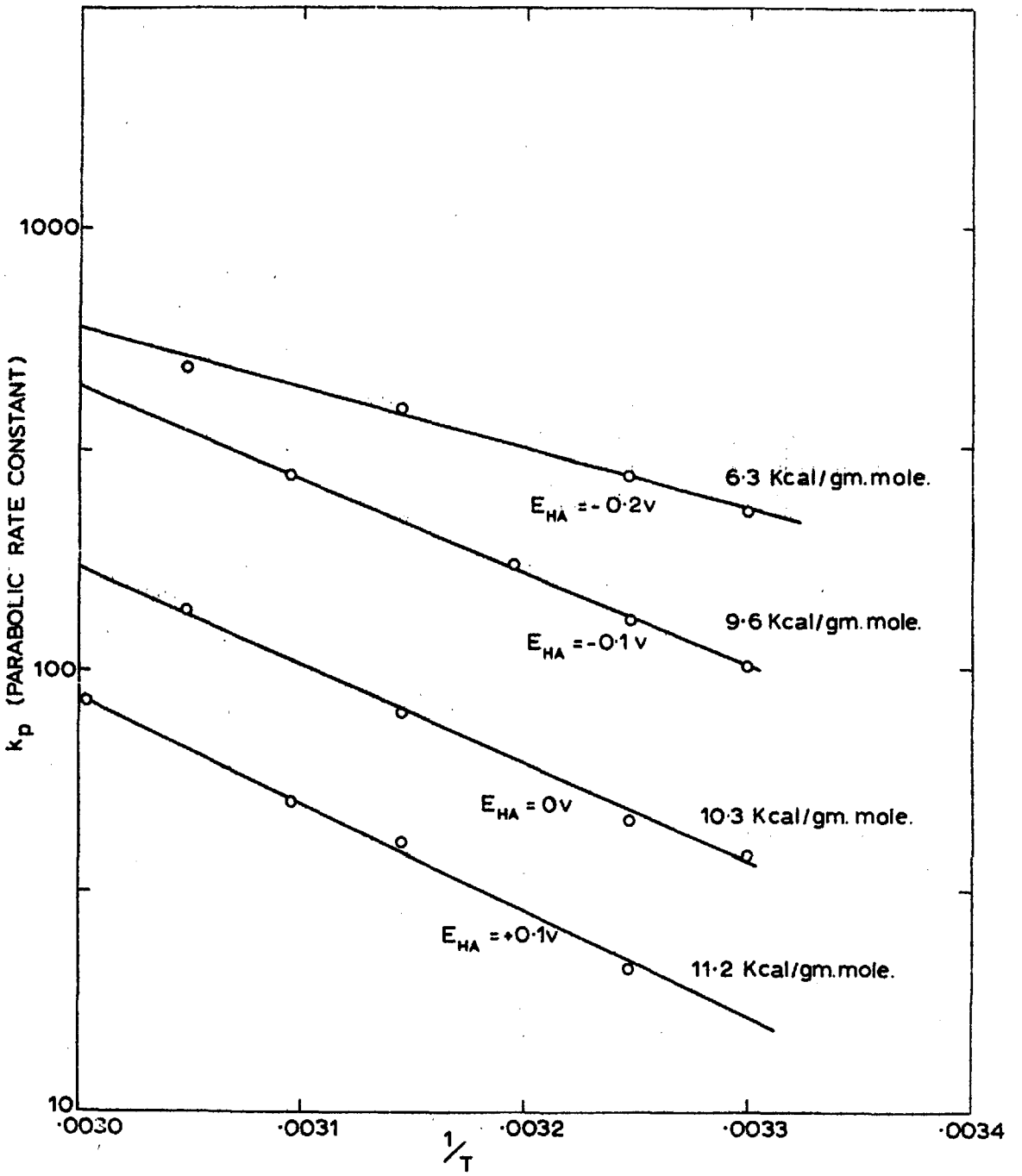

FIG. 40. TEMPERATURE DEPENDENCE OF CORROSION-RATE.
PURE URANIUM.
pH 5·4 SOLUTION.
O_2 FREE.

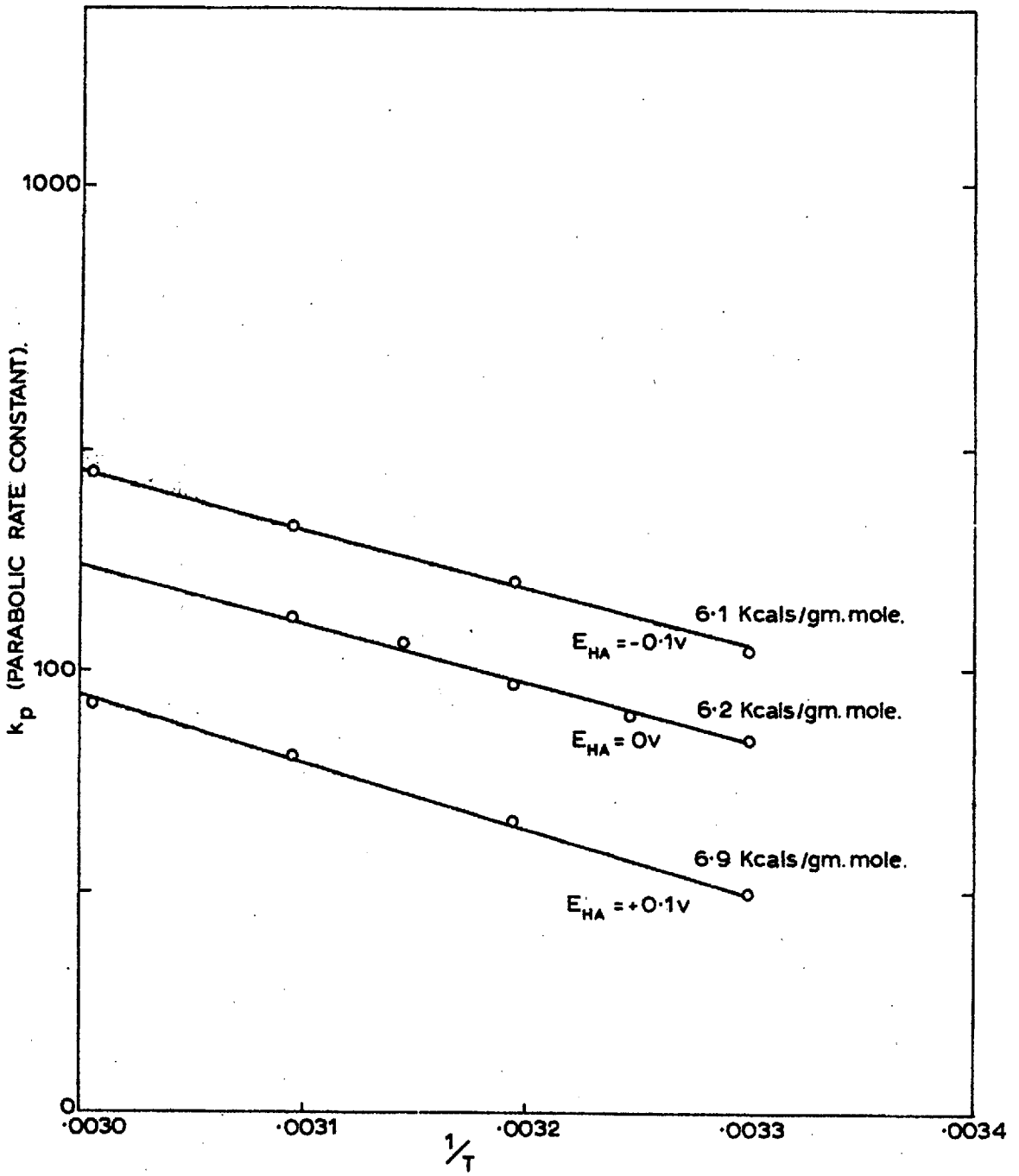

FIG. 41. TEMPERATURE DEPENDENCE OF CORROSION-RATE.
U – 5wt % Zr.
pH 5·4 SOLUTION.
O_2 FREE.

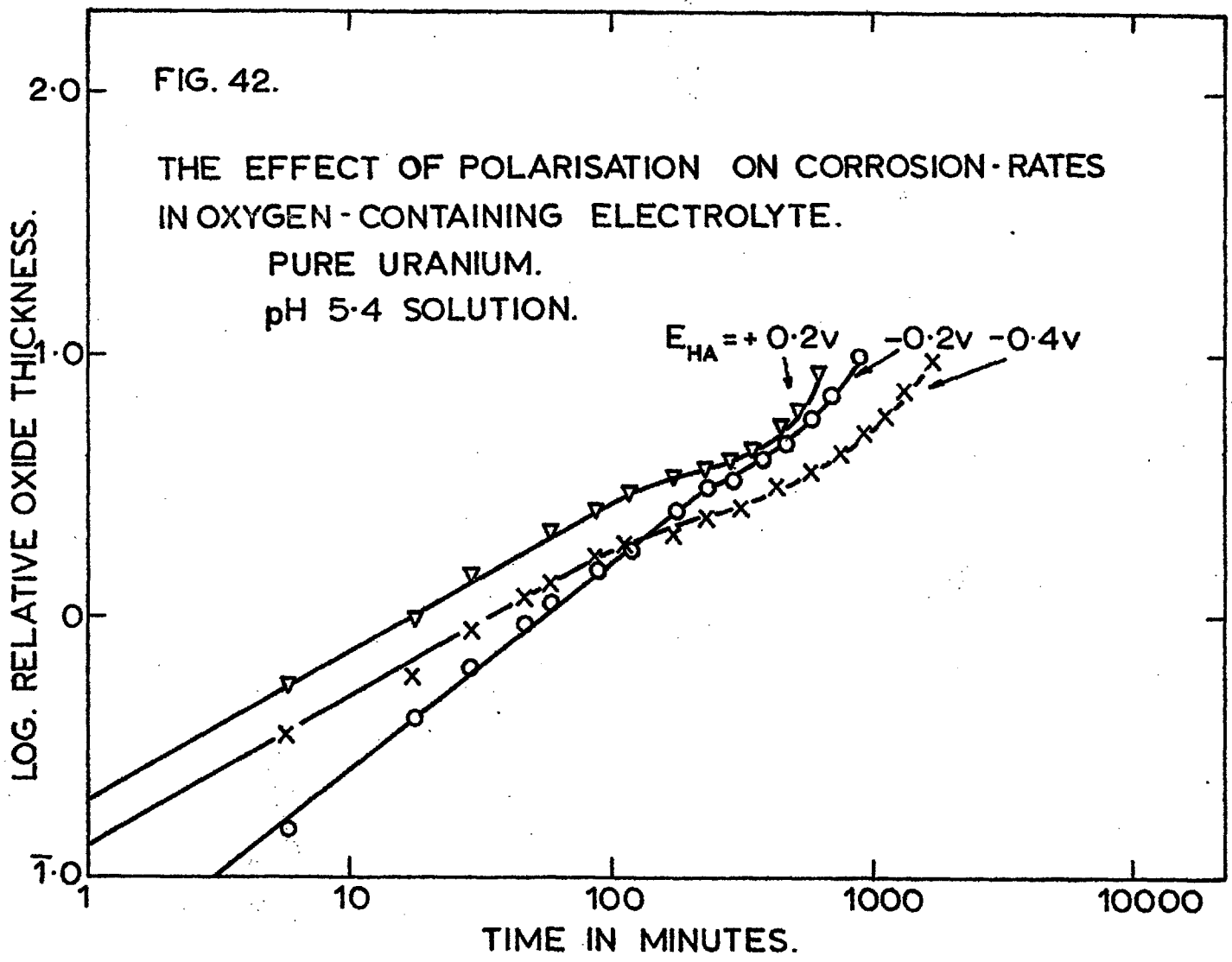
FIG. 42.
THE EFFECT OF POLARISATION ON CORROSION-RATES IN OXYGEN-CONTAINING ELECTROLYTE.
PURE URANIUM.
pH 5·4 SOLUTION.
E_{HA} = + 0·2v
-0·2v
-0·4v
LOG. RELATIVE OXIDE THICKNESS.
2·0
1·0
0
1·0
1
10
100
1000
10000
TIME IN MINUTES.

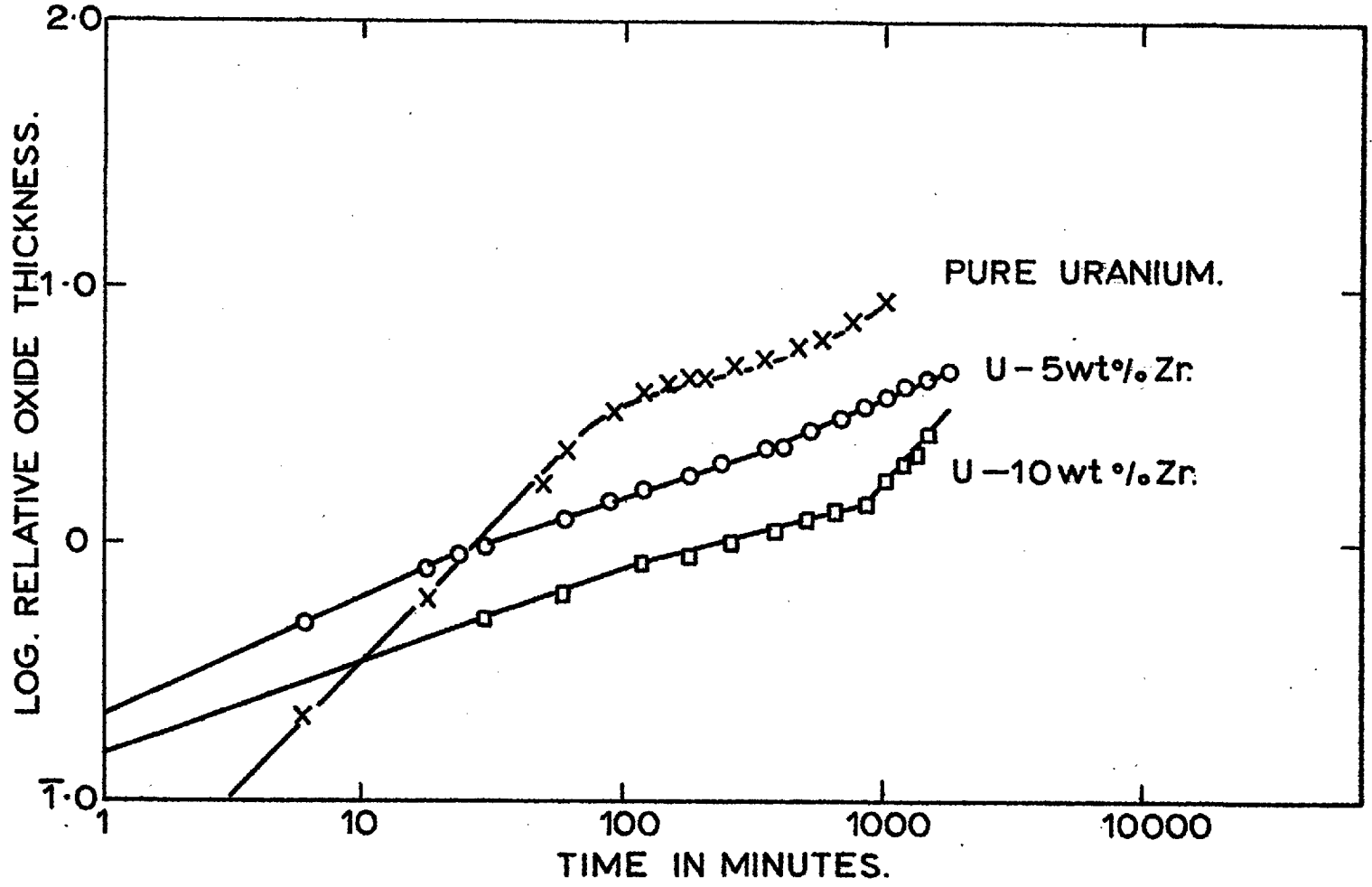

FIG. 43. FREE CORROSION OF URANIUM AND ALLOYS.
pH 5·4 SOLUTION.
O_2 FREE.

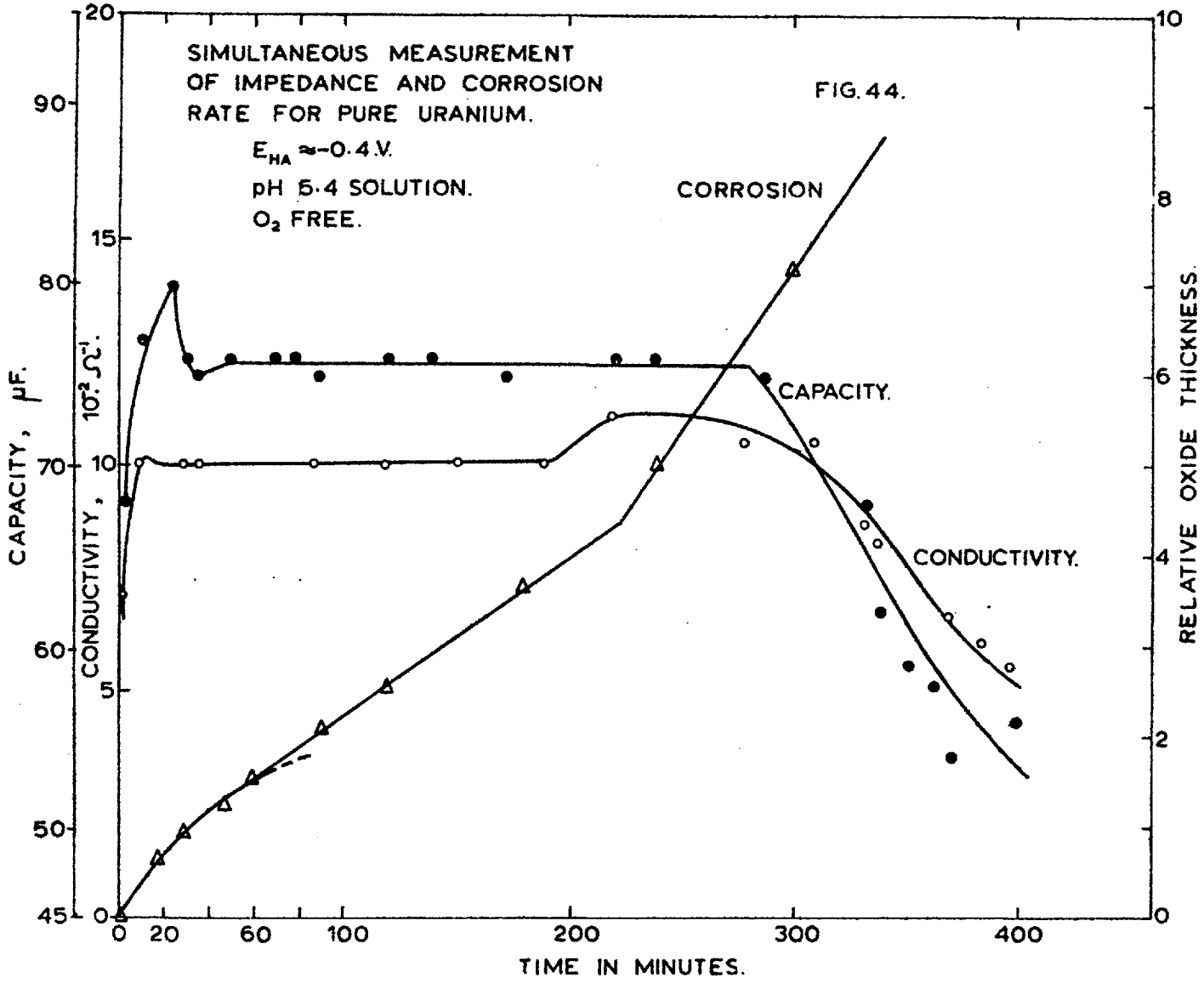
SIMULTANEOUS MEASUREMENT
OF IMPEDANCE AND CORROSION
RATE FOR PURE URANIUM.
E_{HA} ≈ -0.4 V.
pH 5.4 SOLUTION.
O_2 FREE.
FIG. 44.
CORROSION
CAPACITY.
CONDUCTIVITY.
CAPACITY, μF.
CONDUCTIVITY, $10^{-2}\,\Omega^{-1}$.
RELATIVE OXIDE THICKNESS.
TIME IN MINUTES.
90
80
70
60
50
45
20
15
10
5
0
10
8
6
4
2
0
0
20
60
100
200
300
400

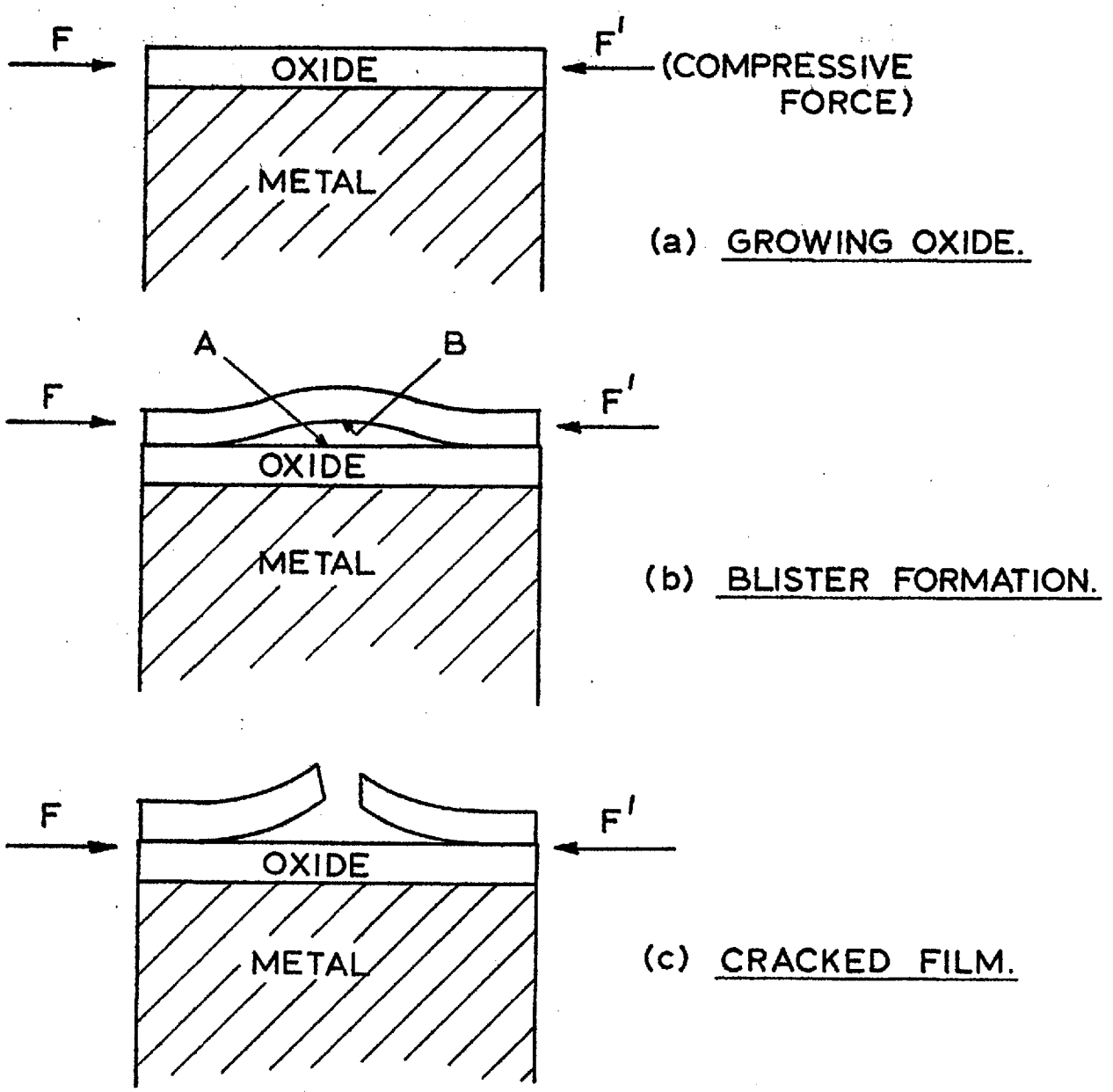

FIG. 45 STAGES IN THE GROWTH AND FRACTURE OF AN OXIDE UNDER LATERAL COMPRESSION.

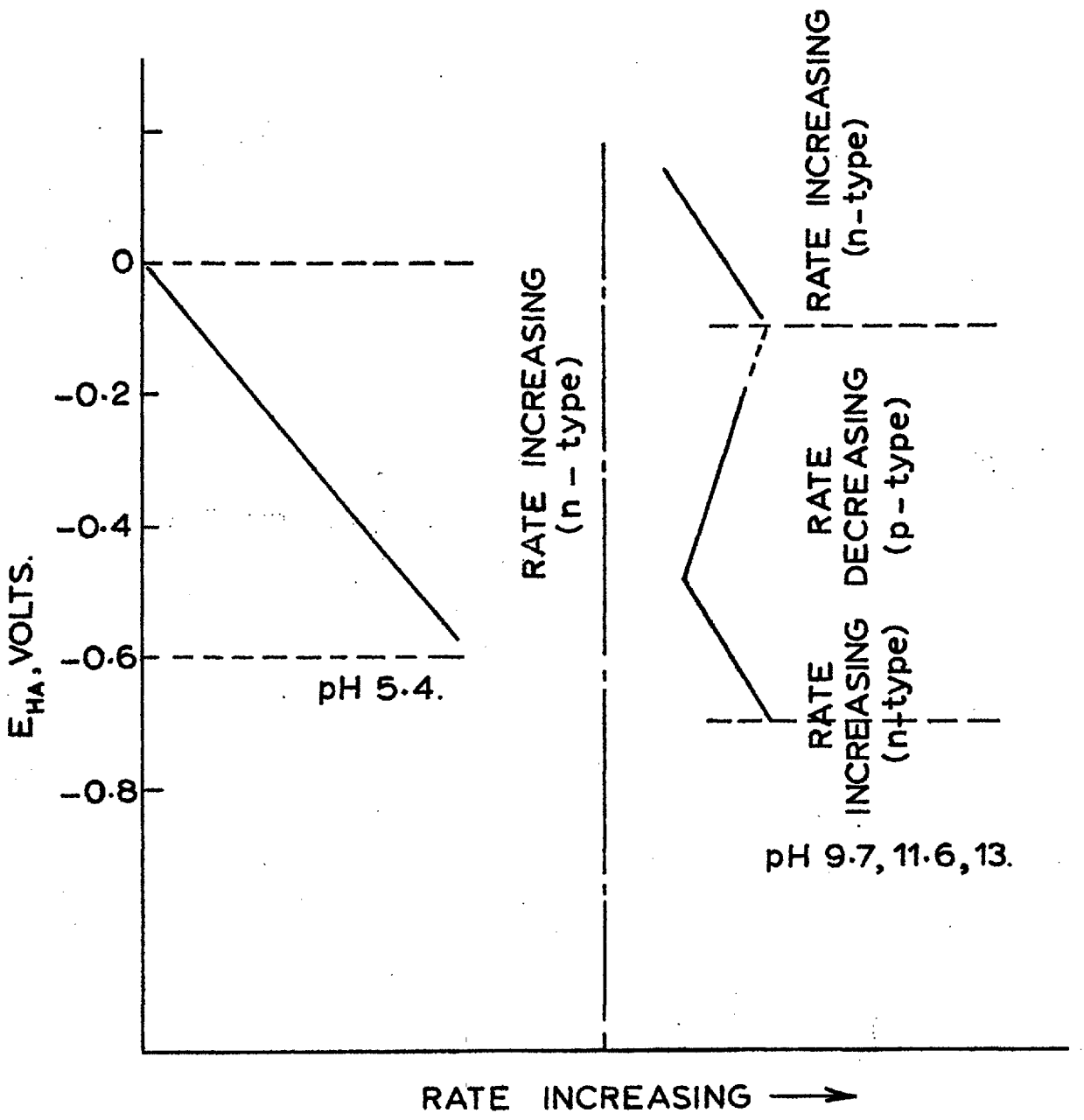

FIG.46. CORROSION RATE AS A FUNCTION OF pH AND POTENTIAL.

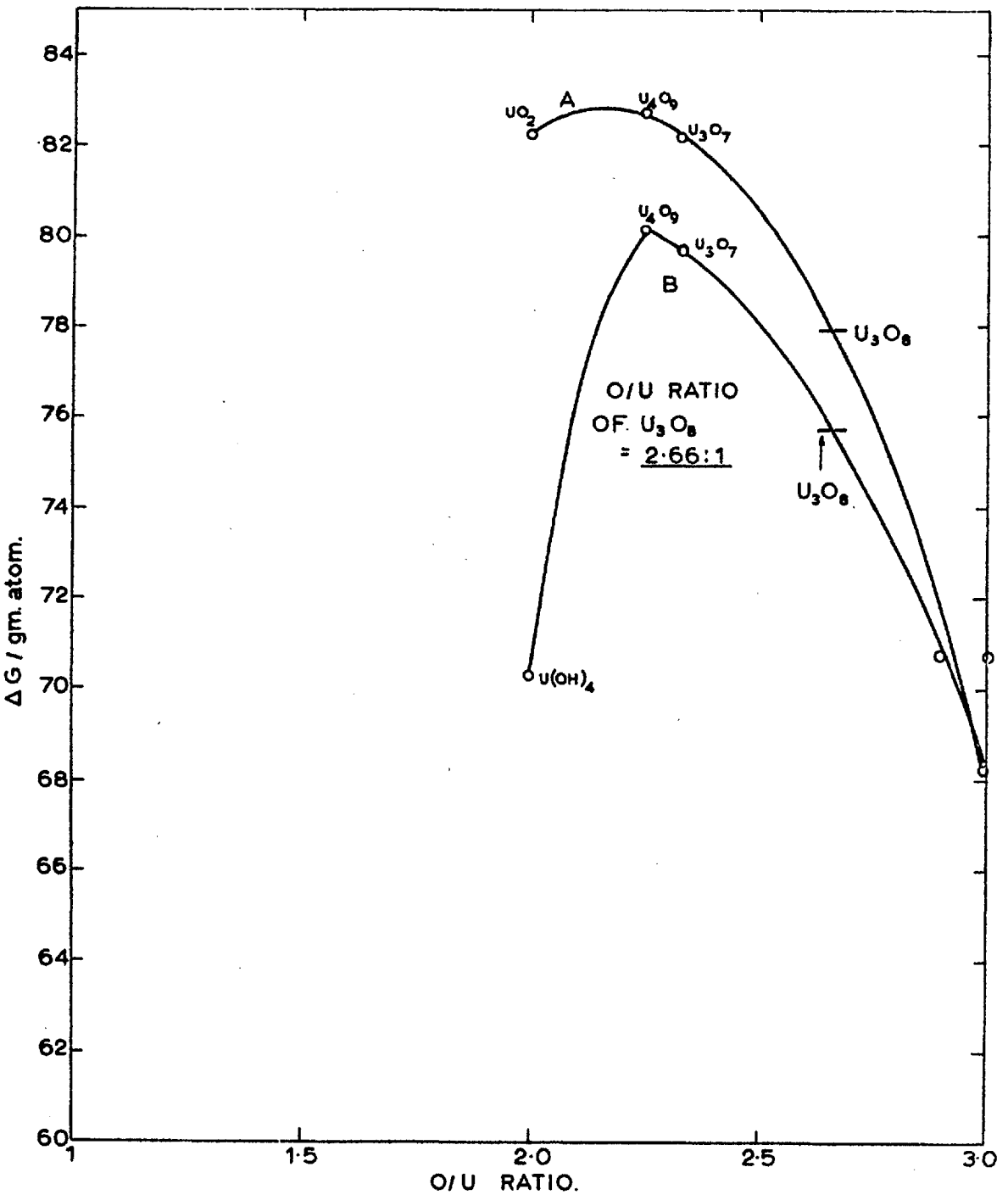

FIG. 47. THEORETICAL CALCULATION OF FREE ENERGY OF FORMATION FOR U_3O_8.

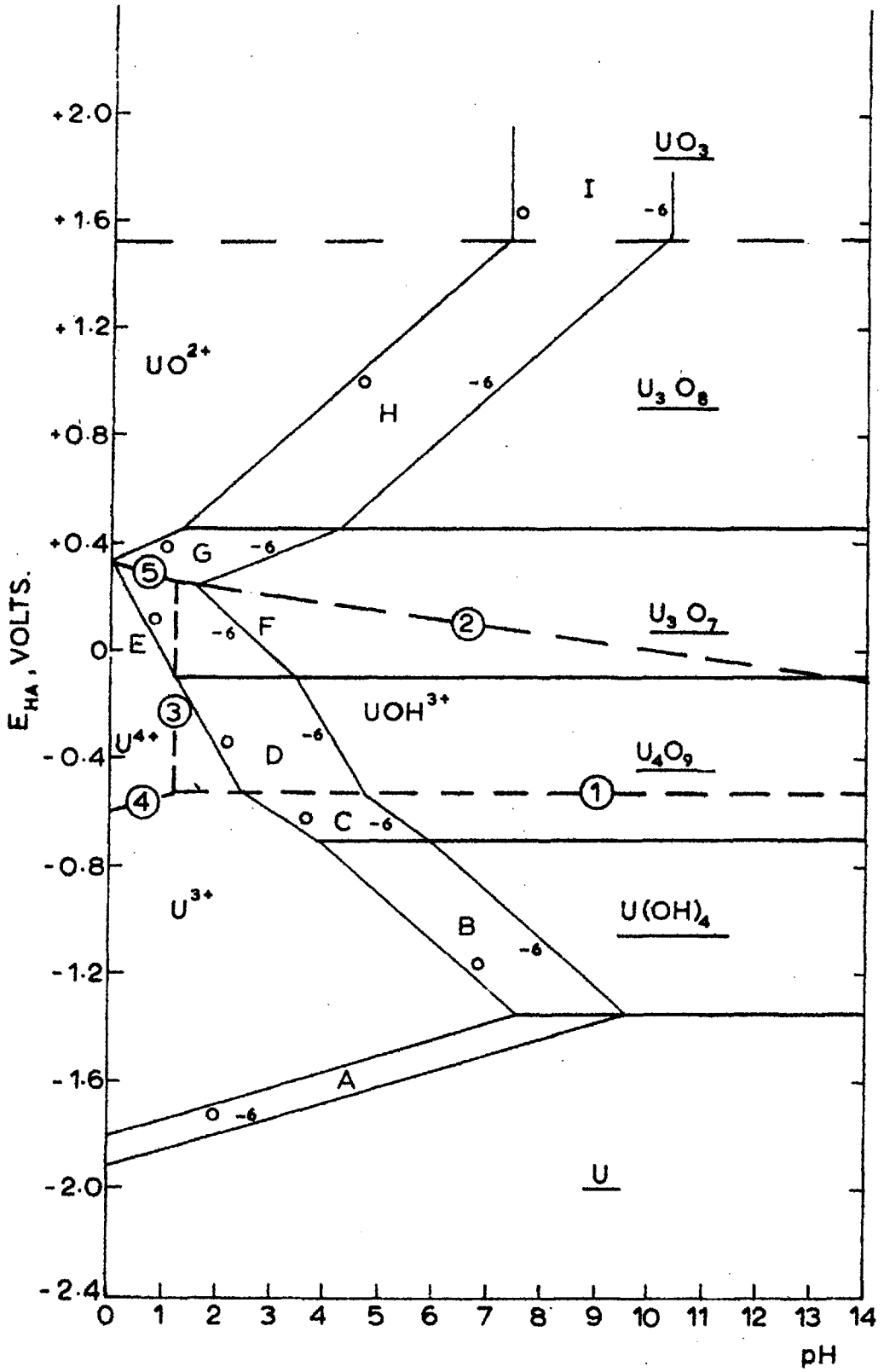

FIG. 48a. pH-POTENTIAL DIAGRAM FOR U-H_2O SYSTEM. (MODIFIED VERSION)

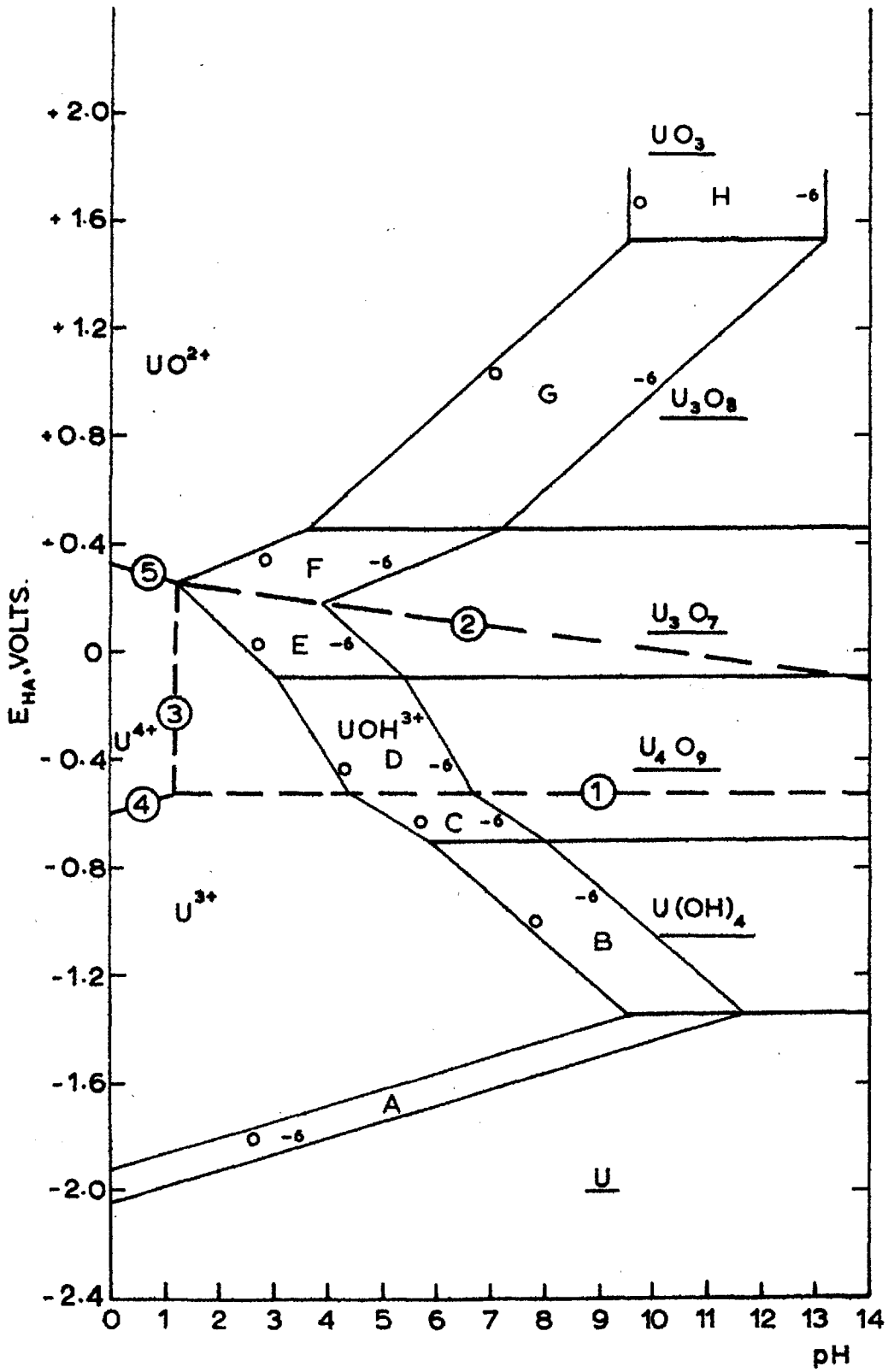

FIG48b. pH–POTENTIAL DIAGRAM FOR U–H_2O SYSTEM.
(MODIFIED VERSION AFTER pH SHIFT)